JPRS L/9121

3 June 1980

USSR Report

METEOROLOGY AND HYDROLOGY

No. 3, March 1980

FBIS FOREIGN BROADCAST INFORMATION SERVICE

NOTE

JPRS publications contain information primarily from foreign newspapers, periodicals and books, but also from news agency transmissions and broadcasts. Materials from foreign-language sources are translated; those from English-language sources are transcribed or reprinted, with the original phrasing and other characteristics retained.

Headlines, editorial reports, and material enclosed in brackets [] are supplied by JPRS. Processing indicators such as [Text] or [Excerpt] in the first line of each item, or following the last line of a brief, indicate how the original information was processed. Where no processing indicator is given, the information was summarized or extracted.

Unfamiliar names rendered phonetically or transliterated are enclosed in parentheses. Words or names preceded by a question mark and enclosed in parentheses were not clear in the original but have been supplied as appropriate in context. Other unattributed parenthetical notes within the body of an item originate with the source. Times within items are as given by source.

The contents of this publication in no way represent the policies, views or attitudes of the U.S. Government.

For further information on report content call (703) 351-2938 (economic); 3468 (political, sociological, military); 2726 (life sciences); 2725 (physical sciences).

APPROVED FOR RELEASE: 2007/02/08: CIA-RDP82-00850R000200090007-3

JPRS L/9121

3 June 1980

USSR REPORT

METEOROLOGY AND HYDROLOGY

No. 3, March 1980

Selected articles from the Russian-language journal METEOROLOGIYA I GIDROLOGIYA, Moscow.

CONTENTS

PUBLICATION DATA

English title	:	METEOROLOGY AND HYDROLOGY
Russian title	:	METEOROLOGIYA I GIDROLOGIYA
Author (s)	:	
Editor (s)	:	Ye. I. Tolstikov
Publishing House	:	Gidrometeoizdat
Place of Publication	:	Moscow
Date of Publication	:	March 1980
Signed to press	:	18 Feb 80
Copies	:	3780
COPYRIGHT	:	"Meteorologiya i gidrologiya", 1980

UDC 551.509.33

DYNAMIC-STATISTICAL PARAMETERIZATION OF THE OCEAN'S THERMAL MEMORY

Moscow METEOROLOGIYA I GIDROLOGIYA in Russian No 3, Mar 80 pp 5-14

[Article by Doctor of Physical and Mathematical Sciences Sh. A. Musayelyan, USSR Hydrometeorological Scientific Research Center, submitted for publication 5 July 1979]

Abstract: The problems of predictability of atmospheric processes and long-range weather forecasting are discussed. Particular attention is devoted to the role of external energy sources. The author emphasizes the role of cloud cover over the ocean as a regulator of the heat influx in the process of absorption of solar radiant energy by the ocean. A dynamic-statistical method for parameterization of the ocean's thermal memory is outlined.

[Text] In the short-range forecasting of meteorological fields the atmosphere in the first approximation can be regarded as an isolated medium and the processes transpiring in it can be regarded as adiabatic. In other words, in the first approximation the short-range forecasting of meteorological fields is the Cauchy problem -- a problem with initial data. Accordingly, in numerical short-range weather forecasting the principal factor is the quality of analysis of the fields of initial data. [The problem of boundary conditions will not be discussed here (Author's note).] In actuality, however, the processes transpiring in the atmosphere are strictly nonadiabatic, and when one speaks of study of atmospheric behavior over long and very long time periods the external energy conditions must be regarded as determining factors. And this means that the problem of modeling of short-period climatic variations or long-range prediction of meteorological fields is the Cauchy problem, but with a source. In other words, in this case it is insufficient to have only qualitatively analyzed initial fields; it is also necessary to take into account, and this is particularly important, the principal macroscale nonadiabatic factors.

The contributions of initial data and external energy sources to numerical weather forecasting for different times in advance have been examined by a number of authors (for example, see [1, 4]). These contributions can also be investigated directly on the basis of the first law of thermodynamics.

Qualitative Analysis of Contributions of Initial Data and Nonadiabatic Factors

As is well known, the mathematical expression for the first law in thermodynamics, applicable to atmospheric conditions, is the energy equation, which can be written in the following form:

$$\frac{\partial T}{\partial t} + \frac{v_\theta}{a}\frac{\partial T}{\partial \theta} + \frac{v_\lambda}{a\sin\theta}\frac{\partial T}{\partial \lambda} - \frac{k}{a^2}\Delta T = E. \tag{1}$$

Here t is time, λ is geographic longitude, $\theta = \pi/2 - \varphi$, φ is latitude, $v_\theta(\theta, \lambda, t)$ and $v_\lambda(\theta, \lambda, t)$ are the velocity components along the θ and λ axes respectively, $T(\theta, \lambda, t)$ is temperature, a is the earth's mean radius, k is the coefficient of horizontal macroturbulent exchange, Δ is the Laplace operator in spherical coordinates and the function $E(\theta, \lambda, t)$ integrally describes all the heat influxes.

We will assume that it is necessary to obtain a solution of equation (1), periodic relative to λ, symmetric relative to the equator and limited at the pole, satisfying the initial condition

$$T(\theta, \lambda, t)|_{t=0} = T_0(\theta, \lambda). \tag{2}$$

For convenience in the subsequent presentation we introduce the notation

$$-\frac{v_\theta}{a}\frac{\partial T}{\partial \theta} - \frac{v_\lambda}{a\sin\theta}\frac{\partial T}{\partial \lambda} = I(\theta, \lambda, t)$$

and equation (1) is rewritten in the following form:

$$\frac{\partial T}{\partial t} - \frac{k}{a^2}\Delta T = E + I. \tag{3}$$

Assuming that the functions $E(\theta, \lambda, t)$, $I(\theta, \lambda, t)$ and $T_0(\theta, \lambda)$ can be represented in the form of series in spherical functions

$$\left.\begin{aligned} E &= \mathrm{Re}\sum_n\sum_m E_n^m(t)\, e^{-im\lambda} P_n^m(\cos\theta), \\ I &= \mathrm{Re}\sum_n\sum_m I_n^m(t)\, e^{-im\lambda} P_n^m(\cos\theta), \\ T_0 &= \mathrm{Re}\sum_n\sum_m T_{0n}^m\, e^{-im\lambda} P_n^m(\cos\theta), \end{aligned}\right\} \tag{4}$$

we will seek a solution of equation (3) in the form

$$T = \mathrm{Re}\sum_n\sum_m T_n^m(t)\, e^{-im\lambda} P_n^m(\cos\theta). \tag{5}$$

In formulas (4) and (5) $E_n^m(t)$, $I_n^m(t)$ and $T_n^m(t)$ are complex functions, $T_{0\,n}^m$ are complex numbers, and $P_n^m(\cos\theta)$ is the adjoint Legendre polynomial.

It is easy to show that the considered problem is reduced to integration of the equation

$$\frac{dT_n^m}{dt} + \frac{k}{a^2} n(n+1) T_n^m = E_n^m + I_n^m \tag{6}$$

with the stipulated condition

$$T_n^m(t)|_{t=0} = T_{0n}^m. \tag{7}$$

The solution of problem (6)-(7) can be written in the form

$$T_n^m(t) = \frac{a^2(\overline{E}_n^m + \overline{I}_n^m)}{kn(n+1)}\left\{1 - \exp\left[-\frac{k}{a^2} n(n+1) t\right]\right\} + + T_{0n}^m \exp\left[-\frac{k}{a^2} n(n+1) t\right]. \tag{8}$$

where $\overline{E}_n^m$ and $\overline{I}_n^m$ are values of the functions $E_n^m(t)$ and $I_n^m(t)$, averaged in the considered time interval.

Formula (8) is prognostic. The second term on the right-hand side of this formula shows that in the prediction of temperature the role of initial data actually decreases with time, and this decrease occurs exponentially. However, the first term on the right-hand side of (8) shows that the contribution of the energy sources increases with time in conformity to the law

$$1 - \exp\left[-\frac{k}{a^2} n(n+1) t\right].$$

It is entirely obvious that both these processes (decrease in the role of initial data with time and increase in the contribution of energy sources) occurs differently for different wave numbers n. In addition, the intensity of both these processes is essentially dependent on the value of the coefficient of horizontal macroturbulent exchange k, which, as is well known, varies in a rather broad range.

For waves of the scale of middle-latitude cyclones $n \approx 5$ and for the value $k = 10^6$ m^2/sec the contributions of the above-mentioned processes are represented in Fig. 1.

In this figure we have plotted time in days along the horizontal axis, and along the vertical axis -- some conditional r_0 value characterizing the contribution of some factor to the precomputed meteorological field (in essence, this is the parameter characterizing the success of the prediction, for example, the correlation coefficient).

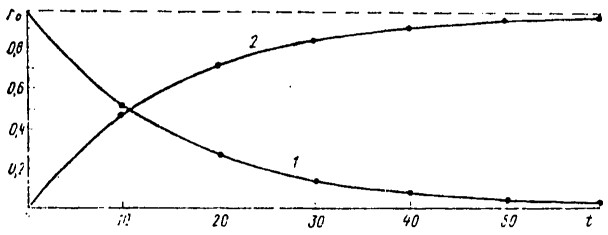

Fig. 1. Contributions of initial data (1) and heat influxes (2).

The following conclusions can be drawn on the basis of an analysis of Fig. 1:

1) In the time interval $0 < t \lesssim 5$ days the success of the forecast is determined primarily by the quality of analysis of the initial field and the contribution of the energy sources is secondary. In this case the forecasting problem in the first approximation can be regarded as the classical problem with initial data. According to the terminology which is now in use forecasts for up to five days are called short-range.

2) In the time interval approximately from one to two weeks the role of the above-mentioned factors is approximately identically important, that is, the success of the forecast is determined to an approximately equal degree both by the quality of analysis of the initial field and the contribution of energy sources. In this case the forecasting problem can be considered as the Cauchy problem with a source; both these factors are identically important. This is a case of intermediate forecasts.

3) In the time interval from two weeks to one-two months there is a continuing decrease in the role of initial data and an increase in the contribution of energy sources. In this case the forecasting problem is evidently the Cauchy problem with a source, but the main role is nevertheless played by energy sources. This is the case of long-range forecasts for a month and a season.

4) Finally, in the time interval from one-two months to infinity the role of initial data becomes negligible and everything (or almost everything) is determined by the external energy conditions. This is the case of a superlong-range or climatic forecast.

Other classifications also exist.

We will return to formula (8). It is easy to show that the time τ_0, at whose end the role of initial data becomes equal to the contribution of the energy sources, is determined using the formula

$$\tau_0 = \frac{0{,}7\, a^2}{kn\,(n+1)}.$$

Below we give the τ_0 values for different wave numbers with $k = 10^6$ m^2/sec.

n	1	2	3	4	5	6	7	8	9	10
τ_0 days	162	54	27	16	11	8	6	5	4	3

The cited data show that the ultralong components of the initial fields (n = 1, 2, 3) are conserved for a very long time in the atmospheric memory and only after one or more months their role becomes less than the contribution of energy sources. Waves of a synoptic scale ($n \approx 5$) in the atmospheric memory, however, are conserved only for approximately two weeks, after which the role of nonadiabatic factors increases.

Finally, for the high-frequency components the role of initial data decreases very rapidly and literally after several days the external energy sources become the determining factor.

Another conclusion which follows from formula (8) relates to the predictability problem.

As is well known, the traditional interpretation of the problem of predictability of atmospheric processes is based on the conclusion that the errors contained in the initial fields are doubled each two to four days, as a result of which predictability is a definite limit equal to five-seven days (for example, see [6]). This, to a certain degree, agrees with the just mentioned formula. Moreover, curve 1 in Fig. 1 shows that the contribution of initial data decreases with time independently of their accuracy -- such is the structure of the equations in hydrothermodynamics. But, according to this same formula, with a decrease in the role of initial data the contribution of energy sources increases. Therefore, to speak of atmospheric predictability, taking into account only the role of initial data and laying aside the contribution of energy sources, means from the very beginning to set a limit to predictability of 5-7 days. This follows from formula (8) and can be seen clearly in Fig. 1. The nature of atmospheric processes is evidently such that allowance for only one factor -- the contribution of initial data -- leads to a sharp limitation on the predictability limit, whereas the addition of another factor -- energy sources -- makes this limit longer. In any case, such is the nature of the equations of hydrothermodynamics, and this rigorously follows from formula (8) and can be seen clearly in Fig. 1.

The structure of the prognostic formula (8) is such that when having even precise initial data, strictly speaking, it is impossible to precompute the predicted field precisely even for one day. However, if in addition precise data are available concerning the sources, using this formula it is possible to precompute the temperature field for any time with the accuracy with which equation (3) is integrated. However, the initial field is known very approximately and only for a part of the earth constituting

about 20% of its entire surface. With respect to the energy sources, judging from everything, our ideas concerning them are extremely vague. Therefore, when reference is to long-range weather forecasting the principal problem is that of discriminating and parameterizing the most important large-scale energy sources controlling the behavior of the global atmosphere over long time intervals. Everything set forth above indicates that when reference is to short-range weather forecasting the term "atmospheric predictability" in general is an apt expression. However, if reference is to long-range forecasting of meteorological fields the traditional problem of predictability must evidently be dealt with in a new way and the term "atmospheric predictability" itself must be replaced by some other, more suitable term, such as the term "long-range predictability of the earth-atmosphere system."

In equation (3) and formula (8) the temperature $T(\theta, \lambda, t)$ and its expansion coefficients $T_n^m(t)$ are functions highly dependent on time. Now we introduce into consideration the climatic temperature $\tilde{T}(\theta, \lambda)$ and we will assume that it is slightly dependent on time (as it actually is), so that $\partial \tilde{T} / \partial t \approx 0$. Then, if we denote the expansion coefficients $\tilde{T}(\theta, \lambda)$ in spherical functions by $\tilde{T}_n^m$ it is easy to show that

$$\tilde{T}_n^m = \frac{a^2 (\bar{E}_n^m + \bar{I}_n^m)}{kn (n+1)}. \tag{9}$$

On the other hand, on the basis of (8) it is easy to find

$$\lim_{t \to \infty} T_n^m(t) = \frac{a^2 (\bar{E}_n^m + \bar{I}_n^m)}{kn (n+1)}. \tag{10}$$

Comparing (9) and (10), we have

$$\tilde{T}_n^m = \lim_{t \to \infty} T_n^m(t).$$

Thus, according to formula (8), modern climate is some asymptomatic state of the real atmosphere with real boundary conditions and external energy sources.

It should be noted that the conclusions drawn above do not have a categorical nature due to a number of simplifications of the considered problem (in particular, no allowance is made for the process of energy exchange between waves of different scales). However, it appears that these conclusions, at least qualitatively, agree with modern concepts.

The enumerated classifications are based on a very important fact: the initial data on the state of the atmosphere sooner or later "are forgotten" and the factors controlling atmospheric behavior over long time intervals will be the external energy sources.

Thus, for developing a long-range weather forecasting method it is necessary that we first discriminate and parameterize those factors which control the processes transpiring in the "earth-atmosphere" system over the course of long time intervals.

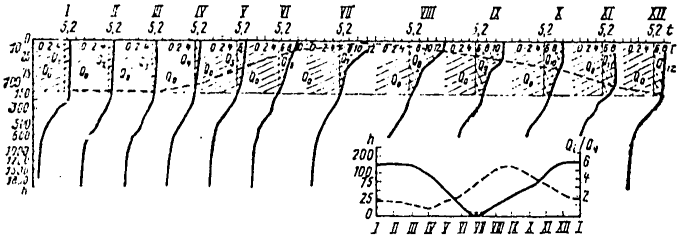

Fig. 2. Mean monthly vertical water temperature profiles and Q_i values.

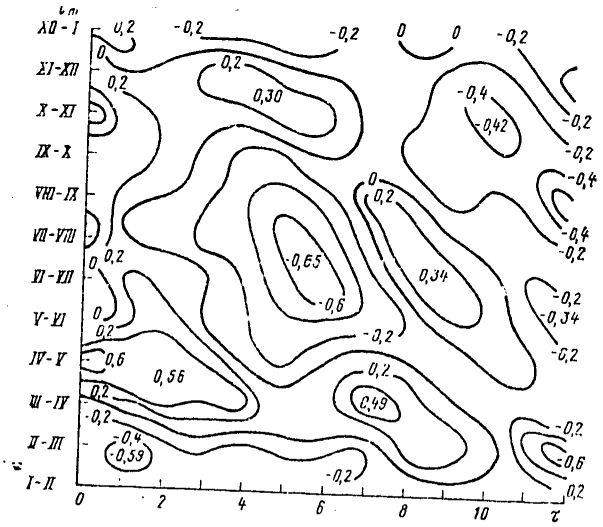

Fig. 3. Cross-correlation matrix of moving averages of the $S'(t_m)$ and $T'(t_m + \tau)$ values for two months.

Comments on Thermal Memory of Ocean

In an investigation of large-scale atmospheric processes it can be assumed that the sun is the only energy source.

The nature of atmospheric-oceanic processes is such that the ocean in the warm half of the year absorbs solar radiant energy, transforms it into thermal energy and "remembers" it, that is, accumulates it in its depths. In the cold half of the year, using different heat exchange processes, the ocean transmits this heat to the atmosphere. In this case the cloud cover is the principal regulator with a feedback [3-5, 7].

In order to trace this process we will turn to Fig. 2, where on the basis of data for weather ship M (66°00'N, 02°00'E) we have shown the mean monthly vertical water temperature profiles for all the months of 1953. Along the vertical axis we have plotted depth in meters, and along the horizontal axis -- time t (the months are denoted by Roman numerals) and temperature T in degrees Celsius. "Q_0" denotes the heat content of an ocean layer with a thickness 150 m with a temperature constant with height, equal to 5.2°C. "Q_i" ($i = 1, 2, \ldots, 12$) denotes deviations of the heat content of the mentioned layer from Q_0 (heavy shading).

An analysis of this figure indicates that an increase in the heat content of the active layer of the ocean occurs in the warm half of the year, whereas in the winter the accumulated heat is transmitted to the atmosphere. This can be seen particularly well in the inset to Fig. 2, where the solid curve represents the approximate depth of the homogeneous layer of the ocean, whereas the dashed curve represents the ratio Q_1/Q_4.

For greater clarity we will cite the following well-known example [4]. If the temperature of the upper 100-m layer of the world ocean is reduced by 0.1°C and it is assumed that all the released heat is expended on heating of the atmospheric air, the temperature of the entire atmosphere to an altitude 30 km is raised by approximately 5-6°C.

Thus, in developing a method for long-range weather forecasts an acute need arises for parameterization of the thermal memory of the ocean.

Role of the Cloud Cover of the Oceans

The process of absorption of solar radiant energy by the ocean, its transformation into internal energy stored in the warm half of the year and the release of this accumulated heat to the atmosphere in the cold half-year cannot for the time being be parameterized in general form with the accuracy necessary for the development of long-range weather forecasting schemes on this basis.

The author of [5, 7] gave a certain phenomenological interpretation of this problem. There, instead of the temperature of sea water, he proposes the use of information on the cloud cover of the oceans received from meteorological satellites. In particular, it was demonstrated that there is a quite close asynchronous correlation between anomalies of summer cloud cover over the ocean, averaged for three-month time intervals, and deviations of winter air temperature on the continent from the norm.

Further investigations indicated that such a correlation also exists with two-month averaging of anomalies of the above-mentioned meteorological elements [2]. As an example, we will examine Fig. 3, where by means of isocorrelates we have represented the correlation matrix for Leningrad. In computing this matrix on the basis of data from meteorological satellites for the 10 years from 1965 through 1974 we formed the mean monthly values for total cloud cover at the points of a geographic grid 5° x 5° for the part of the North Atlantic bounded by latitudes 40 and 65°N. Using these data we determined the norms for each month in the year and then computed the corresponding anomalies and averaged them for the considered part of the ocean. The monthly temperature anomalies used were those employed in the operational work of the USSR Hydrometeorological Center.

Using these data we computed the moving mean two-month anomalies of the considered meteorological elements.

Along the horizontal axis in Fig. 3 we have plotted the time shift τ, and along the vertical axis -- the months of the year. The nature of the field of isocorrelates in this figure is approximately the same as for the case of three-month averaging [5, 7], to wit: the field of isocorrelates is represented by alternating positive and negative correlation regions extending along the main diagonal of the matrix. It is easy to discriminate a region of negative correlation between the characteristics of summer cloud cover and winter temperature.

Such cross-correlation matrices were computed for each of 31 stations uniformly distributed over the European USSR. An analysis of these matrices made it possible to discriminate the most informative indicators for formulating a statistical scheme for predicting air temperature anomalies for the European USSR on the basis of cloud data registered over the North Atlantic. These predictors are listed in the table. One of the important peculiarities of this table is that in the prediction of the temperature anomaly for the cold half of the year the number of predictors invariably includes the cloud cover anomaly for the warm half-year. A prognostic regression equation was written on the basis of this table. The regression coefficients were determined using data from a teaching sample for 10-12 years by the least squares method. Then, using data from an examination sample we computed a series of forecasts of two-month air temperature anomalies for the European USSR. These predictions are usually poorly successful with respect to sign, especially in those cases when there is a predominance of zonal circulation in the lower half of the troposphere.

At the present time the prediction method is in the stage of operational tests. The preliminary results of these tests are encouraging.

Thus, like the earlier published studies [5, 7], the results presented in this article convincingly demonstrate that there is a quite close negative asynchronous correlation between summer cloud cover anomalies over the North Atlantic and deviations of winter air temperature from the norm in

the European USSR. And this means that the heat absorbed and accumulated in the active layer of the ocean during the warm half of the year is retained for a very long time in its depths and is released to the atmosphere during the winter months.

Predictor Months Using Cloud Cover Anomaly for Temperature Anomalies

Prediction months	Predictor months
January-February	April-May
February-March	August-September
March-April	September-October
April-May	September-October
May-June	February-March
June-July	February-March
July-August	January-February
August-September	June-July
September-October	April-May
October-November	June-July
November-December	May-June
December-January	July-August

Dynamic-Statistical Approach to the Problem of Parameterization of the Oceanic Thermal Memory

On the basis of the results obtained in the preceding sections we will attempt to formulate some phenomenological approach to the problem of dynamic-statistical parameterization of the process of the thermal effect of the ocean on the atmosphere [5].

Bearing in mind the above-mentioned conclusions as a first approximation, we will assume that the quantity of heat $Q_r(\theta, \lambda, t)$ accumulated in the active layer of the ocean during some summer month is proportional to the function

$$N_r(\theta, \lambda, t) = 1 - 0{,}1\ S_r(\theta, \lambda, t),$$

where r is the numbering of the months during the warm half-year, $S_r(\theta, \lambda, t)$ is the corresponding total quantity of clouds. It then can be written that

$$Q_r(\theta, \lambda, t) = \chi_r(\theta, \lambda, t)\ N_r(\theta, \lambda, t), \tag{11}$$

where χ_r are some still unknown functions to be determined and which are assumed to be quasiuniversal.

It is obvious that

$$Q_r = \begin{cases} \chi_r, & \text{when } S_r = 0/10 \\ 0, & \text{when } S_r = 10/10 \end{cases}$$

It evidently can be postulated that the quantity of heat Q^q released by the ocean into the atmosphere in the q-th winter month consists of the quantity of heat accumulated in the active layer of the hydrosphere during each of all the summer months. The contribution of each month of the warm half-year must enter with its weight. Now we will assume that as a teaching sample we have an archives containing observational data for years. For each pair of successive warm and cold halves of the year belonging to this sample we have, on the basis of (11)

$$Q^q = \sum_r \chi_r^q N_r. \tag{12}$$

Accordingly, the heat influx equation for predicting air temperature (with stipulated initial and boundary conditions and known horizontal velocity components) of the q-th winter month, with (12) taken into account, can be written in the form

$$\frac{\partial T}{\partial t} + \frac{v_\theta}{a}\frac{\partial T}{\partial \theta} + \frac{v_\lambda}{a\sin\theta}\frac{\partial T}{\partial \lambda} - \frac{k}{a^2}\Delta T = \sum_r \chi_r^q N_r. \tag{13}$$

For convenience in exposition, we will call the functions $\chi_r^q(\theta, \lambda)$ the asynchronous influence functions.

Our objective is a determination of elements of the matrix $\|\chi_r^q(\theta, \lambda)\|$ functions for each pair of numbers $r \subset \eta$ and $q \subset \eta$ possible for real atmospheric-oceanic conditions.

Equation (13) describes the change in air temperature caused by the thermal effect of the ocean on the atmosphere, advection and horizontal macroturbulent exchange. A distinguishing characteristic of this equation is that its right-hand side was written in a form with a "lagging" argument and its computation requires the availability of data on cloud cover only for the times which have elapsed (that is, cloud cover need not be predicted).

Since our objective is a determination of the asynchronous influence function χ_r^q, therefore, assuming that in equation (13) the functions T, v_θ, v_λ and N_r are known, and χ_r^q are to be found, we denote its right-hand side by $F^q(\theta, \lambda)$ and rewrite it in the following form:

$$\sum_r N_r \chi_r^q = F^q.$$

Hence the asynchronous influence functions χ_r^q can be determined by different methods. However, it seems that in this case the spectral method is the most natural. In this case the problem essentially involves solution of a system of linear algebraic equations for the expansion coefficients of the sought-for functions [5].

The degree of practical applicability of the asynchronous influence functions determined in this way can be judged only after carrying out extensive diagnostic and prognostic experiments during which there should also be a study of the nature of the temporal variability of these functions.

Using the proposed method for parameterization of the oceanic thermal memory it is evidently impossible to study atmospheric-oceanic processes with any detail. However, we hope that on the basis of such parameterization it will be possible, in a rough approximation, to describe the principal large-scale processes of the thermal effect of the ocean on the atmosphere during the cold half of the year.

BIBLIOGRAPHY

1. Blinova, Ye. N., "Hydrodynamic Prediction of Mean Monthly Temperature Anomalies for the Earth's Northern Hemisphere Using IGY Data," DOKLADY AN SSSR (Reports of the USSR Academy of Sciences), Vol 131, No 2, 1960.

2. Zadorozhnaya, T. N., "Evaluations of the Correlations Between Cloud Anomaly Fields Over the Ocean and Temperature Anomalies Over the Continent With a Two-Month Averaging Interval," TRUDY GIDROMETTSENTRA SSSR (Transactions of the USSR Hydrometeorological Center), No 192, 1977.

3. Marchuk, G. I., Musayelyan, Sh. A., "Methods for Computing Variations of the Total Flux of Radiant Energy for the Purposes of Long-Range Prediction of Large-Scale Meteorological Fields," METEOROLOGIYA I GIDROLOGIYA (Meteorology and Hydrology), No 8, 1974.

4. Monin, A. S., "Physical Mechanism of Weather Changes," METEOROLOGIYA I GIDROLOGIYA, No 8, 1963.

5. Musayelyan, Sh. A., O PRIRODE NEKOTORYKH SVERKHDLITEL'NYKH ATMOSFERNYKH PROTSESSOV (Nature of Some Super-Prolonged Atmospheric Processes), Leningrad, Gidrometeoizdat, 1978.

6. Lorenz, E. N., "The Predictability of Hydrodynamic Flow," TRANS. NEW YORK ACAD. SCI., Ser. 2, Vol 25, 1963.

7. Mussaelyan, Sh. A., "The Use of Cloud Cover Satellite Information for Quantitative Long-Term Forecasting," PROCEEDINGS OF THE SYMPOSIUM ON METEOROLOGICAL OBSERVATIONS FROM SPACE, Philadelphia, Pennsylvania, USA, 8-10 June 1976 (19th COSPAR).

UDC 551.(58+576.2)(100)

ZONAL DISTRIBUTION OF CLOUD COVER OVER THE EARTH

Moscow METEOROLOGIYA I GIDROLOGIYA in Russian No 3, Mar 80 pp 15-23

[Article by Doctor of Geographical Sciences T. G. Berlyand, Candidate of Geographical Sciences L. A. Strokina and L. Ye. Greshnikova, Main Geophysical Observatory, submitted for publication 11 September 1979]

Abstract: A study was made of the latitudinal distribution of the quantity of clouds on the basis of new global monthly maps of cloud cover compiled on the basis of data from the world network of meteorological stations. It is shown that in both hemispheres the mean quantity of clouds over the oceans is greater than over the land (by approximately one-tenth). The monthly quantity of clouds for the earth as a whole is virtually constant, regardless of season of the year. The results are compared with similar data from earlier studies made for climatological generalization of cloud cover distribution.

[Text] Status of problem and data used. The study of characteristics of the global cloud cover regime is now attracting considerable attention in connection with work on estimating the earth's energy balance, modeling of climate and its changes and also solution of many other timely problems of a scientific and practical nature.

One of the first climatological generalizations of cloud cover data was made by Brooks, who in 1927, on the basis of a relatively limited volume of observational data obtained the zonal distribution of the quantity of clouds over the oceans, land and the earth's surface as a whole [9]. After this study the zonal characteristics of cloud cover were virtually not investigated for a long time. Only after three decades did K. Telegadas and J. London [10] compute the zonal values of the quantity of clouds over the northern hemisphere for two months (April, October) and two seasons (winter, summer). In characterizing cloud cover over the oceans they employed data from the atlas of climatic maps of the oceans

prepared by McDonald [12]. The results of these studies have found use in a number of climatological investigations, in particular, devoted to the modeling of climate.

During the last 10-15 years the volume of cloud cover information has increased considerably as a result of the increasing series of observations, the implementation of international geophysical programs, determining the expansion of the ground network of stations in poorly studied regions, and also the launching of meteorological earth satellites. This facilitated the further study of the patterns of spatial-temporal distribution of cloud cover.

Using data from two years of observations from a satellite (1965-1966), J. Sadler [14] obtained the zonal distribution of the quantity of clouds for the tropical zone (30°N-30°S).

H. van Loon [18] used both ground and satellite information on cloud cover. On the basis of a generalization of [9, 14 and others] he investigated the characteristics of the latitudinal distribution of the quantity of clouds in the southern hemisphere for January and July.

In the fundamental publication ATLAS OF THE OCEANS [2], recently published in the USSR, there is a series of monthly cloud cover maps of the Pacific, Atlantic and Indian Oceans. They were compiled using data from regular and expeditionary observations on ships over a long period of time (from the end of the last century through 1965-1970).

Z. M. Makhover and L. A. Nudel'man [1] prepared an atlas containing a considerable number of different climatic characteristics of cloud cover for the southern hemisphere. In the course of preparation of the atlas maps they generalized for all months of the year an extensive volume of daily data from ground observations for a five-year period (1967-1972).

Data on the distribution of the quantity of clouds over the earth's surface, except for the equatorial zone (13°N-5°S), are cited in studies by C. Shutz and W. Gates [15, 16]. They were prepared for the purpose of obtaining initial material for investigations for the modeling of climate. As the characteristics of the cloud cover regime in the northern hemisphere the authors used the results of surface and satellite observations. The latter were made only at two times (midday and midnight). For the southern hemisphere the data were taken from the mentioned study by van Loon [18]. They also drew upon the results of generalization of a four-year series of observations (1967-1970) from a satellite, taken from the atlas published by D. Miller [13], relating only to the interval 1400-1600 hours local solar time and characterized the cloud cover conditions for a limited part of the day.

The use of inadequately uniform observational data on cloud cover from the point of view of methods for collecting information concerning it, the observations made once or twice during the day and the relatively short (not

always corresponding to climatological requirements) observation periods -- all this could not but exert an influence on the accuracy of the values and completeness of the characteristics in the above-mentioned studies.

World monthly maps of the distribution of the total quantity of clouds based on more uniform material, covering a long period of observations, were compiled by T. G. Berlyand and L. A. Strokina. Some of these maps were published in 1975 [3]. The initial data used in their compilation was the information included in numerous handbooks, monographs, atlases, monthly summaries and yearbooks published by the meteorological services of different countries. The results of modern investigations of the cloud cover regime in individual regions of the earth were also taken into account [4, 5, 7, 8, 17, 19] in this investigation. In the course of analysis of the various initial data, in addition to surface data, use was made of data from satellite observations of cloud cover [6, 13, 14]. In compiling monthly maps of the quantity of clouds on the continents the authors of [3] used data for about 3,500 points, of which 950 were for Europe, 1,150 for Asia, 450 for Africa, 300 for North America, 460 for Central and South America, 140 for Australia and Oceania and 30 for Antarctica (we note that in the mentioned study by Brooks data for a total of 1,000 stations were used for compiling such maps [9]). At most stations the observation periods exceeded 30 years, whereas for stations situated in the low latitudes -- from 15 to 20 years. The distribution of cloud cover over the oceans was determined for the most part using data from the MARINE CLIMATIC ATLAS [17], which contains data on the probability of the total quantity of clouds for individual regions characterizing the principal climatic regions of the oceans. For the area of the Atlantic Ocean the initial values were given for 93 regions, for the Pacific Ocean -- for 111 regions, for the Indian Ocean -- for 48 regions.

This article is devoted to a further development of [3]. In that paper, on the basis of data taken from new world monthly maps, the authors computed the zonal values of the quantity of clouds for the continents, oceans and the earth's surface as a whole.

Computation of Zonal Characteristics of Cloud Cover

The mean latitudinal cloud quantities were determined by averaging the values for 35 circles of latitude $\varphi_i = \pm 0, 5, 10, 15, \ldots, 85°$ with a longitude interval 5°. A total of more than 30,000 values were taken from all the monthly maps; these characterize the quantity of clouds at the intersections in a regular 5° grid.

The mean value for a 10° i-th latitude zone, taking the oceans and continents separately into account, was determined using the formula

$$\overline{n_i} = \frac{0{,}5 \cos \varphi_{i-5} \sum_{j}^{N_{i-5}} n_{(i-5)j} + \cos \varphi_i \sum_{j}^{N_i} n_{ij} + 0{,}5 \cos \varphi_{i+5} \sum_{j}^{N_{i+5}} n_{(i+5)j}}{0{,}5 N_{i-5} \cos \varphi_{i-5} + N_i \cos \varphi_i + 0{,}5 N_{i+5} \cos \varphi_{i+5}},$$

where n_{ij} is the quantity of clouds at the j-th point of intersection of a regular grid at the circle of latitude φ_i; N_i is the number of points of grid intersection at the circle φ_i, the subscript $i = \pm 0, 5, 10, \ldots, 85$.

The zonal value of the quantity of clouds over the earth's surface was computed as the mean weighted value of the corresponding data for the oceans and continents, taking into account the areas of the latter. The results are given in tables accompanying the paper. The data in the table make it possible, more completely than up to this time, to ascertain the peculiarities of the latitudinal and annual variation of the quantity of clouds over the earth's surface.

Tables 1 and 2 give the annual variation of the zonal values of cloud cover in tenths over the land, oceans and for the earth as a whole respectively. Table 3 contains data on the mean monthly quantity of clouds for individual continents and individual oceans.

Analytical Results

Table 1 indicates that during the course of the year both for the land and for the oceans in both hemispheres an identical latitudinal variation in the quantity of clouds with maxima in the temperate and equatorial latitudes and minima in the tropics is characteristic. The difference between the extremal values sometimes exceeds 3/10. The position of the maximum and minimum values does not remain constant during the course of the year. In each hemisphere during the warm half-year they shift in direction toward the higher latitudes; during the cold season the shift is toward the low latitudes. This shift is quite great, being 10-15° in latitude. The greatest withdrawal of the maxima of the quantity of clouds in the direction from the equator to the north is observed in the period from May through September; in the opposite direction -- from November through March. Twice a year (April, October) the extrema are situated in both hemispheres almost symmetrically relative to the equator.

The results of this analysis of the mean monthly cloud quantities for each of the 10° zones for the most part show that during the course of the year there is one maximum and one minimum. A maximum in the warm season and a minimum in the cold season is the most commonly observed type of annual variation. It is characteristic of latitude zones situated above 50° in both hemispheres; with advance toward the poles there is an increase in the annual amplitude. The amplitude attains its maximum values (4/10) over the north pole; this amplitude is twice as great as over the south pole.

The noted type of annual variation is also characteristic of the equatorial zone (20°N-20°S), where the annual amplitude is about 3/10 over the land and 1/10 over the oceans.

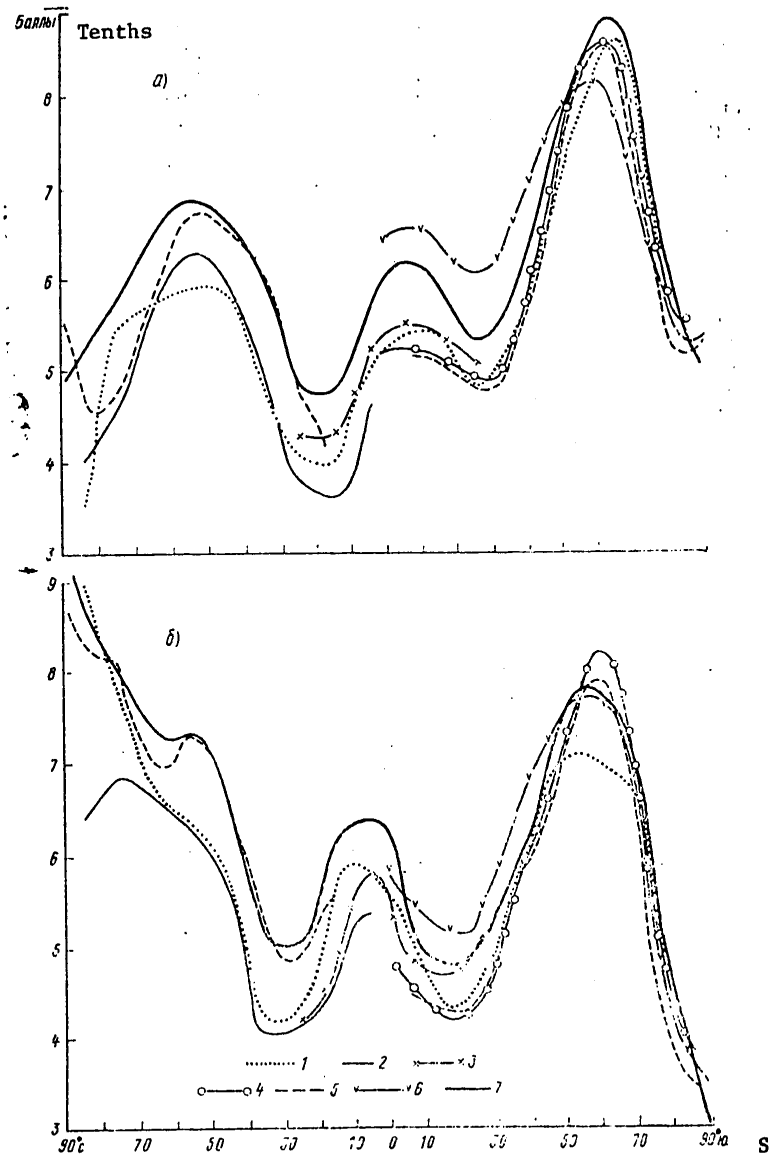

Fig. 1. Zonal distribution of cloud quantities according to data from different authors. a) January; b) July; 1) C. Brooks; 2) J. London; 3) J. Sadler; 4) H. ve[illegible] Loon; 5) C. Shutz and W. Gates; 6) Z. M. Makhover and L. A. Nudel'man; 7) T. G. Berlyand, L. A. Strokina and L. Ye. Greshnikova

Table 1

Annual Variation of Cloud Quantities

Широта 1	I	II	III	IV	V	VI	VII	VIII	IX	X	XI	XII	Год 9
7 Над сушей													
80—70° с 2	5,6	5,6	5,1	5,7	7,0	7,2	7,3	7,2	7,7	7,4	6,3	5,3	6,5
70—60	6,3	6,1	5,9	6,2	7,1	7,1	7,1	7,3	7,8	7,8	6,9	6,5	6,8
60—50	6,3	6,1	6,1	6,5	6,7	6,7	6,6	6,6	6,8	7,1	7,0	6,7	6,6
50—40	5,7	5,8	5,9	6,1	5,9	5,5	5,0	4,7	4,7	5,1	5,8	6,1	5,5
40—30	5,1	5,0	5,0	4,9	4,5	3,9	3,8	3,7	3,4	3,5	4,0	4,7	4,3
30—20	3,7	3,6	3,7	3,6	3,6	3,7	4,0	4,2	3,7	3,0	3,4	3,6	3,7
20—10	3,5	3,6	3,8	4,0	4,6	5,2	6,0	6,2	5,6	4,1	3,9	3,6	4,5
10—0	5,4	5,6	6,0	6,6	6,7	6,7	6,9	7,1	6,7	6,0	5,8	5,1	6,2
0—10° ю 3	7,2	7,3	7,3	6,8	6,4	5,6	5,0	5,4	6,0	6,2	6,8	7,0	6,4
10—20	6,4	6,3	6,0	5,4	4,0	3,3	3,1	3,0	4,2	5,2	5,7	5,3	4,8
20—30	4,5	4,5	4,3	3,8	3,5	3,3	3,0	2,7	3,2	3,9	4,1	4,2	3,8
30—40	3,9	3,4	3,7	3,8	4,7	4,8	4,7	3,9	3,9	4,2	3,8	3,8	4,1
40—50	4,9	5,3	4,9	5,4	6,6	6,1	5,8	5,8	5,9	5,3	5,9	5,8	5,6
50—60													
60—70	7,1	6,7	6,7	6,5	5,8	5,7	5,9	6,4	6,4	6,4	6,2	6,3	6,3
70—80	6,2	6,3	6,4	5,7	5,9	4,9	5,0	5,7	5,8	6,2	5,8	6,2	5,7
80—90	5,4	5,7	5,9	4,5	4,2	4,1	3,9	5,0	5,0	5,0	5,4	5,7	5,0
Северное полушарие 4	5,2	5,5	5,2	5,4	5,6	5,5	5,6	5,6	5,5	5,3	5,3	5,2	5,4
Южное полушарие 5	5,9	5,9	5,8	5,3	4,8	4,4	4,2	4,4	4,9	5,3	5,4	5,6	5,2
Суша в целом 6	5,4	5,4	5,4	5,4	5,3	5,2	5,1	5,2	5,3	5,3	5,4	5,3	5,3
8 Над океанами													
90—80° с	5,3	5,2	5,3	5,7	7,7	8,5	8,7	9,0	8,8	8,0	6,2	5,4	7,0
80—70	6,0	5,9	5,7	6,3	7,7	8,0	8,1	8,4	8,5	8,1	6,8	6,0	7,1
70—60	7,0	6,8	6,3	7,0	7,6	7,7	7,7	7,8	8,0	7,8	7,4	7,1	7,4
60—50	7,6	7,5	7,5	7,7	8,1	8,2	8,3	8,1	7,8	7,6	7,7	7,7	7,8
50—40	7,5	7,4	7,3	7,5	7,7	7,9	7,7	7,4	7,1	7,0	7,2	7,4	7,4
40—30	6,5	6,6	6,5	6,5	6,6	6,6	6,1	5,7	5,6	6,1	6,2	6,4	6,3
30—20	5,5	5,5	5,3	5,3	5,3	5,6	5,7	5,3	5,2	5,4	5,3	5,5	5,4
20—10	5,2	5,0	5,0	5,3	5,4	6,1	6,3	6,1	6,0	5,8	5,4	5,4	5,6
10—0	5,8	5,6	5,7	5,9	6,0	6,3	6,2	6,1	6,0	6,0	5,8	5,9	5,9
0—10° ю	5,9	5,7	5,6	5,6	5,3	5,2	5,3	5,3	5,6	5,6	5,7	5,8	5,5
10—20	5,7	5,5	5,6	5,3	5,1	5,0	5,3	5,4	5,5	5,7	5,8	5,7	5,5
20—30	5,6	5,5	5,7	5,6	5,5	5,4	5,6	5,6	5,8	6,0	5,9	5,7	5,7
30—40	6,0	6,0	6,1	6,1	6,2	6,2	6,1	6,0	6,4	6,5	6,2	6,1	6,1
40—50	7,0	7,1	7,0	7,1	7,2	7,1	7,0	6,9	7,1	7,2	7,1	7,1	7,1
50—60	8,4	8,2	8,1	8,1	7,9	7,8	7,8	7,7	7,6	8,0	8,4	8,3	8,0
60—70	9,0	8,6	8,3	8,1	7,8	7,5	7,7	7,7	7,6	8,2	8,4	8,4	8,1
70—80	8,4	7,9	7,7	7,6	6,6	6,5	6,5	6,7	6,8	7,6	7,4	7,4	7,2
Северное полушарие 4	6,0	6,0	5,9	6,1	6,3	6,6	6,6	6,4	6,2	6,3	6,1	6,1	6,2
Южное полушарие 5	6,6	6,4	6,4	6,4	6,2	6,1	6,2	6,2	6,3	6,5	6,6	6,5	6,4
Океаны в целом 6	6,4	6,3	6,2	6,3	6,3	6,4	6,4	6,3	6,3	6,5	6,4	6,4	6,3

KEY TO TABLE 1

1. Latitude
2. N
3. S
4. Northern hemisphere
5. Southern hemisphere
6. Land as a whole
7. Over land
8. Over oceans
9. Year

Table 2

Annual Variation of Zonal Cloud Quantities Over Earth's Surface

Широта 1	I	II	III	IV	V	VI	VII	VIII	IX	X	XI	XII	Год 2
90° с.	4,9	4,8	5,5	5,5	7,7	8,9	9,2	9,2	9,0	7,9	6,0	5,3	7,0
90—80 3	5,3	5,2	5,3	5,7	7,7	8,5	8,7	9,0	8,8	8,0	6,2	5,4	7,0
80—70	5,9	5,8	5,5	6,1	7,5	7,8	7,9	8,0	8,3	7,9	6,7	5,8	6,9
70—60	6,5	6,3	6,2	6,4	7,2	7,3	7,3	7,4	7,9	7,8	7,0	6,7	7,0
60—50	6,9	6,7	6,7	7,0	7,3	7,3	7,3	7,2	7,2	7,3	7,3	7,1	7,1
50—40	6,6	6,6	6,6	6,8	6,8	6,6	6,3	6,0	5,8	6,0	6,5	6,7	6,4
40—30	5,9	5,9	5,9	5,8	5,7	5,4	5,1	4,8	4,7	5,0	5,3	5,7	5,4
30—20	4,8	4,8	4,7	4,7	4,7	4,9	5,1	4,9	4,6	4,5	4,6	4,8	4,8
20—10	4,8	4,6	4,7	5,0	5,2	5,7	6,2	6,1	5,9	5,4	5,0	4,9	5,3
10—0	5,7	5,6	5,8	6,1	6,2	6,4	6,4	6,3	6,2	6,0	5,8	5,7	6,0
0—10° ю.	6,2	6,1	6,0	5,9	5,6	5,3	5,2	5,3	5,7	5,7	6,0	6,1	5,8
10—20	5,9	5,7	5,7	5,3	4,9	4,6	4,8	5,0	5,2	5,6	5,8	5,6	5,3
20—30 4	5,3	5,3	5,4	5,2	5,0	4,9	5,0	4,9	5,2	5,5	5,5	6,4	5,2
30—40	5,8	5,7	5,8	5,8	6,0	6,0	5,9	5,8	6,1	6,2	5,9	5,8	5,9
40—50	6,9	7,0	6,9	7,0	7,2	7,1	7,0	6,9	7,1	7,1	7,1	7,1	7,0
50—60	8,4	8,2	8,1	8,1	7,9	7,8	7,8	7,7	7,6	8,0	8,4	8,3	8,0
60—70	8,8	8,4	8,1	7,9	7,6	7,3	7,5	7,6	7,5	8,0	8,2	8,2	7,9
70—80	6,8	6,8	6,8	6,3	5,5	5,4	5,4	6,0	6,1	6,6	6,3	6,6	6,2
80—90	5,4	5,7	5,9	4,5	4,2	4,1	3,9	5,0	5,0	5,0	5,4	5,7	5,0
90° ю.	5,0	4,6	4,5	3,1	2,6	3,0	3,1	3,5	4,5	5,2	4,0	4,9	4,0
5 Северное полушарие	5,7	5,6	5,6	5,8	6,0	6,2	6,2	6,1	6,0	5,9	5,8	5,8	5,9
6 Южное полушарие	6,5	6,1	6,3	6,2	6,0	5,8	5,9	5,9	6,1	6,3	6,4	6,4	6,2
7 Земля в целом	6,1	6,0	6,0	6,0	6,0	6,0	6,0	6,0	6,0	6,1	6,1	6,1	6,0

KEY:

1. Latitude
2. Year
3. N
4. S
5. Northern hemisphere
6. Southern hemisphere
7. Earth as a whole

The remaining latitude zones are characterized by a different type of annual variation. A winter maximum or an autumn minimum is characteristic of this type. In this case the annual amplitude for the land and oceans is 1-1 1/2 and 1/2-1 tenth respectively.

The cloud quantities averaged by hemispheres for both continental and oceanic conditions reflect the patterns of the first of the mentioned types of annual variation. The annual amplitude for the land and ocean in the

northern hemisphere varies about 1/2 tenth, whereas the amplitude for the land in the southern hemisphere is three times greater. The latter circumstance is attributable to the peculiarities of distribution of the land in this hemisphere and the corresponding effect of equatorial monsoons with well-expressed intra-annual cloud cover variations.

Table 3

Mean Monthly Cloud Quantities for Continents and Oceans

	I	II	III	IV	V	VI	VII	VIII	IX	X	XI	XII	Год
Континенты													
Африка	4,4	4,4	4,4	4,4	4,1	3,9	4,2	4,5	4,6	4,5	4,5	4,2	4,3
Азия	4,9	5,0	5,2	5,7	5,7	5,7	5,7	5,6	5,4	4,9	4,9	5,0	5,3
Южная Америка	6,4	6,4	6,5	6,2	6,0	6,4	5,0	5,2	5,5	5,9	6,2	5,9	5,9
Северная Америка	5,8	5,7	5,5	5,5	6,1	6,1	6,0	6,0	6,1	6,1	5,2	6,0	5,9
Австралия	4,7	5,0	4,7	4,3	4,3	4,3	3,9	3,5	3,5	4,1	4,3	4,8	4,3
Европа	7,2	7,0	6,7	6,4	6,3	5,9	5,5	5,6	6,0	6,9	7,7	7,6	6,6
Антарктида	6,1	6,2	6,3	5,5	4,9	4,8	4,7	5,5	5,8	5,8	5,7	6,0	5,6
Океаны													
Ледовитый	5,9	5,7	5,7	6,2	7,6	7,9	8,0	8,4	8,4	8,0	6,7	6,0	7,0
Атлантический	6,2	6,0	5,9	6,0	6,0	6,0	6,0	5,9	6,0	6,3	6,4	6,2	6,1
Тихий	6,5	6,4	6,4	6,5	6,4	6,6	6,6	6,5	6,5	6,5	6,4	6,5	6,5
Индийский	6,3	6,2	6,2	6,0	6,1	6,1	6,2	6,2	6,0	6,2	6,3	6,3	6,2

KEY:

1. Year
2. Continents
3. Africa
4. Asia
5. South America
6. North America
7. Australia
8. Europe
9. Antarctica
10. Oceans
11. Arctic
12. Atlantic
13. Pacific
14. Indian

In a comparison of the mean annual cloud quantities relating to both hemispheres one can see some predominance of cloud cover over the land in the northern hemisphere in comparison with the southern hemisphere.

The relationship of the considered value over the ocean has a different character. It is somewhat greater in the southern hemisphere.

It is of interest to ascertain the zonal distribution of cloud cover over the oceans on the basis of the independent material given in [2]. For this purpose use was made of the method described above for the averaging of the quantity of clouds by 10° latitude zones and for the hemispheres

as a whole. The results confirmed the conclusions drawn above.

On the basis of the data in Table 2 it can be concluded that the quantity of clouds over the earth's surface in general in the course of the year remains virtually constant and is about 6/10. It should be noted that this value characterizes the cloud cover regime during daylight, since in the overwhelming number of countries observations are not made at nighttime. (In order to ensure the uniformity of all the initial material in this study we have not included data for nighttime for the few countries for which such data are available). Taking into account the tendency to a decrease in cloud cover at nighttime, it can be postulated that the various mean daily cloud cover quantities over the earth, with nighttime data taken into account, can be somewhat less than the value obtained and are in the range from 5/10 to 6/10.

According to Table 3, the annual variation is most clearly expressed over continents which are situated entirely in the northern or southern hemispheres. Over these continents, except for Europe, there is an appreciable increase in the quantity of clouds during the summer months in the corresponding hemispheres, whereas during winter periods, on the other hand, a decrease is observed. As was demonstrated above, such a type of annual variation of the quantity of clouds is characteristic for most latitude zones.

The singularity of the conditions for the formation of a cloud cover over Europe (increase in the quantity of clouds in the cold half-year in comparison with the warm half-year) is determined by the influence of cyclonic activity over the Atlantic Ocean. It is precisely this influence which explains the fact that among all the continents the greatest quantity of clouds is observed over Europe.

The annual variation of cloud cover for the African continent, situated in both hemispheres, is expressed considerably more weakly than over the remaining continents. Africa and Australia are the least cloudy continents.

Since the conditions for the formation of clouds are more uniform over the oceans than over the continents, the differences in the annual variation of the quantity of clouds over individual oceans, except for the Arctic basin, are small. Over the Arctic Ocean the quantities of clouds during the summer and autumn seasons are much greater than in winter and spring. As a result, as an average for the year it is the cloudiest region of the world ocean.

It is of interest to compare the collected data on the zonal distribution of the quantity of clouds with similar data published by other authors.

Figure 1 shows the zonal distribution of the quantity of clouds for the earth as a whole for January and July on the basis of data in this article, data from other investigations [1, 9, 14, 15, 16, 18], and also

the data in [10] for the northern hemisphere, winter and summer, since in [10] there is no information on the zonal distribution of the quantity of clouds for January and July. All the values have been reduced to a 10/10 scale.

An analysis of the curves shown in the figure shows that the distribution of the considered value, obtained by individual authors, in general is in agreement. However, there are discrepancies between the absolute values which can exceed 1/10. We note the lower (in comparison with the remaining values) quantities of clouds obtained on the basis of data from surface observations in the studies by Brooks and London [9, 10]. A rather close coincidence of the latitudinal variation curves is noted for the extratropical latitudes of the southern hemisphere. The virtual coincidence of the data published by C. Shutz and W. Gates with the data published by Van Loon is attributable to the fact that Gates and London used for the most part the results obtained by Van Loon as their initial data in characterizing the southern hemisphere.

The lower values obtained in [14-16, 18], in comparison with ours, are possibly associated with the difference in determining cloud cover on the basis of satellite and surface observations. The satellite data, used for the most part in [14-16], do not always make possible a sufficiently reliable estimate of the quantity of clouds over some types of underlying surface having a high reflectivity (ice, snow, desert), which leads to an understatement of the actual quantity of clouds. On the other hand, the surface observations, which we used for the most part, give some exaggeration of this value because the lateral surfaces of cloud elements also fall in the observer's field of view. The discrepancy in the data of a number of authors plotted in the figure is also attributable to their use of short and inadequately uniform observation series.

Summary

The results presented in this study make it possible to draw a number of conclusions concerning the characteristics of the cloud cover regime over the earth:

-- the zonal distribution of the quantity of clouds both over the land and over the oceans in both hemispheres is identical and is characterized by the presence of maxima situated in the temperate and equatorial latitudes, whereas the minima are situated in the tropical latitudes;

-- during the course of the year the maxima and minima are dispaced in each hemisphere by 10-15° in latitude in the direction of the higher latitudes in the warm half-year and toward the low latitudes during the cold half-year;

-- in the majority of the latitude zones there is a fundamental predominance of the quantity of clouds over the oceans in comparison with the land on the average by 1/10;

-- the most widespread type of annual variation of the quantity of clouds (zones 20°N - 20°S and above 50° in both hemispheres) is characterized by the onset of a maximum during the warm season of the year and a minimum in the cold half-year;
-- the quantity of clouds over the earth's surface as a whole virtually does not change during the course of the year.

The results obtained on the zonal distribution of the quantity of clouds in the annual cycle for the conditions of the continents, ocean and the surface of the earth as a whole, based on a generalization of a great volume of modern information on cloud cover, can find a broad range of application.

The authors express appreciation to L. S. Vysotskaya, who carried out a considerable volume of computations for preparing the tables.

BIBLIOGRAPHY

1. ATLAS KLIMATICHESKIKH KHARAKTERISTIK OBLACHNOSTI NAD YUZHNYM POLUSHARIYEM (Atlas of Climatic Characteristics of Cloud Cover Over the Southern Hemisphere), edited by Z. M. Makhover and L. A. Nudel'man, Moscow, Gidrometeoizdat, 1975.

2. ATLAS OKEANOV. T. 1. TIKHIY OKEAN, T. 2. ATLANTICHESKIY I INDIYSKIY OKEANY (Atlas of the Oceans. Vol. 1. Pacific Ocean. Vol. 2. Atlantic and Indian Oceans), VMF SSSR, 1974, 1977.

3. Berlyand, T. G., Strokina, L. A., "Cloud Cover Regime on the Earth," TRUDY GGO (Transactions of the Main Geophysical Observatory), No 338, 1975.

4. Zav'yalova, I. N., "Cloud Cover Regime Over Antarctica," TRUDY AANII (Transactions of the Arctic and Antarctic Scientific Research Institute), Vol 328, 1976.

5. METEOROLOGICHESKIY REZHIM ZARUBEZHNOY ARKTIKI (Meteorological Regime of the Foreign Arctic), edited by I. M. Dolgin, Leningrad, Gidrometeoizdat, 1971.

6. Morozova, I. V., "Cloud Cover Regime in the Tropical Part of the North Atlantic (in the GATE Region)," METEOROLOGIYA I GIDROLOGIYA (Meteorology and Hydrology), No 1, 1975.

7. Prik, Z. M., "Principal Results of Meteorological Study of the Arctic," PROBLEMY ARKTIKI I ANTARKTIKI (Problems of the Arctic and Antarctic), No 4, 1960.

8. Strokina, L. A., Beyeva, I. M., "On the Problem of the Distribution of Cloud Cover Over the Oceans," TRUDY GGO, No 307, 1974.

9. Brooks, C. E. P., "The Mean Cloudiness Over the Earth," MEM. ROY. METEOROL. SOC., Vol 1, No 10, 1927.

10. London, J., "A Study of the Atmospheric Heat Balance," FINAL REPORT, CONTRACT NAF 19 (122)-165. Dept of Meteorology and Oceanography, New York University, 1957.

11. Malberg, H., "Comparison of Mean Cloud Cover Obtained by Satellite Photographs and Ground-Based Observations Over Europe and the Atlantic," MON. WEATHER REV., Vol 101, No 12, 1973.

12. McDonald, W. E., ATLAS OF CLIMATIC CHARTS OF THE OCEANS, WB No 1247, U. S. Govt. Printing Office, Washington, 1938.

13. Miller, D. B., GLOBAL ATLAS OF RELATIVE CLOUD COVER 1967-70 BASED ON DATA FROM METEOROLOGICAL SATELLITES, Washington, 1971.

14. Sadler, J. C., AVERAGE CLOUDINESS IN THE TROPICS FROM SATELLITE OBSERVATIONS, Honolulu, East-West Center Press, 22 pages and 12 maps, 1969.

15. Shutz, C., Gates, W. L., SUPPLEMENTAL GLOBAL CLIMATIC DATA: JANUARY, The Rand Corporation R-915/2 ARPA Santa Monica, 1973.

16. Shutz, C., Gates, W. L., SUPPLEMENTAL GLOBAL CLIMATIC DATA: JULY, The Rand Corporation R-1029/1 ARPA Santa Monica, 1974.

17. U. S. NAVY MARINE CLIMATIC ATLAS OF THE WORLD, Vol I-VII, Washington, D. C., Chief of Naval Operations, 1955-1959, 1965.

18. Van Loon, H., "Cloudiness and Precipitation in the Southern Hemisphere," METEOROLOGY OF THE SOUTHERN HEMISPHERE, edited by C. W. Newton, Meteorological Monographs, Vol 13, No 35, 1972.

19. WMO TECHNICAL NOTE No 87. Polar Meteorology. WMO-No 211. TP. 111, Geneva, 1967.

UDC 543.4

DETERMINATIONS OF THE MASS CONCENTRATION OF AEROSOLS IN THE PLUMES OF INDUSTRIAL PLANTS USING A LIDAR

Moscow METEOROLOGIYA I GIDROLOGIYA in Russian No 3, Mar 80 pp 24-32

[Article by Candidates of Technical Sciences I. M. Nazarov and Sh. D. Fridman, Candidate of Physical and Mathematical Sciences V. I. Rozhdestvenskiy and V. F. Zhuravlev, Institute of Applied Geophysics, submitted for publication 26 July 1979]

Abstract: This paper gives the results of a lidar investigation of aerosols emanating from metallurgical combines. The authors propose a new method for processing data from lidar sounding. The aerosol microstructure is determined using a parametric model of the polydisperse scattering function, obtained by an analytical integration of a Fredholm equation of the first kind. The approximated Mie function, taking into account the real refractive index, is used as the kernel of this equation. There is a satisfactory agreement between the mass concentrations of aerosols in the plume determined using laser sounding and data from direct sampling of aerosols from an aircraft.

[Text] Introduction. One of the aspects of the problem of monitoring of contaminants and preservation of the environment is an investigation and evaluation of the mass concentration of aerosol emanating from the stacks of industrial plants. This problem can be solved by different methods: by sampling, by monitoring production processes, and by the remote method of lidar sounding of the plume [7].

This paper gives the results of an experiment for investigating the aerosols emitted by a large metallurgical combine. The experiment was made using remote laser sounding of the plume and also by direct sampling of aerosols from an aircraft. A method is proposed for processing data from laser sounding for determining the mass concentration and distribution of aerosols in

the plume, based on an analytical solution of a Fredholm equation of the first kind. A comparison of data on the mass concentration obtained using a lidar and by direct sampling is given. It is shown that for investigating such rapidly transpiring processes of propagation of contaminants as plumes lidar sounding makes it possible to determine the spatial-temporal variations of aerosols and thus merits broad application for the monitoring of contaminants due to its operational properties and mobility.

Concise Information on Measuring Instruments and Work Method. Determination of Volume Scattering Coefficient

Sounding was with a two-frequency lidar with an Al-Na garnet laser emitting wavelengths $\lambda = 1.06\mu m$ and $\lambda = 0.532\mu m$, with a receiving antenna designed using a Cassegrainian scheme with a diameter of the large dish 0.26 m. The pulse power at a wavelength $0.532\mu m$ was 0.2-1.0 MW; the radiation pulse duration was 7-20 nsec; beam divergence was 30'. The time required for shifting from one wavelength to another was 1-1.5 minute. The received signal was registered using an oscillograph with subsequent photographing of the pulse shape. At the same time, using the RDV instrument there was continuous measurement of the meteorological range of visibility, a knowledge of which made it possible to take into account the attenuation of the signal on the sounding path using the formula $V = 3.0/\beta(\lambda, z)$. The data masses were obtained as the means of a series of signals at one wavelength from one and the same sounding volume. Sounding at one wavelength at a distance up to 3 km with 150-m intervals requires 4-5 minutes. The switching to another wavelength is accomplished in one minute. A lidar mounted on a ZIL-157 truck was set up at a distance of 2 km from the mouth of the stack. The geometry of the experiment is shown in Fig. 1. The depth of penetration of the signal into the plume, depending on the density of the plume, varied from 30-40 m to 200-250 m. The transverse dimensions of the plume at a distance of 2 km from the mouth attained 300 m.

Table 1

Results of Microphysical Measurements of Samples

Element	r μm	σ
Zinc	0.32	5
Iron	0.60	1.8
Nickel	0.45	1.5
Copper	0.65	1.9

Simultaneously with laser sounding an aircraft was employed in sampling the aerosol in the plume. For this purpose the aircraft flew at different altitudes along horizontal paths across the plume (Fig. 1). The sampling was accomplished using three-layer filters with a linear velocity of the air flow 1.7-1.9 m/sec. After ending the sampling each layer of the filter was analyzed for its dust content and the atomic absorption method was employed for determining the content of zinc, iron, nickel and copper. The background

content of the mentioned ingredients was separately determined using an unexposed filter. Next, at the Scientific Research Physicochemistry Institute imeni L. Ya. Karpov specialists used the method developed by V. I. Skitovich to determine the fractional composition of the aerosol samples: median particle radius r and standard geometrical deviation σ on the assumption of a log-normal distribution. The collected data are given in Table 1. The volumetric dust concentration, according to aircraft sampling, was 100±30 $\mu g/m^3$.

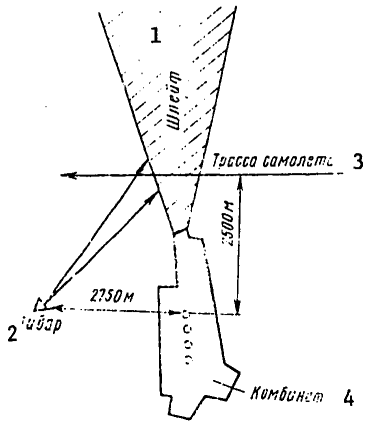

Fig. 1. Geometry of experiment.

KEY:
1. Plume
2. Lidar
3. Aircraft path
4. Combine

The characteristic appearance of the echo signal received from the plume at a distance of 800 m from the stack mouth is shown in Fig. 2. Calculation of the volumetric scattering coefficient profile with depth of penetration of the sounding pulse into the plume was accomplished using the symptotic signal method [5]. The echo signal oscillogram has a smooth character with one maximum. The volumetric scattering coefficient also increases smoothly from $6.2 \cdot 10^{-5}$ to $2.5 \cdot 10^{-2}$ m^{-1}. Figure 3 gives examples of the scattering coefficients for two wavelengths. It is easy to see from these figures that a high gradient of the scattering coefficient is observed in the first 25 m of penetration into the plume; the value of the scattering coefficient changes by 2-4 orders of magnitude. This is indicative of the exceptional variability of the microstructure of smoke plumes, that is, one must speak only of estimates of the aerosol parameters.

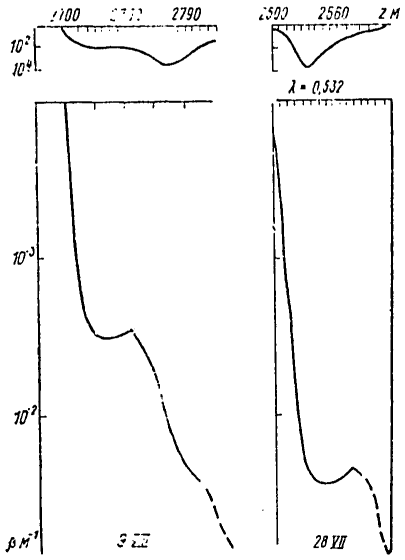

Fig. 2. Profile of echo signal from plume at distance of 800 m from mouth of stack. 1977.

For the power of the registered signal P(z), scattered by the aerosols in the plume, on the assumption of single scattering we can write

$$P(z) = P_0 z^{-2} A \sigma_\pi \exp\left\{-2\int_{z_1}^{z_2}\beta(z)\,dz\right\}, \qquad (1)$$

where P_0 is the initial pulse power, A is the receiver instrument function, z is the distance to the scattering volume, σ_π is the inverse scattering indicatrix, τ is the optical thickness

$$\tau = 2\int_{z_1}^{z_2}\beta(z)\,dz,$$

$\beta(z)$ is the volumetric scattering coefficient -- the sought-for parameter in the laser sounding of aerosols.

The solution of the laser sounding equation (1) by the asymptotic signal method makes it possible with an accuracy 10% to determine the $\beta(z)$ value under the condition of a constancy of the inverse scattering indicatrix along the entire sounding path $\beta_\pi(z)$ = const and in the presence of an echo signal from a great optical thickness, for example, $\tau = 2$. In this case the strength of the back-scattered signal received by the lidar receiving antenna, related to atmospheric parameters and expressed through the instrument functions at the photomultiplier output, has the form

$$P(z) = \frac{P_0 S \sigma_\pi \frac{c\tau_u}{2}}{z^2} \times$$

$$\times \exp\{-2\beta(z)\, z\}, \qquad (2)$$

[= pulse] where s is the effective antenna area, c is the speed of light, τ_{pulse} is pulse duration.

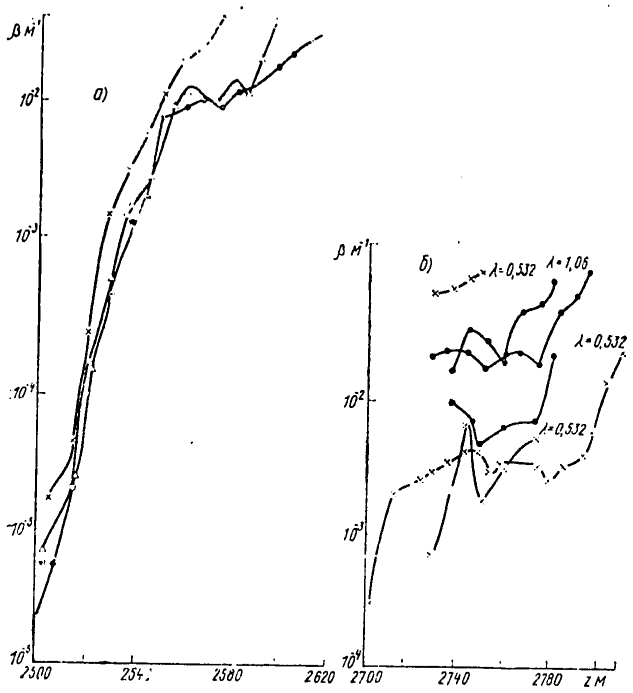

Fig. 3. Dependence of the volumetric scattering coefficient on depth of penetration. a) for a case monitored by an aircraft, b) for an unmonitored case.

It can be seen that this equation contains the two unknown parameters σ_π and $\beta(z)$. For an unambiguous determination of each of them we used additional information on the meteorological range of visibility, obtained using the RDV-2 instrument. The scattering coefficients carry information on the mass concentration, size, distribution and composition of aerosols present in the plume.

Method for Evaluating the Microstructure of Aerosols Using Data from Laser Sounding

The extraction of data on the microstructure of aerosols on the basis of their optical properties involves the solution of a certain incorrectly formulated problem in mathematical physics. Existing methods for solution of the inverse problem in atmospheric optics essentially involve solution of Fredholm equations of the first kind. They have not been brought into routine use; the literature contains only a few examples of processed experimental data [1, 3]. Therefore, in actual practice, instead of solution of this problem in each specific case it is common to use calibration by contact methods, carried out simultaneously with laser sounding [2]. However, these measures are time-consuming and can give considerable errors, especially when there is a noncoincidence of the site of sampling and the volume of laser sounding. Below we will give a method for solving the inverse problem, making it possible to carry out routine processing of the results of laser sounding. The proposed method for solving the integral equation is a mathematical modeling method.

The volume scattering coefficient is related to the microstructure of an aerosol by a Fredholm equation of the first kind

$$\beta(z, \lambda) = \int_{r_1}^{r_2} \pi r^2 K(r, \lambda, n) f(r)\, dr, \qquad (3)$$

where K(r, λ, n) is the kernel of an equation known from the Mie theory, f(r) is the particle-size distribution function, requiring determination in this problem, r is the radius of the aerosol on the assumption of spherical particles, n is the refractive index of particles, λ is radiation wavelength.

A parametric model of the polydisperse scattering coefficient was obtained by analytical integration of equation (3). As the kernel K(r, λ, n) we used the Mie approximation function [8]:

$$K(r, \lambda, n) = \begin{cases} K_{11}(\rho, n) = \frac{1}{3} K(\rho) \left(\frac{a\rho}{n-1}\right)^2 \left(1 + \frac{2}{5} \frac{n^2 - 1.5^6}{n^2} a\rho\right), \\ \qquad \rho < \rho_n \\ K_{12}(\rho, n) = \frac{n}{f(n)} K(\rho) + 2\left[1 - \frac{n}{f(n)}\right] + 2(\sqrt{n} - 1) e^{-\frac{n-1}{10 n^2}\rho}, \\ \qquad \rho > \rho_n, \end{cases} \qquad (4)$$

where K(ρ) is the Van de Hulst function.

$$K(\rho) = 2\left[1 - \frac{2\sin\rho}{\rho} + \frac{\sin^2\frac{\rho}{2}}{\left(\frac{\rho}{2}\right)^2}\right],$$

$\rho = \frac{4\pi(n-1)r}{\lambda}$ is a dimensionless parameter,

$$f(n) = \begin{cases} 1{,}05; & n < 1{,}5; \\ 1{,}00; & n > 1{,}5; \end{cases} \qquad a = \frac{n+1}{n^2+2}.$$

This function is correct for any real values of the refractive index of particles. The mean approximation error is 4% for a refractive index 1.5. Failure to take absorption into account in $K(\rho, n)$ gives errors of a few percent for polydisperse media. The particle size function was stipulated in the form of a three-parameter gamma function

$$f(r) = Br^{\mu} e^{-br} \quad (\mu > -1); \quad b = \frac{\mu+1}{\bar{r}}, \tag{5}$$

which with a broad change in the b and μ parameters describes well the diverse spectra of particles observed in the atmosphere. With (4) and (5) taken into account, the expression of the scattering function for the adopted model has the form [6]

$$\beta(\lambda) = \frac{4\pi N}{b^2}\left\{\frac{(\mu+1)(\mu+2)}{2} + y^2 - \frac{y^{\mu+3}}{(1+y^2)^{\frac{\mu+2}{2}}}\left[(\mu+1)\sin(\mu+2)\varphi + \right.\right. \tag{6}$$

$$\left.\left. + \sqrt{1+y^2}\cos(\mu+1)\varphi\right]\right\} + \frac{2\pi N}{b^2}(\mu+1)(\mu+2)\times$$

$$\times\left[1 - \frac{n}{f(n)} + \frac{\sqrt{n}-1}{c^{\mu+3}}\right],$$

$$y = \frac{b}{2\alpha}; \quad c = 1 - \frac{n-1}{8nb}\alpha; \quad \alpha = \frac{\rho}{\bar{r}}.$$

An analytical model of the volume scattering coefficient (6) can be used in determining the mass concentration and parameters of an aerosol in the interpretation of data from laser sounding. It makes it possible to reduce the problem of determining the microstructure of an aerosol to the optimization problem in parameter space by means of minimizing the functional

$$F(\mu, \bar{r}, N) = \sum_{i=1}^{k} [\beta_i(\lambda, z) - \beta_i^{\tau}(\lambda)]^2, \tag{7}$$

constituting the sum of the squares of nonclosures of the differences in the measured values of the scattering coefficients and the corresponding values in the model. In principle, for determining the four parameters of the distribution it is necessary to know the measured scattering coefficients at four wavelengths. However, taking into account that the

variations of the refractive index in the range from 1.3 to 1.7 lead to a change in the scattering coefficients $\beta(\lambda)$ by not more than 10-15% [10], with an accuracy in measuring $\beta(\lambda, z)$ of 20% the value of the refractive index can be selected taking into account the specific conditions of the investigated object, additional measurements of composition or taken as a mean. In other words, with a fixed value of the refractive index in determining the aerosol parameters it is possible to limit ourselves to three wavelengths. Having specific experimental data on $\beta(\lambda, z)$, using an electronic computer we obtain the numerical values of the selected $\beta(\lambda)$ model. The end result of the calculations is evaluations of the model parameters with a stipulated accuracy, determined by the sum of the squares of the difference in the values of the parameters in two successive iterations. With a fixed value of the refractive index n, the accuracy of the method gives an error in determining the parameters of 3-5% [10]. An assumption concerning the particle-size distribution function does not limit the possibilities of the model employed because using the variations of r and μ it is possible to obtain the most diverse particle distribution spectra. In order to obtain multimodal spectra it is necessary to have measurements at a great number of wavelengths.

Analysis of Inversion Results

Due to the fact that two wavelengths were used in our experiment in sounding the plume, our method makes it possible to determine two parameters of the model. In this case the most interesting parameters of the plume should be the mean particle size and the numerical concentration. Precisely these parameters were determined in this experiment. Two other parameters -- distribution width μ and the refractive index of particles $\hat{n}$ -- were selected from the accompanying samplings. The results of the samplings cited in Table 1, on the basis of the dispersion value, made it possible to assume that the investigated aerosols have a quite broad size spectrum and therefore the μ value should be selected equal to 0 or 2. The value of the real part of the refractive index for particles of zinc, iron and copper, according to the Ivlev model [4] and cited in the book by Van de Hulst, can vary in the range 1.40-1.47. As mentioned above, such changes in n cannot introduce significant errors into the determination of mass concentration.

In addition, for work with the optimum parameterization method using an electronic computer it is necessary to select two initial points containing the surmised sought-for parameters μ, n, the mean particle size r, numerical N or mass $M = N\delta\, 4/3\pi r^3$ concentration, where δ is aerosol density. In our experiment these data were also taken from microphysical measurements. We note that in principle we can select any reasonable values of the parameters as the initial points. Their choice influences only the convergence of the problem when seeking the minimum of the F function and the expenditure of computer time. In order to stipulate these points it is not at all mandatory to carry out simultaneous microphysical measurements, but with the availability of the latter the choice of initial points is simplified.

Thus, as a result of inversion of equation (3) by the optimum parameterization method we obtained evaluations of model parameters as indicated in Table 2.

Table 2

Evaluation of Aerosol Parameters by Optimum Parameterization Method

μ	n	$\bar{r}$ мкм μm	N см$^{-3}$	M мкг/м^3 μg/m^3	ΔM %
2,0	1,40	0,20	$5,0 \cdot 10^7$	3,2	90
0	1,47	0,50	$3,7 \cdot 10^7$	74	40
2,0	1,44	0,58	$5,7 \cdot 10^7$	98,5	50

Table 3

Values of Volume Scattering Coefficients and Aerosol Parameters for Pure Atmosphere

λ мкм 1	$\beta(\lambda, z)$ см$^{-1}$	Параметры распределения 2	N см$^{-3}$	V км
0,532	$4 \cdot 10^{-6}$	$\bar{r}$=0,22	790	10
0,694	$3 \cdot 10^{-6}$	μ=2,0		
1,064	$1,7 \cdot 10^{-6}$	n=1,33		
0,532	$2,1 \cdot 10^{-6}$	$\bar{r}$=0,20	530	20
0,694	$1,5 \cdot 10^{-6}$	μ=2,0		
1,064	$7 \cdot 10^{-7}$	n=1,33		

KEY:
1. μm
2. Distribution parameters

The magnitude of the error in determining the mass concentration ΔM (with a density δ = 2 g/cm^3) was determined from the minimum nonclosure ΔF, which characterizes the minimum deviation of our model $\beta^T(\lambda)$ from the set of experimental data.

The mean radius of the particles falls in the region 0.3-0.6 μm and varies in dependence on the spectral variation of the scattering coefficient [2]. The concentration was equal to $5 \cdot 10^7$ cm^{-3}. The mass concentration with a 50% error was 75 μg/m^3, which corresponds to data from the sampling. Table 2 shows that the parameters most sensitive to variations of experimental

data are N and the mean size of particles, and hence, to a high degree, also the mass concentration. Such high errors in determining M are attributable to this circumstance. For example, the inversion of the volume scattering coefficients (Fig. 3) for a case when there were accompanying aircraft samplings with stipulated values $\mu = 0$, $n = 1.47$ made it possible to obtain $r = 0.5\mu m$ and a value of the mass concentration $M = 74\mu g/m^3$. The minimum value of the mass concentration, corresponding to the background value $\beta(\lambda, z) = 5 \cdot 10^{-4}$ cm^{-1}, is $2.6 \cdot 10^{-2}$ $\mu g/m^3$, whereas the concentration N is $1.3 \cdot 10^4$ cm^{-3}. The maximum M value is 400 $\mu g/m^3/m^3$ and was observed with $\beta(z) = 9.0$ cm^{-1}. The computed value of the scattering coefficient in the model for the assumed particle distribution with N = 1 cm^{-3} is $\beta(\lambda) = 3.77 \cdot 10^{-8}$ $cm^{-1} \pm 1.5 \cdot 10^{-8}$ cm^{-1}. The accuracy in determining the mass concentration in this case is 40%.

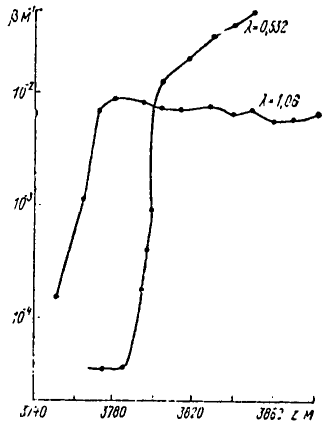

Fig. 4. Dependence of the volume scattering coefficient on depth of penetration.

Similar computations were made for other series of laser sounding of the plume; these are shown in Fig. 4. The mean values of the distribution and mass concentration parameters for these series are given in Table 2.

As an illustration of the method described above we will give an example of inversion of the results of three-frequency laser sounding of the free atmosphere at Leningrad carried out in 1978. In this experiment we used an Al-Na garnet laser ($\lambda = 1.06\mu m$ and $0.532\mu m$) and a ruby laser ($\lambda = 0.69\mu m$) with a common receiving antenna designed in a Cassegrainian system with a diameter of the large mirror 0.26 m. Table 3 gives data on the composition of aerosol obtained with values of the meteorological range of visibility 10 and 20 km.

The refraction coefficient for the pure atmosphere was assumed equal to 1.33. The use of three sounding wavelengths made it possible to evaluate three aerosol parameters. The n value was stipulated, taking the experimental conditions into account. The determined values of the concentration N are in agreement with data in the literature for the free atmosphere [10].

Conclusion

The results of this investigation of aerosol in smoke plumes using two-frequency laser sounding and the employed method for inversion of the volume scattering coefficients indicated that the mass concentration of particles obtained by this method agrees well with the results of sampling. This confirms the considerable possibilities of remote sensing and monitoring of smoke plumes using laser techniques. In the case of three-frequency sounding the mass concentration can be obtained in the absence of accompanying microphysical measurements. Two-frequency sounding also can be used without accompanying microphysical measurements if the element composition of the effluent is known.

With an increase in the number of sounding frequencies the method described here makes it possible to obtain multimodal aerosol distribution spectra.

Taking into account that enterprises of the same class give close spectra of aerosol particles in effluent, for solution of typical problems in monitoring effluent it is sufficient to obtain statistically representative characteristics of effluent for individual branches of industry. This will make it possible to organize remote routine monitoring of effluent by means of laser systems.

BIBLIOGRAPHY

1. Badayev, V. V., Georgiyevskiy, Yu. S., Pirogov, S. M., "Aerosol Attenuation in the Spectral Region 0.25-2.2μm," IZV. AN SSSR, FIZIKA ATMOSFERY I OKEANA (News of the USSR Academy of Sciences, Physics of the Atmosphere and Ocean), Vol II, No 5, 1975.

2. Zhitkov, L. V., Kaul', B. V., et al., "Use of a Lidar for Investigating the Dynamics of a Smoke Plume," TRUDY 5-go VSESOYUZNOGO SIMPOZIUMA PO LAZERNOMU I AKUSTICHESKOMU ZONDIROVANIYU ATMOSFERY (Transactions of the Fifth All-Union Symposium on Laser and Acoustic Sounding of the Atmosphere), Tomsk, 1978.

3. Zuyev, V. Ye., et al., "Optical Experiment and Results of Inversion of Data from Multifrequency Laser Sounding of the Microstructure of Aerosol in the Surface Layer," PROBLEMY DISTANTSIONNOGO ZONDIROVANIYA ATMOSFERY (Problems in Remote Sensing of the Atmosphere), Tomsk, SO AN SSSR, In-t Optiki Atmosfery, 1976.

4. Ivlev, L. S., Popova, S. I., "Complex Refractive Index of Matter of the Disperse Phase of Atmospheric Aerosol," IZV. AN SSSR, FIZIKA ATMOSFERY I OKEANA, Vol 9, No 10, 1973.

5. Kovalev, V. A., "One Method for Processing a Laser Signal," TRUDY GGO (Transactions of the Main Geophysical Observatory), No 312, 1973.

6. Martynova, V. I., "Polydisperse Scattering Coefficient for the Mie Approximation Function," TRUDY IPG (Transactions of the Institute of Applied Geophysics), No 17, 1973.

7. Nazarov, I. M., Nikolayev, A. N., Fridman, Sh. D., DISTANTSIONNYYE I EKSPRESSIVNYYE METODY OPREDELENIYA ZAGRYAZNENIYA OKRUZHAYUSHCHEY SREDY (Remote and Express Methods for Determining Environmental Contamination), Moscow, Gidrometeoizdat, 1977.

8. Pakhomov, P. V., Martynova, V. I., "Mie Approximation Function for the Factor of Effectiveness of Scattering," TRUDY IPG, No 17, 1973.

9. Rozhdestvenskaya, V. I., "Determination of the Concentration and Parameters of Aerosols from the Results of Twilight Measurements," TRUDY IPG, No 32, 1977.

10. Rozhdestvenskaya, V. I., RASEYANIYE SVETA NA POLIDISPERSNYKH SISTEMAKH AEROZOL'NYKH CHASTITS (Light Scattering on Polydisperse Systems of Aerosol Particles), Moscow, IPG, 1977.

UDC 551.509.616

CHANGE IN MICROSTRUCTURE OF STRATIFORM CLOUDS UNDER INFLUENCE OF CONDENSATION NUCLEI

Moscow METEOROLOGIYA I GIDROLOGIYA in Russian No 3, Mar 80 pp 33-38

[Article by K. B. Yudin, Institute of Experimental Meteorology, submitted for publication 19 July 1979]

Abstract: The article gives the results of field experiments for the modification of warm stratiform cloud cover by artificial hygroscopic condensation nuclei. The author gives some characteristics of a modified cloud medium and describes the nature of restructuring of the spectrum of cloud element sizes as a result of modification.

[Text] The problem of artificial modification of warm clouds and fogs is of great scientific and practical interest. One of the objectives of artificial modification is an improvement in visibility in clouds and fogs. Their total dissipation is not always necessary. It follows from the theory of light attenuation of dispersive media [10] that it is possible to improve visibility by a restructuring of the microstructure of a cloud or fog. After Yu. S. Sedunov [6] proposed a method for the modification of microstructure by the introduction of additional finely disperse condensation nuclei directly prior to the onset of cloud formation, a series of theoretical studies [1, 2, 5] was carried out in which a study was made of the effect of nuclei with different characteristics. The experimental studies carried out in an aerosol chamber [3, 8] indicated that the considered method affords a possibility for modification of the process of forming of the droplet spectrum. A merit of the method is a high degree of use of the reagent, attributable to the fact that in the process of formation of the microstructure the total mass, which can be extremely small, participates, and to a certain degree determines its large number of condensation nuclei.

The objective of this study was a field investigation of the regularities in changes in the microstructure of the cloud medium with introduction of a reagent. Artificial hygroscopic particles were introduced into the cloud near the condensation level. They must be entrained into a cloud by ascending flows, and competing with natural nuclei, change the course

Table 1

№ опыта 1	Синоптические условия 2	Вид облака 3	Высота нижней границы, м 4	Мощность, м 5	Температура нижней границы, °С 6	Стадия измерения 7	Время после воздействия, мин 8	$\overline{R}$ мкм 9	N см$^{-3}$	$\alpha \cdot 10^3$ м$^{-1}$
1	Фронт окклюзии 10	St	350	1050	+7	фон 17 след 18 след	5—6 12—14	2,9±0,6 2,7±0,6 2,8±0,9	335±60 375±80 355±65	28±9 30±12 28±9
2	Передняя часть теплого фронта 11	Sc	500	800	—3	фон след	6—7	3,3±0,4 3,2±0,4	280±40 320±45	40±4 44±6
3	Передняя часть циклона 12	дымка 16	650	—	+3	фон след след	4—5 9—11	1,3±0,4 1,2±0,4 1,3±0,4	90±30 190±80 120±50	1,3±0,6 1,7±1,1 1,3±0,7
4	Малоподвижный фронт 13	Sc	900	1450	—2,5	фон след	4—5	1,1±0,4 1,0±0,6	180±110 280±300	1,1±0,9 2,8±2,4
5	Передняя часть теплого фронта 14	St	800	1500	+1,5	фон след след	5—6 15—16	2,3±0,6 2,2±0,7 2,3±0,6	280±26 380±72 230±25	12±6 18±10 14±6
6	Ложбина перед фронтом окклюзии 15	St	500	600	+4	фон след	4—6	3,1±0,5 2,6±0,6	315±80 470±150	29±7 32±11

KEY:

1. No of experiment
2. Synoptic conditions
3. Type of cloud
4. Altitude of lower boundary, m
5. Thickness, m
6. Temperature of lower boundary, °C
7. Measurement stage
8. Time after modification, minutes
9. μm
10. Occluded front
11. Front part of warm front
12. Front part of cyclone
13. Very slowly moving front
14. Front part of warm front
15. Trough before occluded front
16. Haze
17. Background
18. Trace

---

of its development. Depending on the dispersivity and mass of the introduced reagent there can be both formation of large droplets capable of initiating coagulation and the creation of a stable fine-droplet system of the haze type [2]. In the modification process use was made of particles of aluminum chloride, in its hygroscopic properties extremely close to sodium chloride particles. In sublimation by pyrothechnic means there was formation of particles having a size distribution close to a log-normal distribution with a mean radius of 0.2μm and a dispersion of logarithms of the radii 1.0.

The level at which it is necessary to introduce the additional nuclei is situated near the lower cloud boundary. However, specifically in this layer there is an increased nonuniformity of all the cloud elements. Here it is common to encounter gaps, individual flocs or "locks" of clouds "hanging" down for tens of meters. Since an aircraft cannot precisely trace all the changes of the lower boundary, the introduced reagent entered both into zones where the droplets still have not formed and in the forming lower part of the cloud. Thus, the conditions for condensation growth of droplets on artificial particles in different parts of the modification zone are different. The modification effect is detected somewhat above the level of introduction of the reagent, but in the lower part of the cloud, where the nonuniformity remains significant.

The nonuniformity of the medium indicates an increased turbulence level in the lower part of the cloud, which, it was found, gives the main contribution to the entrainment and propagation of the reagent. The reagent was introduced from aboard the aircraft-laboratory during flight along a straight line. The conditions of its propagation were studied using radar corner reflectors [9]. In accordance with the measurement results,

Table 2

№ опыта 1	Стадия измерений 2	Обводненные ядра 3: A мкм$^{-1}$·см$^{-3}$	ν	n см$^{-3}$	Капли 4: $\bar{r}$ мкм 5	m см$^{-3}$	$\sigma/\bar{r}$	$\alpha \cdot 10^3$ м$^{-1}$
1	фон 6	60±18	4,3±0,8	180±80	3,1±0,3	160±35	0,35±0,10	28±9
	след 7	95±24	3,6±0,7	220±110	3,1±0,4	170±35	0,38±0,12	30±12
2	фон	15±5	6,4±0,5	120±60	5,5±0,5	160±20	0,37±0,10	40±4
	след	35±20	5,6±0,6	180±85	5,2±0,5	150±20	0,46±0,24	44±6
3	фон	40±10	2,3±0,7	75±40	4,0±0,4	25±5	0,33±0,08	1,3±0,6
	след	60±25	3,6±1,1	140±115	4,2±0,4	50±10	0,4 ±0,18	1,7±1,1
4	фон	80±20	3,3±0,4	170±60	2,1±0,2	30±5	0,48±0,20	1,8±0,9
	след	120±50	2,7±0,7	230±150	2,5±0,3	70±10	0,45±0,20	2,8±2,4
5	фон	35±7	4,2±0,3	120±30	2,5±0,3	180±10	0,43±0,17	12±6
	след	80±13	4,0±0,3	215±50	2,7±0,4	190±15	0,52±0,26	18±10
6	фон	40±8	5,5±0,8	200±75	4,6±0,3	120±30	0,38±0,12	29±7
	след	70±12	5,3±0,9	320±120	4,2±0,4	130±40	0,48±0,26	32±11
Увеличение параметра 8		1,7	—	1,5	—	1,1	—	1,2
Уровень значимости 9		85%	—	95%	—	60%	—	60%
Увеличение флуктуаций 10		2,0	—	1,8	—	—	1,6	1,5
Уровень значимости 9		80%	—	80%	—	—	80%	80%

KEY:

1. No. of experiment
2. Measurement stage
3. Water-enveloped nuclei
4. Droplets
5. μ m
6. Background
7. Track
8. Increase of parameter
9. Significance level
10. Increase of fluctuations

the modification zone can be represented as an elliptical cylinder with a horizontal axis of 7-8 km. The lengths of the axes of the ellipse, lying at the base of the cylinder, 5 minutes after modification were 600 and 200 m, and after 10 minutes -- 1,200 and 400 m. The mean concentration of reagent after 5 and 10 minutes was 20μ g/m^3 and 5μg/m^3 respectively. However, the reagent, diffusing in the cloud under the influence of dynamic turbulence, does not fill the entire volume uniformly and at individual points of its concentration can differ considerably from the mean values. For the monitoring and registry of changes in microstructure the aircraft repeatedly returned to the modification track at an altitude exceeding by 20-30 m the altitude at which the reagent is introduced. The flight trajectory, the moments of entry into the modification zone and emergence from it were registered by a ground radar. The time of presence of the aircraft in the modification zone was about two minutes.

The principal instruments for investigating microstructure and its changes were a photoelectric instrument for measuring the sizes and concentration of cloud droplets in the range from 0.5 to 40μm [4] and an instrument for measuring aerosol scattering in clouds. During presence in the modification zone 100-120 microstructure samples were taken for analysis. The number of droplets in the sample varied from 500 to 6,000, depending on their concentration in the cloud. The background data on the state of clouds were collected in regions adjacent to the modification zone during aircraft maneuvers for return to the modification track.

Table 1 gives data on the synoptic conditions under which the experiments were made and some integral characteristics of microstructure computed from the measured spectra. A preliminary analysis indicated that in the modification zone there is an increase in the concentration of hydrometeors and aerosol scattering. However, there is no direct proportionality between these changes, which indicates a restructuring of the spectra. In order to explain the nature of this restructuring each of the measured spectra was divided into two parts -- water-enveloped nuclei and droplets [7]. The part of the spectrum containing water-enveloped nuclei was described by a power-law distribution in the form

$$f(r) = A\left(\frac{r}{r_0}\right)^{-\nu},$$

where A is a normalizing factor numerically equal to the value of the above power function with $r = r_0 = 1\mu$ m. The A and ν parameters were computed by the least squares method. The parameters of the distribution function, describing the droplet part of the spectrum, were computed from the modal values of the radius and distribution function and the liquid water content value, computed from the measured spectrum. Table 2 gives the parameters of the distribution function (and not the parameters of the mean spectrum), averaged from individual spectra, and their variability in background measurements and in the modification zone 5-7 minutes after introduction of the reagent. The last four lines in the table generalize data on change in the parameters as a result of modification and on the significance levels for these changes, evaluated using the Bartlett and Fisher tests.

An analysis of the table indicates that as a result of introduction of the reagent there was an increase in the concentration n of water-encased nuclei, that is, most of the additional nuclei were encased in water, but could not form droplets. The droplet concentration m and the aerosol scattering coefficient α increase somewhat. The changes of the exponent in the inverse power-law distribution ν, the mean radius $\bar{r}$ of droplets and the relative dispersion of the droplet part of the spectrum $\sigma/\bar{r}$ are insignificant at the level of the natural inhomogeneity of clouds. A substantial increase in fluctuations of some parameters is also observed in the wake of the effect.

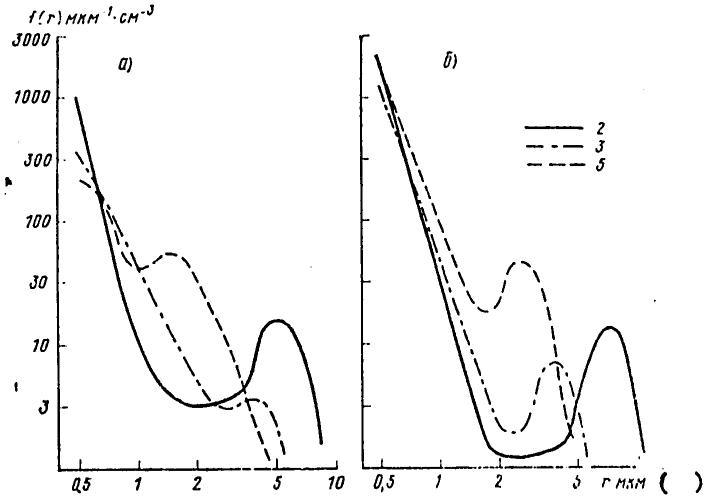

Fig. 1. Spectra of size of hydrometeors before modification and 5-7 minutes after cloud modification. a) background, b) wake of modification; 2) in stratocumulus cloud, 3) in haze under clouds, 5) in stratiform cloud

The additional information on restructuring of the spectra is shown in the figure. The numbers on the curves in this figure correspond to the numbers of the experiments. The figure shows that in the modification zone the value of the distribution function in the region 0.5-0.7 μm increases by a factor of 2-3, there is a deepening of the "dip" between the parts of the spectrum, and droplets which are larger than those observed in background measurements appear. However, droplets capable of causing coagulation ($r > 20\mu$ м) have not been registered.

Our work demonstrated that the introduction of additional artificial condensation nuclei somewhat modifies the microstructure of clouds. Under natural conditions the process is traced for 13-15 minutes after introduction of the reagent. At the end of this period the concentrations of

the diffusing reagent and modified droplets become so small that the modification effect is insignificant and all the measured parameters of the cloud medium approach the background levels. On the other hand, this circumstance indicates that repeated flights of an aircraft through the modification zone do not result in substantial changes in stratiform clouds and exert no influence on "purity" of the experiment. It is evidently possible to trace the further course of the process only with a marked increase in the seeding area. A significant effect from modification which could be used for practical purposes has not yet been established.

The author expresses appreciation to A. V. Lachikhin, V. P. Bedrenko and B. S. Yurchak, specialists at the Institute of Experimental Meteorology, for assistance in carrying out field experiments and measurements.

BIBLIOGRAPHY

1. Aleksandrov, E. L., Klepikova, N. V., "Influence of Artificial Condensation Nuclei on the Kinetics of Formation of Cloud Droplets," TRUDY IEM (Transactions of the Institute of Experimental Meteorology), No 8(46), 1974.

2. Aleksandrov, E. L., Klepikova, N. V., "Effect of Artificial Condensation Nuclei on Development of the Cloud Spectrum," TRUDY IEM, No 9(52), 1975.

3. Aleksandrov, E. L., Yasevich, N. P., "Results of Preliminary Experiments for Fog Modification in a Condensation Nuclei Chamber," TRUDY IEM, No 20, 1971.

4. Aleksandrov, E. L., Lachikhin, A. V., Posadskiy, V. I., Yudin, K. B., "Aircraft Photoelectric Instrument for Measuring Cloud Droplets," TRUDY IEM, No 19(72), 1978.

5. Klepikova, N. V., Sedunov, Yu. S., "Kinetics of the Droplet Spectrum in the Initial Stage of Condensation," TRUDY IEM, No 3(37), 1973.

6. Sedunov, Yu. S., "Numerical Experiment for Modifying the Kinetics of Formation of the Cloud Spectrum by the Introduction of Additional Condensation Nuclei," TRUDY IEM, No 6, 1969.

7. Sedunov, Yu. S., FIZIKA OBRAZOVANIYA ZHIDKOKAPEL'NOY FAZY V ATMOSFERE (Physics of Formation of the Liquid Droplet Phase in the Atmosphere), Leningrad, Gidrometeoizdat, 1972.

8. Smirnov, V. V., "Restructuring the Microstructure of Fogs Under the Influence of Hygroscopic Particles," TRUDY IEM, No 25(93), in press.

9. Skhirtladze, G. I., Yurchak, B. S., "Measurement of the Coefficient of Horizontal Diffusion in Cumulus Clouds by the Radar Method," IZV. AN SSSR, FIZIKA ATMOSFERY I OKEANA (News of the USSR Academy of Sciences, Physics of the Atmosphere and Ocean), Vol 15, No 2, 1979.

10. Shifrin, K. S., RASSEYANIYE SVETA V MUTNOY SREDE (Light Scattering in a Turbid Medium), Moscow, Gostekhizdat, 1951.

UDC 551.509.314

PROBABILISTIC APPROACH TO THE OBJECTIVE CLASSIFICATION PROBLEM

Moscow METEOROLOGIYA I GIDROLOGIYA in Russian No 3, Mar 80 pp 39-44

[Article by A. A. Burtsev, USSR Hydrometeorological Scientific Research Center, submitted for publication 13 July 1979]

Abstract: In the probabilistic approach to objective classification the meteorological fields are not characterized as belonging unambiguously to some class, but by degrees of reliability of belonging to all classes. It is demonstrated that the proposed probabilistic approach is more universal and has a number of advantages in comparison with the traditional deterministic approach. In order to ascertain the degrees of reliability of such a determination the author proposes the synthesis of a Golovkin algorithm with a potential functions method algorithm and its realization using actual data. The results indicate an objective character of the restored degrees of reliability.

[Text] Recently in meteorology ever-increasing attention is being devoted to the problem of objective classification of the fields of meteorological elements. The timeliness of this problem is attributable not only to theoretical and cognitive considerations, but also to the fact that the results in one form or another can be used in weather forecasting. Many authors, concerned with classification, indicate the difficulty [2], and some [7] even suggest the impossibility of creating a universal objective classification in meteorology. The author of [6] makes an attempt to create such a classification, but by virtue of the factors which will be considered below, this approach can be considered universal only to a limited degree. In this article we propose a new approach making it possible to come close to solution of this problem.

Among the objective classification algorithms special attention should be given to the B. A. Golovkin algorithm [5]. For the first time in meteorology it was applied in [4] and then with some modifications -- in [3].

This algorithm, constituting an approximate solution of the problem of linear programming with Boolean variables, makes it possible to discriminate in the set of objects X the centers of clustering of objects $x_i \in X$, and specifically, obtain a set of the most typical, or as they are usually called, "standard" objects. Then the entire ensemble of objects $x_i \in X$, $i = 1,\ldots,N$ (N is the number of objects) is broken down into classes by assigning each x_i to that class the distance to whose standard object is minimum. A merit of this algorithm is that it is completely free of any a priori assumptions concerning the spatial structure of the set of objects to be classified and in the best way possible evaluates the number of classes and unambiguously distributes all the objects by classes. In this algorithm there is no need to stipulate any threshold distances; the only input data are the matrix (measuring N x N) of distances between each pair of objects.

If the spatial structure of the set X is such that all x_i can be broken down into classes which are adequately compact and distant from one another, the Golovkin algorithm rather qualitatively solves the classification problem. The situation is far more complex in a case when the characteristic regions of the classes are situated close to one another and particularly when the characteristic regions intersect. In this case objects which are extremely close to one another, situated in a zone of intersection of the characteristic regions, can be assigned to different classes and in this case the probability of a classification error will be very high. And precisely such a peculiarity is characteristic for some large-scale fields of meteorological elements. For example, it was established in [3] that the fields of summer mean monthly anomalies of H-500 (registered in the latitude zone 75-40°N during the period 1948-1977) have the property of intersection of characteristic regions. This circumstance followed from the fact that after constructing a classification on the basis of the Golovkin algorithm the zero hypothesis of equality of intraclass means could not be refuted on the basis of the Fisher test with a 5% significance level. The classification became significant only after exclusion of a number of objects falling in the zone of intersection of the characteristic regions. But such an artificial procedure evidently cannot be considered justified because we obtain a number of objects unrelated to any one of the classes.

Returning to [6], it should be noted that the theory of a universal objective classification constructed there in the considered case is inapplicable since at its basis is the hypothesis of nonintersection of the characteristic regions of classes. Thus, the classification in [6] can be regarded as universal only in a limited class of fields of meteorological elements.

In this article the author does not attempt to dispute the position that in the atmosphere there are some stable states around which the entire ensemble of temporal realizations of atmospheric processes tends to be

grouped. However, the objectively established fact of the existence of some individual meteorological fields not similar to one of the standard fields of determined classes forces us to seek a more flexible approach to the objective classification problem than used now and before.

Now we will examine still another aspect of objective classification theory. In developing different meteorological classifications it is customary to limit ourselve to the construction of "standard" fields of classes, assuming in this case that these standards are an exhaustive characteristic for all fields combined with them into a single class. Now we will consider the problem of the informational properties of the standards, for clarity in description examining the case of two classes. We will denote these classes by A and B, and their standards by x_A^* and x_B^*. The quantity of information I(y) concerning some field $y \in X$ consists of two parameters, to wit: the quantity of information about y included in x_A^* and the quantity of information on y included in x_B^*.

$$I(y) = I(y/x_A^*) + I(y/x_B^*).$$

The I(y/x) parameter is determined in the following way:

$$I(y/x) = H(x) + H(y) - H(x, y),$$

where

$$H(x) = -\int_{-\infty}^{\infty} p(x) \log p(x)\, dx$$

is the statistical entropy of the x field and p(x) is probability density.

If y belongs to the region where $p(x^*_A, y)$ is close to $p(x^*_B, y)$, it is obvious that $I(y/x^*_A)/I(y/x^*_B)$ do not differ so much that one of them can be neglected. Should we formally assign y to that class for which the p(x, y) value is maximum, we lose a considerable part of the information, which is scarcely justifiable. Thus, in the considered case of intersections of the characteristic regions the informational properties of the standards do not enable us to solve the classification problem successfully if we employ traditional methods for breaking down the objects by classes.

Another problem which must be dealt with in solving classification problems is the availability of a teaching sequence of sufficient length. V. N. Glivenko has demonstrated the theorem of uniform convergence of the empirical distribution curve to the distribution function with an increase in the volume of the sample. It follows from this theorem that the length of the teaching sequence l_{ad} adequate so that after ending the teaching process it will be possible to recognize the newly appearing objects is proportional to the dimensionality of criterial space and inversely proportional to the probability of classification error. Applicable to our data, in particular, for the above-mentioned mean monthly ΔH_{500} fields, it was established in [3] that $l_{ad} \approx 6000$, which is an order of magnitude greater than the archives of field data at our disposal. In order to reduce l_{ad} it is

necessary to reduce considerably the dimensionality of criterial space. This can be achieved by the approach of expansion in natural orthogonal functions. However, since in order to obtain λ_{ad} in our data we were forced to limit ourselves to a very small number of the first expansion terms, some percentage of the variability (dispersion) of the fields remains not taken into account.

In addition to what has been stated above, this circumstance indicates that solution of the classification problem, which in essence is a compression of the useful information, in the considered case a transformation of this information into a loss.

It seems that this difficulty also cannot be overcome by any effective method if we remain within the framework of the traditional, that is, deterministic theory of breakdown by classes. Accordingly, we will proceed to formulation of a fundamentally new, probabilistic classification problem: we will characterize each field $x_i \in X$ not by an unambiguous assignment to the class A or B, but instead we will introduce the concept of the degree of reliability of belonging $D_A(x_i)$ and $D_B(x_i)$, that is, we will say that the x_i field belongs to the class A with the degree of reliability $D_A(x_i)$ and belongs to the class B with the degree of reliability $D_B(x_i)$. In the case of M classes each x_i will be characterized by the vector $\bar{D}(x_i) = \{D_{i1}, \ldots, D_{iM}\}$, $i = 1, \ldots, M$. Such an approach is far more universal than the deterministic approach, and in addition, with such a representation there is no information loss.

In actuality, if we find all the degrees of reliability, the determined vector $\bar{D}(x_i)$ will unambiguously characterize x_i, that is, rigorously fix its position in the space X, not leaving room for uncertainty. It is convenient to use a probabilistic characteristic as the degree of reliability. Thus, we will assume that in all X there are functions $D_A(x)$ and $D_B(x)$ which are the conditional probabilities that x belongs to class A or class B respectively. We note that such a probabilistic formulation of the problem is a special case of the deterministic approach, characterized by the fact that $D_A(x)$ and $D_B(x)$ only assume values equal to or close to 0 or 1 in objects of A and B, as occurs in the case of adequate compactness and a considerable distance between A and B.

Now our problem is, using the objects $x_i \in X$ appearing in the teaching process, to restore $D_A(x)$ and $D_B(x) = 1 - D_A(x)$. In order to approximate $D_A(x)$ we will use the adaptive algorithms approach, and specifically the potential functions method [1]. This method is attractive, first of all, because it is free of any a priori assumptions concerning the nature of the distribution of objects, that is, we need only assume that there is some non-zero probability of the appearance of objects $x_i \in X$; second, the method is attractive due to its simplicity and the economy of computer time; third, the potential functions method allows successful synthesis with a Golovkin algorithm. Applying the Golovkin algorithm, we will seek the optimum set of standard objects and then we will "fix" them as the most typical representatives of the classes, and after this, applying the potential functions

approach, we will ascertain the degree of reliability of whether each x_i belongs to these standard objects.

Thus, assuming that $D_A(x)$ is representable by a series in the form

$$D_A(x) = \sum_i c_i \varphi_i(x),$$

where $\varphi_i(x)$ is some complete system of functions, we will use the recurrent procedure

$$f_A^{n+1}(x) = f_A^n(x) + r_n K(x^{n+1}, x), \tag{1}$$

where $f_A^n(x)$ is the n-th approximation to $D_A(x)$, $K(x^{n+1}, x)$ is a potential function. In general form K has the following form:

$$K(x, y) = \sum_{i=1}^{\infty} \lambda_i^2 \varphi_i(x) \varphi_i(y), \tag{2}$$

where the following conditions are imposed on λ_i

$$\begin{cases} \sum_{i=1}^{\infty} \lambda_i^2 < \infty \\ \text{all } \lambda_i \neq 0. \end{cases} \tag{3}$$

In the teaching process, the following four situations can arise in the representation of any object x: AB, BA, AA and BB. The first letter in these notations is the designation of the class to which the object x must be assigned, taking into account which of the values $f_A^n(x)$ or $f_B^n(x)$ is maximum. The second letter is the designation of the class to which x must be assigned, being guided by the criterion of a minimum of the distance to the standard. The coefficients r_n are determined in the following way:

$$r_n = \begin{cases} \gamma_n, & \text{if BA,} \\ -\gamma_n, & \text{if AB,} \\ 0, & \text{if AA or BB,} \end{cases} \tag{4}$$

where γ_n is a series satisfying the conditions

$$\begin{cases} \sum_1^{\infty} \gamma_n > \infty \\ \sum_1^{\infty} \gamma_n^2 < \infty. \end{cases} \tag{5}$$

When using the recurrent procedure (1) with the potential function (2) and adhering to the conditions (3), (4), (5), it can be demonstrated [1] that

$$\int_X [f_A^n(x) - D_A(x)]^2 \, p(x) \, dx \xrightarrow{p} 0,$$

where p(x) is probability density.

As a result of synthesis of the Golovkin algorithm and the potential functions method each x_i field in our archives will be characterized by the vector $\underline{D}_i = \{D_{i\,1}, \ldots, D_{i\,M}\}$, where M is the number of classes. In addition to solving the information compression problem, such a representation can find use in prognostic practice. In actuality, the components of the $\underline{D}_i$ vector are in fact the conditional probabilities and accordingly, for further investigations it is possible to apply all the advantages of the mathematical statistics method.

Some methods for long-range weather forecasting are now known. They are based on the forming of different classifications. In these methods the standard field of the most probable class is stipulated as the prediction material [4]. It appears that it is possible to increase the guaranteed probability of such prognostic schemes if it is not the appearance of some class which is predicted, but a set of parameters $D_{i\,pre}$. In such a way we will predict a specific field unambiguously determined by its degrees of reliability $D_{i\,pre}$. Then, using our archives of data, it is possible to find some real field x_p with the set D_{ip} closest to $D_{i\,pre}$, and as the forecast --- give this x_p field.

We note that when using the potential functions method we solve still another problem related to the presence of a teaching series. The use of the recurrent procedure (1) allows a cyclic representation of the set of presented objects. The algorithm is stopped after such a teaching cycle for which all the coefficients r_n were equal to zero, that is, when $f^n(x)$ approximates D(x) with an adequate degree of accuracy. Thus, the possibility of use of cyclic teaching is still another merit of the potential functions method of importance to us.

In conclusion we will cite the result obtained using real data (the above-mentioned mean monthly $\underline{H}_{500}$ anomalies). This example indicates that the degrees of reliability $\underline{D}_i$ restorable by the described method are an adequately effective method for representation of the fields of meteorological elements and the distance between $\underline{D}_i$ of two fields can be used as a measure of the similarity of these fields. Using the classification obtained in [3], for each field we restored $\underline{D}_i$. It was found that the pairs of fields for which the value

$$S_{ij} = \sqrt{\sum_{k=1}^{m} (D_{ik} - D_{jk})^2}$$

is small are characterized by a quite high similarity index ρ, and on the other hand, the pairs of fields with large S_{ij} are characterized by small ρ.

The figure shows five curves. Along the y-axis we have plotted the S_{ij} value, where $i \in P$, $j \in Q_i$, P is a set of standard objects, Q_i is a set of objects belonging to a class with the i-th standard object. For the first standard $\underline{D}_{stan\,1} = \{1, 0, 0, 0, 0\}$; for the second $\underline{D}_{stan\,2} = \{0, 1, 0, 0, 0\}$ etc., that is, the i-th standard was assumed to belong to

the i-th class with the degree of belonging 1, and to the remaining classes -- with the degree of reliability 0. The approximately identical character of all five curves indicates a nonrandomness of such a correspondence. At first glance it appears strange that some fields are characterized by very small ρ values, but it was found that precisely these fields are in the zone of intersection of the characteristic regions of classes. We note that if any field x_j belongs to the zone of intersection of the k-th and l-th classes then D_{kj} is close to D_{ij}.

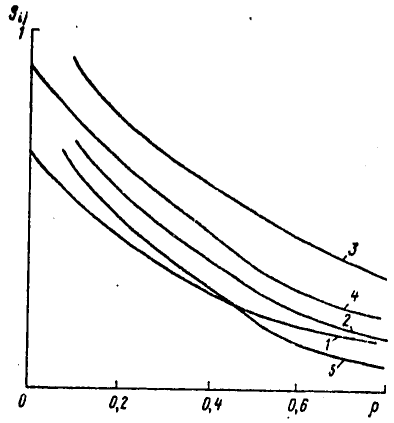

Fig. 1. Curves of the dependence of S_{ij} on ρ for five classes.

In summarizing what has been said above, it can be said that the proposed probabilistic approach to the problem of objective classification of the fields of meteorological elements is quite universal and has a number of advantages over the traditional deterministic approach.

BIBLIOGRAPHY

1. Ayzerman, M. A., Braverman, E. M., Rozonoer, L. N. METOD POTENTSIAL'NYKH FUNKTSIY V TEORII OBUCHENIYA MASHIN (Potential Functions Method in the Theory of Teaching of Machines), Moscow, Nauka, 1970.

2. Bagrov, N. A., "Classification of Synoptic Processes," METEOROLOGIYA I GIDROLOGIYA (Meteorology and Hydrology), No 5, 1969.

3. Burtsev, A. A., "Experiments for the Objective Classification of the Fields of Meteorological Elements," TRUDY GIDROMETTSENTRA SSSR (Transactions of the USSR Hydrometeorological Center), 1979.

4. Vil'fand, R. M., "Application of an Objective Classification of Meteorological Fields to a Monthly Forecast of Air Temperature Anomalies in the European USSR," METEOROLOGIYA I GIDROLOGIYA, No 10, 1977.

5. Golovkin, V. A., MASHINNOYE RASPOZNAVANIYE I LINEYNOYE PROGRAMMIROVANIYE (Computer Recognition and Linear Programming), Moscow, Sovetskoye Radio), 1973.

6. Semenovskiy, Yu. V., "Methods in the Theory of Recognition of Images and Problems in the Analysis and Prediction of Meteorological Fields," METEOROLOGIYA I GIDROLOGIYA, No 12, 1978.

7. Sonechkin, D. M., "Mathematical Theory of Classification and its Application in Meteorology), No 12, 1969.

UDC 551.515.2

STRUCTURE OF TROPICAL CYCLONE "CARMEN" DETERMINED FROM AEROLOGICAL SOUNDING MEASUREMENTS OVER THE OCEAN

Moscow METEOROLOGIYA I GIDROLOGIYA in Russian No 3, Mar 80 pp 45-50

[Article by V. V. Galushko, Doctor of Physical and Mathematical Sciences V. N. Ivanov, V. A. Korobkov, L. A. Mikhaylova and Candidate of Physical and Mathematical Sciences A. Ye. Ordanovich, Institute of Experimental Meteorology, submitted for publication 13 July 1979]

Abstract: A study was made of the thermo- and hydrodynamic parameters of the atmosphere in different synoptic situations using radiosonde data collected by a group of scientific research ships. The article examines the characteristic thermo- and hydrodynamic peculiarities of the atmosphere on the periphery and in the central cloud mass of a typhoon and situations with few clouds outside the zone of typhoon influence.

[Text] At the present time a number of fundamental problems related to the genesis and development of tropical cyclones (TC) remain unsolved. Such problems include study of the spatial-temporal structure of thermohydrodynamic processes in the tropical atmosphere.

In order to carry out this type of investigations the principal meteorological characteristics of the atmosphere and their gradients much be spatially averaged with averaging scales not greater than 100-300 km, since in such distances the variability of the investigated mesoscale formations has the same order of magnitude. A decrease in the averaging scales is also undesirable, since in addition to the measurement errors, increasing in this case, there is a decrease in the stability of the experimental results with respect to fluctuations of meteorological parameters due to atmospheric turbulence.

In this paper we examine the thermo- and hydrodynamic characteristics of the tropical atmosphere in different synoptic situations, computed using radiosonde data in an aerological polygon formed by a group of three scientific research ships of the "Tayfun-78" expedition. The side of the triangle formed by the ships was approximately 200 km.

Table 1

Location of Aerological Polygon Relative to Center of Typhoon and Central Cloud System

Число августа 1	Время, ч 2: гринвичское 6	местное 7	Координаты, град 3: с. ш. 8	в. д. 9	Стадия 4	Расстояние, км 5: от центра тайфуна 10	от края облачного массива 11
			Северная периферия 12				
10	12	22	23	147	ТД *	800	—500 **
10	18	04	23	147	ТД 15	800	—400
11	00	09	23	147	Т	800	—400
11	06	16	23	147	Т	800	—400
11	12	22	23	147	Т 16	800	—250—300
			13 *Центральный облачный массив*				
12	06	16	23	147	Т	450	+50
12	12	22	23	147	Т	350	+100
12	18	04	23	147	Т	300	+200
			14 *Хвостовая конвективная полоса*				
13	01	11	23	147	Т	700	+400
13	06	16	23	147	Ту	700	+400
13	12	22	23	147	Ту	800	+600
13	18	04	23	147	Ту 17	1000	+800

KEY:

1. Day in August
2. Time, hours
3. Coordinates, degrees
4. Stage
5. Distance, km
6. Greenwich
7. Local
8. N
9. E
10. from center of typhoon
11. from edge of cloud mass
12. Northern periphery
13. Central cloud mass
14. Tail convective zone
15. Tropical depression
16. Tropical storm
17. Tropical hurricane

Note. The sign in the column with the double asterisk denotes the position of the center of the polygon relative to the cloud mass: minus -- degree of withdrawal, plus — degree of penetration

---

Among the hydrodynamic characteristics of the atmosphere considered in this paper are the two horizontal and vertical wind velocity components and relative vorticity. The method for computing these parameters is similar to that described in [2].

As the thermodynamic characteristics of the atmosphere we will examine latent heat LQ = Lq and static energy

$$\mathrm{EL}=c_pT+Lq+gz-\mathrm{EL}_0.$$

Here T is the temperature of moist air, K; q is the specific moisture content of air at the altitude z; L is the specific heat of vaporization; c_p is the specific heat capacity of air at constant pressure; g is the acceleration of free falling; EL_0 is a constant determined in such a way that near the ocean surface the EL value is close to zero:

$$\mathrm{EL}_0=c_pT_0+Lf_0q_H(T_0)\approx 84.$$

Here $q_H(T_0)$ is the saturating value for specific humidity at the temperature T = 300 K; f_0 is mean relative humidity, equal to 80%.

In this paper we investigate the vertical distribution of these thermodynamic characteristics and influxes of the values LQ and EL (FLQ and FEL respectively) per unit time in an air column with a base area of 1 cm^2 and a height of 50 mb for different synoptic situations.

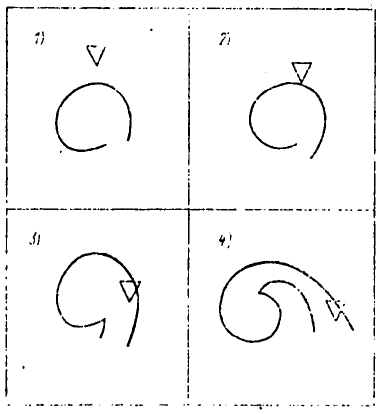

Fig. 1. Schematic image of location of aerological polygon (triangle) relative to typhoon "Carmen." 1, 2 -- northern periphery, 3 -- central cloud mass, 4 -- tail convective zone

During the period 10-15 August 1978 the aerological polygon of the expedition was situated in the zone of influence of typhoon "Carmen" (7811), in its different regions. The characteristics of the synoptic conditions for generation of the typhoon and its structure were described in [1]. Table 1, taken from [1], gives data characterizing the stage of typhoon development and the location of the aerological polygon relative to the center of the typhoon and its central cloud system. A schematic representation of location of the polygon is shown as Fig. 1.

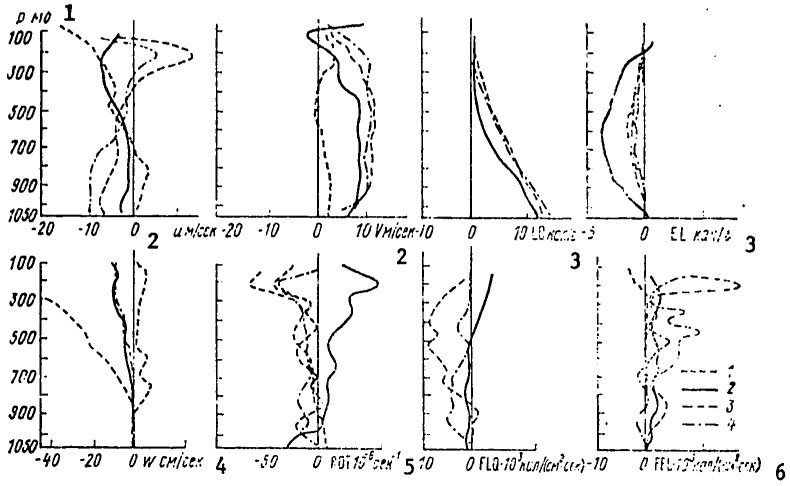

Fig. 2. Hydrodynamic and thermodynamic characteristics of atmosphere in zone of influence of typhoon "Carmen." 1) cloudless Trades zone, 2) northern periphery, 3) central cloud mass, 4) tail convective zone.

KEY:

1. mb
2. m/sec
3. cal/g
4. cm/sec
5. sec
6. cal/(cm^2·sec)

All the experimental data obtained during this period were grouped in accordance with the synoptic situations in the polygon region. It was possible to discriminate several such situations:

1) Northern periphery of typhoon "Carmen";
2) Central cloud mass;
3) Tail convective zone.

It should be noted that the proposed classification of synoptic situations reflects quite well the peculiarities of the state of the troposphere in the region of the aerological polygon. The distribution of the thermohydrodynamic parameters of the atmosphere is qualitatively similar within each group, which makes it possible to consider the results of the computations as objective characteristics of the corresponding synoptic situations.

The results of computations of the thermo- and hydrodynamic characteristics of the troposphere for the above-mentioned situations are presented in Fig. 2. The horizontal components of wind velocity u and v are determined in a Cartesian coordinate system with a reading origin situated at the center of the polygon. The coordinate system is oriented in such a way that the OX-

axis is directed from the center of the typhoon. Here u and v are the radial and tangential components of wind velocity, directed along the OX and OY axes respectively. The positive direction of the tangential velocity component is counterclockwise. The positive sign for the vertical velocity component w corresponds to an upward direction, whereas relative vorticity ROT corresponds to counterclockwise rotation.

Figure 2 also shows the thermodynamic characteristics of the atmosphere: latent heat LQ, static energy EL, and also their influxes (FLQ and FEL) per unit time in an air column with a base 1 cm^2 and an altitude 50 mb.

Now we will examine the most significant characteristics of the troposphere structure over the waters traversed by typhoon "Carmen" in its different zones. The aerological polygon of 10-11 August was to all intents and purposes situated outside the zone of active influence of the typhoon (Table 1, Figure 1), on its northern periphery, at a distance of about 800 km from the center in a cloudless zone. As a result of typhoon movement on 12 August the aerological polygon was within the cloud mass at a distance of about 400 km from the center. Then the typhoon moved and the aerological polygon occupied a position in its tail cloud system at distances from the center of 800 km on 13 August and from 1,200 to 1,400 km on 14 August.

The greatest changes in the characteristics of the troposphere occurred with movement of the polygon from the northern periphery of the typhoon into its central cloud mass. The northern periphery of the typhoon, in all probability, was a slightly disturbed zone, subjected only to a limited influence from the typhoon. This can be seen most clearly from the profile of the radial component of wind velocity, which does not have traits characteristic for zones of strong influence of typhoons (small influx in lower troposphere, no upper tropospheric outflow). Other distinguishing characteristics of the considered zone are positive relative vorticity, the presence of weak but noticeable ascending air flows, small heat influx and virtually zero moisture influx, on the average, in the entire thickness of the atmosphere.

The central cloud mass differs appreciably in its characteristics from the considered situation. This difference was manifested most clearly in the following facts:
-- there is a considerable change in the profile of wind radial velocity -- there is a great influx in the lower troposphere and an outflow in the upper troposphere;
-- there is a change in the stage of vorticity from positive on the northern periphery to negative (anticyclonic) within the cloud mass, especially at great altitudes;
-- the descending flows in the entire thickness of the troposphere increase by a factor of 4-5;
-- in comparison with the preceding situation the total tropospheric moisture content increases by a factor of 1.4;

-- there was a considerable warming of the troposphere -- a minimum in the profile of static energy (in the case of the northern periphery situated in the layer 600-700 mb) was smoothed and the static energy in the entire air column increased.

There was a substantial change in the energy flux in a vertical column of the troposphere. There was an increase in the influx of static energy FEL. It was distributed for the most part in two layers; 950-700 and 700-300 mb. In the first layer the influx averaged about $2 \cdot 10^{-3}$ cal/(cm^2·sec), in the second -- approximately $5 \cdot 10^{-3}$ cal/(cm^2·sec). However, the influx of latent heat FLQ became negative and in the middle layers of the troposphere attained values $8 \cdot 10^{-3}$ cal/(cm^2·sec) (the integral moisture outflow from a vertical unit air column in this case attained 0.85 g/day). It should be noted that the energy influx of 10^{-3} cal/(cm^2·sec) in an air column with a height of 50 mb and with a base of 1 cm^2 can heat (under the condition that energy is expended only on heating) air by 7°C per day. Thus, in the central cloud zone of the typhoon the troposphere was intensively heated.

The tail convective zone of the typhoon, in which the aerological polygon was present on 13 August, differed little with respect to hydrodynamic characteristics from the central cloud mass. As on the preceding day, there were descending vertical flows, but their velocities decreased by a factor of 4-5. Vorticity remained negative. The profile of radial wind velocity retains features characteristic of the central cloud mass, but the outflow in the upper troposphere substantially decreased.

There was a considerable change in the energy balance of the troposphere. Although the vertical distribution of EL and LQ virtually did not differ from the central cloud zone, the energy balance (that is, the influxes of heat and moisture into an air column) decreased by a factor of 6-7. The total influx of all types of heat (static energy) was close to zero.

Table 2

Coordinates of Polygons and Observation Times (Cloudless Situation)

Число сентября 1	Время (гринвичское), ч 2	Координаты полигона, *град* 3		Число 1 сентября	Время 2 (гринвичское), ч	Координаты полигона, *град* 3	
		с. ш. 4	в. д. 5			с. ш.	в. д.
9	12	15,1	143,5	29	12	12,2	146,0
9	00	15,1	143,5	29	18	12,2	146,7
11	00	13,3	138,8	30	00	12,2	146,9
12	00	13,2	141,6	30	06	12,1	146,8
12	00	12,8	141,3	30	12	11,5	141,4
12	12	15,8	143,5	2	12	12,3	145,5
29	06	12,1	146,8	12	00	12,6	145,5

KEY: 1. Day in September
2. Time (GMT), hours
3. Polygon coordinates
4. N
5. E

Thus, an analysis of the thermodynamic characteristics of typhoon "Carmen" makes it possible to draw the following conclusions:

1. The tail convective zone of a typhoon is characterized by a considerable heat content, differing little from the heat content of the central cloud mass, but differing appreciably from the little-disturbed northern periphery of the typhoon.

2. The tail convective zone is relatively conservative in the sense that the influx of latent heat FLQ and especially the total energy balance of the influxes FEL into a vertical air column are not great.

3. Both in the central cloud mass and in the tail convective zone of the typhoon there is a considerable anticyclonic vorticity in the entire thickness of the troposphere. It is particularly great in the layer 400-200 mb.

4. The vertical velocities both on the northern periphery and in the tail convective zone of the typhoon -- its eastern periphery -- are great. In this way the periphery differs appreciably from the central cloud mass of the typhoon, in which the vertical velocities are considerable.

Some thermodynamic characteristics are given in Figures 2 and 3 for a comparison of the thermodynamic characteristics of typhoon "Carmen" with the characteristics of the troposphere under undisturbed conditions. These thermodynamic characteristics are for the cloudless Trades zone, whose frequency of recurrence during the time of the expedition was rather great. In order to compute these characteristics we averaged the experimental data obtained at different times during the course of the expedition and characterizing a relatively extensive cloudless zone. This fact was established using satellite photographs, nephanalysis maps and meteorological evaluations of cloud cover over the polygon. Table 2 gives the coordinates of the polygons and the observation times for such cases. It should be noted that in this case (in the absence of typhoons near the polygon) the coordinate system is oriented in such a way that the OX-axis is directed to the east and the OY-axis is directed to the north, that is, u is the zonal component of wind velocity, v is the meridional component. We note the most characteristic features of the thermohydrodynamic parameters represented on the graphs. These include:
1) Weak positive vorticity in the boundary layer of the troposphere and a considerable negative vorticity at great altitudes.
2) Weak, virtually zero ascending flows in the entire thickness of the troposphere.
3) A virtually complete absence (on the average) of exchange of heat and moisture. The influx of static energy into an air column is virtually equal to zero.

Thus, as follows from the computations, the cloudless Trades zone is characterized by a considerable conservatism, that is, a constancy of the vertical profiles of the principal thermodynamic characteristics and small (on the average) heat influxes into an air column.

BIBLIOGRAPHY

1. Minina, L. S., Arabey, Ye. N., "Structure of the Troposphere Under Tropical Cyclogenesis Conditions," METEOROLOGIYA I GIDROLOGIYA (Meteorology and Hydrology), No 12, 1979.

2. Petrova, L. I., Nesterova, A. V., "Dynamic and Energy Characteristics of the Troposphere on the Periphery of Typhoons and in Zones of Their Maximum Frequency of Recurrence," TAYFUN-75 (Typhoon-75), Vol I, Leningrad, Gidrometeoizdat, 1977.

UDC 551.521.3

ACCURACY IN DETERMINING ATMOSPHERIC OZONE CONTENT USING DATA FROM MEASUREMENTS OF OUTGOING RADIATION

Moscow METEOROLOGIYA I GIDROLOGIYA in Russian No 3, Mar 80 pp 51-58

[Article by Candidates of Physical and Mathematical Sciences Yu. M. Timofeyev and M. S. Biryulina and V. P. Kozlov, Leningrad State University, submitted for publication 15 January 1979]

Abstract: Computations of the informativeness and optimum conditions for measurements of outgoing thermal radiation in the O_3 absorption band 9.6 m are given in the problem of indirect determination of the vertical profile and total content of ozone in the earth's atmosphere. The article gives an analysis of the physical reasons for the low informativeness and accuracy of the indirect method relative to the q(p) profile. Different ways are proposed for increasing the accuracy in determining the characteristics of ozone content using measurements from meteorological artificial earth satellites. It is shown that heterodyne measurements of outgoing radiation (with a resolution 10^{-2}-10^{-3} cm^{-1}) make possible a substantial increase in the accuracy of the indirect method in the upper stratosphere.

[Text] Measurements of the total content of ozone U_{O_3} and the vertical profile of its concentration in the atmosphere, already carried out for a quite long time, have become particularly timely during recent years, in particular in connection with the problem which is arising of possible changes in the thickness of the ozone layer as a result of change in the chemical composition of the atmosphere [10, 18].

Present-day requirements for obtaining global information on atmospheric characteristics stimulated the development of special satellite methods for determining ozone content based on interpretation of data on outgoing radiation in different spectral ranges. In one of these methods use is made

of measurements of outgoing thermal radiation in the region of the O_3 absorption band 9.6μm. Sources [7, 12, 16] give the results of a theoretical analysis of the accuracy of this indirect method. The meteorological artificial earth satellites "Nimbus-3" and "Nimbus-4" were used in measuring outgoing radiation, making it possible to evaluate its real accuracy, and also to obtain a great volume of valuable information on the global field of ozone content [13]. After analyzing the principal results of these studies it is possible to come to the following conclusions:

a) Theoretical investigations and satellite experiments indicated that the informativeness of the considered indirect method when using an average spectral resolution ($\Delta\nu$ = 2-5 cm^{-1}) is small. In particular, with the present-day accuracy of measurements of outgoing radiation it is possible to determine only 1-2 independent parameters of the vertical structure of the ozone content profile (for example, 1-2 coefficients in the expansion of the profile in the characteristic empirical base). As a result, it is not possible to obtain sufficiently reliable data on the vertical structure of the O_3 content profile in the atmosphere.

b) The indirect method makes it possible to determine the total ozone content with a relatively high accuracy. In particular, both theoretical investigations and the interpretation of satellite data indicate the possibility of determining U_{O_3} with an accuracy of 6-10% relative to the true or mean U_{O_3} value.

c) In not a single one of the studies with which we are acquainted was any attempt made to analyze the physical reasons for a low informativeness of the indirect method or to find ways to increase it. In particular, until now there have been no computations of the optimum conditions for measurements of outgoing radiation in the absorption band 9.6μm. Experience has indicated that a correct solution of this problem in a number of cases will considerably increase the accuracy of indirect methods [3].

In this study an attempt is made to fill the existing gaps.

The mathematical basis for solution of inverse problems in the theory of transfer of thermal radiation is the well-known integral form of the transfer equation [4]. After linearization of the equation the considered problem is reduced to solution of the following operator equation of the first kind:

$$\delta\vec{I} = A \times \delta\vec{q}, \tag{1}$$

[It is assumed that the atmospheric temperature profile is known on the basis of solution of the problem of thermal sounding of the atmosphere [4]].

where $\delta\vec{I}$ is the vector of deviations of the measured (with different frequencies ν_i, i = 1, 2,...,m) radiation $I(\nu_i)$ from the radiation $\bar{I}(\nu_i)$, corresponding to the mean profile of of the mixture ratio O_3 - $\bar{q}(p)$,

$\delta\vec{q}$ is the corresponding vector of deviation of the mixture ratio (at different atmospheric levels p_j, $j = 1, 2, \ldots, n$), A is a matrix m x n, whose elements have a simple physical sense -- they characterize the sensitivity of outgoing radiation in the i-th spectral range to variations of the q(p) profile at the level with the pressure p_j.

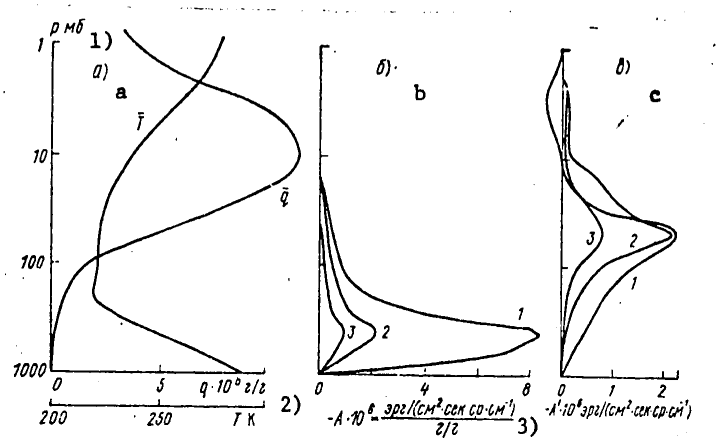

Fig. 1. Vertical temperature profile $\bar{T}$ and mean ozone profile $\bar{q}$ for which computations were made (a), the kernels A(p) for the absolute variations of ozone concentration in three registry channels (b) and the kernels A'(p) for relative variations of the ozone concentration (c). 1) $\nu = 1055$ cm^{-1}, 2) $\nu = 995$ cm^{-1}, 3) $\nu = 1125$ cm^{-1}.

KEY:
1) mb
2) g/g
3) erg/(cm^2·sr·cm^{-1})/g/g

Figure 1b shows examples of computation of $A_i(p)$ for three spectral ranges at the center and in the wings of the absorption band with a spectral resolution of the measurements $\Delta\nu = 5$ cm^{-1}. The computations were based on use of a statistical absorption model [9] and for the mean profiles $\bar{q}(p)$ and $\bar{T}(p)$ corresponding to the period May-September [17].

An analysis of the behavior of the $A_i(p)$ curves shows that for all the considered spectral intervals (we examined 20 intervals in the range from 965 to 1155 cm^{-1}) the maximum influence on outgoing radiation is exerted by absolute variations of ozone content at approximately one and the same level, situated in the troposphere, that is, substantially below the level where the maximum O_3 content is situated (see Fig. 1a, which gives the mean q(p) profile. A change in the optical density of the spectral intervals (with movement from the center of the band to its edges) leads only

to changes in the absolute values $A_i(p)$, but not to a displacement of the curves in the vertical coordinate. This leads to the conclusion that for the considered indirect method the information available for layers above and near the ozone content maximum is very low. A similar behavior of the $A_i(p)$ curves is also observed for other seasons.

The $A_i(p)$ curves shown in Fig. 1 characterize the sensitivity of $I(\nu)$ to absolute variations of q(p). However, due to the strong variability of q(p) within the limits of the ozone layer (q(p) varies by two orders of magnitude) it is useful to analyze the behavior of the $A_i(p)$ curves corresponding to an operational equation relative to the $\delta q/q$ values (it is easy to see that $\tilde{A}_i(p) = q \cdot A_i(p)$. Figure 1c shows $\tilde{A}_i(p)$ curves for these same spectral intervals. It can be seen that although the $\tilde{A}_i(p)$ curves are situated higher in the atmosphere, they are characterized by the above-mentioned peculiarities.

Under conditions of a low information yield of the indirect method it is desirable to make computations of the optimum conditions for measuring outgoing radiation for the purpose of maximum use of the information contained in the $I(\nu)$ spectrum. In this study we used the optimization method proposed by one of the authors [1] and involving the optimum combining of the radiation of different spectral intervals in different measurement channels. The choice of the optimum number of measurements (N) is accomplished on the basis of the known criterion [2]

$$\lambda_k \geqslant \sigma_I^2, \tag{2}$$

where λ_k is the k-th eigenvalue of the covariation matrix of radiation $K_{II} = AK_{qq}A^T$, σ_I^2 is the dispersion of random error, A^T is a transposed matrix.

Table 1

Eigenvalues λ_k $(erg/(cm^2 \cdot sec \cdot sr \cdot cm^{-1}))^2$ for Different Seasons

k	V-IX	X-XII	I-IV
1	$0.4135 \cdot 10^2$	$0.4375 \cdot 10^2$	$0.1558 \cdot 10^2$
2	0.3694	0.2382	0.1565
3	$0.3167 \cdot 10^{-2}$	$0.1480 \cdot 10^{-2}$	$0.1700 \cdot 10^{-2}$

Table 1 gives the first three eigenvalues for three seasons when using covariation matrices of ozone content K_{qq} from [17].

It follows from the data in Table 1 that with the present-day accuracy in measurements (σ_I =0.1-1.0 erg/(cm^2·sec x sr·cm^{-1}) with a spectral resolution $\Delta\nu$ = 5 cm^{-1}) the criterion (2) is satisfied by 1-2 eigenvalues.

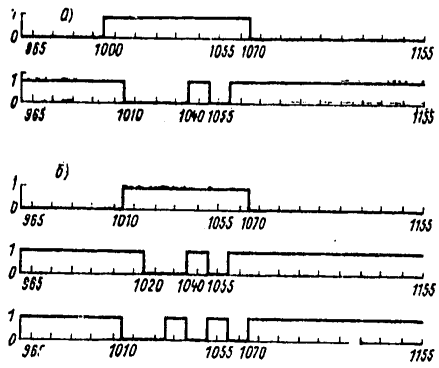

Fig. 2. Configuration of optimum plan for combining spectral intervals. a) for two-channel instrument (N = 2); b) for three-channel instrument (N = 3) (with a value of the ordinate equal to unity a channel is cut in to the combining operation).

Table 2

p мб 1	s_I =0,1 эрг/(см²·сек·ср·см⁻¹) 2					s_I =1,0 эрг/(см²·сек·ср·см⁻¹) 2				
	$(1-\hat{s}_q/s_q)\cdot 100\%$				$\hat{s}_q/\bar{q}\cdot 100\%$ N=3	$(1-\hat{s}_q/s_q)\cdot 100\%$				$\hat{s}_q\,\bar{q}\cdot 100\%$ N=3
	N=20	N=2	N=3	N=3+3		N=20	N=2	N=3	N=3+3	
1	2	3	4	5	6	7	8	9	10	11
0,045	0	0	0	16,3	77	0	0	0	11,7	77
0,425	0	0	0	37,4	27	0	0	0	26,6	27
6	7,0	4,0	13,7	40,5	16,5	3,8	4,0	4,3	17,4	18,7
10	10,2	6,3	19,8	66,0	10,1	1,8	5,1	5,9	25,8	11,9
20	27,5	28,2	28,4	31,5	9,1	3,9	25,2	25,6	28,6	9,5
100	33,2	33,3	33,3	33,8	21,0	29,4	32,9	33,0	33,4	21,1
200	56,5	56,3	57,2	59,2	26,2	52,8	55,9	55,9	57,3	27,0
400	29,5	28,5	31,6	40,6	19,4	12,1	25,5	26,7	34,7	21,7
800	4,7	2,6	9,4	17,6	32,3	1,2	10,7	11,4	9,8	31,6
$1-\frac{\hat{\sigma}_U}{\sigma_U}$	92,0	94,90	96,16	96,61	$\frac{\hat{\sigma}_U}{U_{O_3}}=0{,}47\%$	63,8	94,75	95,49	95,53	$\frac{\hat{\sigma}_U}{U_{O_3}}=0{,}55\%$

KEY:

1. mb
2. erg/(cm^2·sec·sr·cm^{-1})

It can be seen in Fig. 2, which shows examples of the optimum plans with N = 2 and 3 for the season May-September, that the optimum measurement channels occupy rather broad and overlapping spectral regions and also

include sectors in different parts of the band. Computations for other seasons indicated an absence of significant variations in the optimum plans.

Now we will proceed to an analysis of the results of evaluations of errors in the indirect method for different measurement schemes. It should be noted that in a large number of studies (for example, see [12]) as the parameters characterizing the error in the method use is made of the relative errors in restoration, determined relative to the true or mean q(p) or U_{O_3} values. However, taking into account that the relative natural variations of the characteristics of ozone content are relatively small (12-60%) [17], such an approach can create the impression of a rather high accuracy of the indirect method. For example, in evaluating accuracy it is more correct to use the parameter

$$\varphi_q(p) = \frac{\sigma_q(p) - \hat{\sigma}_q(p)}{\sigma_q(p)},$$

characterizing the relative decrease in a priori uncertainty in knowledge of the profile q(p) after carrying out a satellite experiment (σ_q and $\hat{\sigma}_q$ are the mean square q(p) variations before and after carrying out the experiment). The $\hat{\sigma}_q(p)$ values were computed in this study using the formulas of the statistical regularization method [4].

Table 2 gives the $\varphi_q(p)$ and φ_U values for two random error levels: σ_I = 1.0 and 0.1 erg/(cm^2·sec·sr·cm^{-1}) for the season May-September. We examined the following experimental schemes: "full" experiment -- measurements in 20 spectral intervals with a resolution $\Delta\nu$= 5 cm^{-1} (second and seventh columns), measurements of outgoing radiation by optimum instruments with N = 2 (third and eighth columns) and N = 3 (fourth and ninth columns in the table). The sixth and eleventh columns, for comparative purposes, give the relative errors of the indirect method $\hat{\sigma}_q/q$ and $\hat{\sigma}_U/U_{O_3}$ with N = 3. An analysis of the data in Table 2 makes it possible to draw the following basic conclusions:

a) The accuracy of the considered indirect method with respect to the q(p) profile, as followed from the earlier investigations and the informativeness analysis which we made, is relatively low. Only in the layer 20-40 mb is there an appreciable decrease ($>20\%^*$) in the a priori uncertainty in knowledge of the q(p) profile. [Except for the case of a "full" experiment with σ_I = 1.0 erg/(cm^2·sec x sr·cm^{-1}) when this decrease is only 8.9% at the 20-mb level.] Thus, when using measurements of outgoing radiation with average spectral resolution the method yields information on ozone content for the most part only below the level of its maximum content.

b) A decrease in the random measurement error by an order of magnitude exerts a significant influence on method accuracy only in the layers $p \geqslant$ 400 mb and $p <$ 20 mb. However, the absolute accuracy increase in these layers is insignificant.

c) In most cases optimum two- and three-channel instruments make it possible to obtain the same or even a higher accuracy in restoring the q(p) profile as the "full" experiment (20 measurements). [The gain in informativeness when using a measurement scheme with combined spectral intervals in comparison with multichannel instruments is ensured by the known nondependence of the response of heat sensors on the registered radiation flux, which in turn is proportional to the width of the spectral interval. Thus, the signal-to-noise ratio is higher for instruments with broad spectral intervals (optimum plans) than for narrow-band instruments.]

d) With a level of random error $\sigma_I = 1.0$ erg/(cm^2·sec·sr·cm^{-1}) the effectiveness of two- and three-channel instruments is virtually identical. However, with $\sigma = 0.1$ erg/(cm^2·sec·sr·cm^{-1}) the accuracy in using a three-channel instrument is somewhat higher than the accuracy of other measurements.

e) The error in the indirect method with respect to the mean values $\bar{q}$ and U_{O_3} ($\hat{\sigma}_q/\bar{q}$ and $\hat{\sigma}_U/U_{O_3}$ is small and creates the impression of a high accuracy of the method).

f) Despite the small values of the relative decreases in a priori uncertainty $\varphi_q(p)$ at most levels in the atmosphere, the considered indirect method makes it possible to obtain a large amount of information on the total ozone content (last line in the table). At first glance this result is unexpected. Physically this is attributable to the fact that outgoing thermal radiation in the band 9.6 μm is highly sensitive only to variations in total content U_{O_3}, but reacts weakly to variations in the vertical structure of the q(p) profile. From the mathematical point of view small values of the remaining uncertainty

$$\hat{\sigma}_U = \sqrt{\int_0^{p_0}\int_0^{p_0} \hat{K}_{qq}(p_1, p_2)\, dp_1\, dp_2}$$

(here K_{qq} is the matrix of method errors) are attributable to the presence of correlations of errors in the indirect method of different signs for different levels in the atmosphere. This specific structure of the matrix of errors leads to a compensation of the restoration errors at different levels when evaluating the accuracy in restoring the total content U_{O_3}.

g) With a high accuracy in measuring outgoing radiation ($\sigma_I = 0.1$ erg/(cm^2·sec·sr·cm^{-1})) the effectiveness of different satellite systems for determining U_{O_3} is virtually identically high, although in this case as well there are definite advantages of two- and three-channel optimum systems. With an error in measuring radiation of 1 erg/(cm^2·sec·sr·cm^{-1}) the advantages of optimum schemes are significant (compare $\varphi_U = 63.8\%$ for N = 20 and $\varphi_U = 94.75\%$ and 95.49% for N = 2 and 3 respectively). We must note the great advantage of optimum schemes, such as a very weak dependence of the accuracy of the indirect method on errors in measuring outgoing

radiation. However, it is necessary to mention that the determined φ_U values (like the very high $\hat{\sigma}_U/U_{O_3}$ values, less than 1%) characterize the limiting possibilities of the indirect method, since in accuracy computations no allowance was made for the errors attributable to errors in determining the vertical temperature profile, uncertainties in stipulating the characteristics of atmospheric absorption, influence of cloud cover, etc. This evidently also explains the substantial understatement of the theoretical error in the method in comparison with the values obtained in real satellite experiments [12].

The relatively low accuracy in restoring the ozone profile even after optimization of measurement conditions requires an analysis of the physical reasons for this phenomenon for the purpose of seeking ways to increase it. For this it is necessary to understand what is responsible for the specific behavior of the $A_i(p)$ curves (Fig. 1). This analysis is carried out most simply on the basis of the expressions for $A_i(p)$, obtained in a study by one of the authors of the article [5]. In the IR spectral range for the case of monochromatic measurements of outgoing thermal radiation $A_i(p)$ can be written in the form

$$A_i(p) = -k(\nu_i, p) \cdot \int_p^{p_0} \frac{\partial B_{\nu_i}(p')}{\partial p'} \overline{P}(\nu_i, p')\, dp', \qquad (3)$$

where $k(\nu_i, p)$ is the absorption coefficient, $B_{\nu i}(p)$ is the Planck function, $\overline{P}(\nu_i, p)$ is the function of transmission from the upper boundary of the atmosphere to the level with the pressure p for the mean q(p) profile.

It can be seen from formula (3) that the $A_i(p)$ value at the level with the pressure p is determined, in particular, by the value of the integral of the product

$$\frac{\partial B_{\nu_i}(p)}{\partial p} \overline{P}(\nu_i, p)$$

from the considered level to the underlying surface (p_0). For the earth's atmosphere the derivatives $\partial B/\partial p$ have different signs: $\partial B/\partial p \leqslant 0$ in the tropopause and stratosphere and $\partial B/p > 0$ in the troposphere. Accordingly, the $A_i(p)$ values (with $\overline{P} > 0$) will be small for all $p < p_{trop}$ (p_{trop} is the pressure at the level of the tropopause). Such a compensation occurs because the transmission functions in the ozone absorption band 9.6 μm are appreciably different from zero even for the level of the underlying surface.

Thus, the position of the $A_i(p)$ curves in the troposphere is governed by:
-- the complex nature of the relationship between variations of radiation and variations of atmospheric composition (see formula (3)), determined by the physics of transfer of thermal radiation:
-- the vertical thermal structure of the earth's atmosphere;
-- by the small optical thicknesses in the region of the considered absorption band.

This analysis makes it possible to indicate a possible means for increasing the informativeness of the indirect method. The phenomenon of the above-mentioned compensation of the contributions to expression (3) will not be observed under the condition that $\overline{P}(\nu, p_{trop}) = 0$. In this case the $A_1(p)$ curves will be situated above the tropopause level in the atmosphere. The condition $\overline{P}(\nu, p_{trop}) = 0$ can be realized with a marked increase in spectral resolution, for example, when using the heterodyne measurement method [15]. As indicated by computations of the parameters, with a spectral resolution $\Delta\nu = 10^{-2}$–10^{-3} cm^{-1} the $A_1(p)$ curves for the centers of the ozone absorption lines were situated substantially above the tropopause. Table 2 (fifth and tenth columns) gives the parameters which are characteristic of the indirect method with the simultaneous use of measurements with a high spectral resolution in spectral lines of different intensity (ν_{01} = 1053.978 cm^{-1}, S_1 = 500.753 cm/g; ν_{02} = 1070.144 cm^{-1}, S_2 = 29.744 cm/g; ν_{03} = 1000.218 cm^{-1}, S_3 = 13.303 cm/g [11]) and three optimum channels (Fig. 2). The data cited in the table show that the use of the heterodyne method appreciably increases the accuracy of the considered indirect method in the upper stratosphere.

In conclusion we will mention other ways to increase the accuracy in determining the ozone content profile from a meteorological artificial earth satellite:

a) the use of correlations between the temperature profiles T(p) and the ozone content. As follows from [17], these correlations in a number of cases will be rather close. A successful example of realization of such an approach in the problem of humidity sounding of the atmosphere is given in [6].

b) Interpretation of measurements of outgoing radiation in the directions of the planetary horizon. The informativeness of this method is rather high, specifically with respect to the q(p) profile in the upper atmosphere [14]. The joint use of two geometries of measurements (nadir and slant), however, involves great difficulties due to the very high requirements on stabilization of the meteorological artificial earth satellite for precise spatial matching of two types of measurements.

c) There is still another satellite method for determining the vertical profile of ozone content, based on an interpretation of measurements of scattered solar radiation in the UV spectral region [8]. As indicated in [8], the $A_1(p)$ curves of the equation for this method, similar to (1), are situated above the level of the ozone content maximum. On the other hand, the UV method gives very little information concerning the q(p) profile in the lower part of the ozone layer. It is evident that joint measurement in the UV and IR spectral regions will make it possible during the daytime to increase substantially the accuracy in determining the ozone content profile in comparison with measurements in individual spectral regions.

BIBLIOGRAPHY

1. Kozlov, V. P., "Restoration of the Vertical Temperature Profile from the Spectrum of Outgoing Radiation," IZV. AN SSSR, FIZIKA ATMOSFERY I OKEANA (News of the USSR Academy of Sciences, Physics of the Atmosphere and Ocean), Vol 2, No 2, 1966.

2. Kozlov, V. P., "Numerical Restoration of the Vertical Temperature Profile from the Spectrum of Outgoing Radiation and Optimization of the Measurement Method," IZV. AN SSSR, FIZIKA ATMOSFERY I OKEANA, Vol 2, No 12, 1966.

3. Kozlov, V. P., Timofeyev, Yu. M., Kuznetsov, A. D., "Optimization of Conditions for Measuring Outgoing Radiation in the Problem of Indirect Restoration of the Vertical Water Vapor Profile," IZV. AN SSSR, FIZIKA ATMOSFERY I OKEANA, Vol 12, No 5, 1976.

4. Kondrat'yev, K. Ya., Timofeyev, Yu. M., TERMICHESKOYE ZONDIROVANIYE ATMOSFERY SO SPUTNIKOV (Thermal Sounding of the Atmosphere from Satellites), Leningrad, Gidrometeoizdat, 1970.

5. Timofeyev, Yu. M., "Use of the Infrared and Microwave Range of Outgoing Radiation for Determining the Vertical Profile of Atmospheric Humidity," PROBLEMY FIZIKI ATMOSFERY (Problems in Atmospheric Physics), No 12, 1974.

6. Timofeyev, Yu. M., Pokrovskiy, O. M., Kuznetsov, A. D., "Possibilities of Refining the Characteristics of Moisture Content Using a Solution of the Problem of Thermal Sounding of the Atmosphere," METEOROLOGIYA I GIDROLOGIYA (Meteorology and Hydrology), No 3, 1972.

7. Shifrin, Yu. A., "Possibilities of the IR Method for Measuring the Vertical Distribution of Ozone from Artificial Earth Satellites," IZV. AN SSSR, FIZIKA ATMOSFERY I OKEANA, Vol 6, No 7, 1970.

8. Aruga, T., Igarashi, T., "Vertical Distribution of Ozone: A New Method of Determination Using Satellite Measurements," APPL. OPTICS, Vol 15, No 1, 1976.

9. Goldman, A., "Statistical Band Model Parameters for Long Path Atmospheric Ozone in the 9-10 Region," APPL. OPTICS, Vol 9, No 11, 1970.

10. Hidalgo, H., Grutzen, P. J., "The Tropospheric and Stratospheric Composition Perturbed by NO Emission of High-Altitude Aircraft," JGR, Vol 82, No 37, 1977.

11. McClatchey, R. A., et al., "AFCRL Atmospheric Absorption Line Parameters Complication," AFCRL-TR-73-0096 ENVIRONMENTAL RESEARCH PAPERS NO434, 26 January 1973.

12. Prabhakara, C., Conrath, B. J., Hanel, R. A., Williamson, E. J., "Remote Sensing of Atmospheric Ozone Using the 9.6 μ Band," J. ATMOS. SCI., Vol 27, No 7, 1970.

13. Prabhakara, C., Rodgers, E. B., Solomonson, V. V., "Remote Sensing of the Global Distribution of Total Ozone and the Inferred Upper Troposphere Circulation from Nimbus IRIS Experiments," PURE APPL. GEOPHYS., Vol 106/108, No 5/7, 1973.

14. Russell, J. H., Drayson, S. R., "The Interference of Atmospheric Ozone Using Satellite Horizon Measurements in the 1042 cm^{-1} Band," J. ATMOS. SCI., Vol 29, No 2, 1972.

15. Seals, R. K., "Analysis of Tunable Laser Heterodyne Radiometry: Remote Sensing of Atmospheric Gases," AIAA J., Vol 12, No 8, 1974.

16. Sekihara, K., Walshaw, C. D., "The Possibility of Ozone Measurements from Satellites Using the 1043 cm^{-1} Band," ANN. GEOPHYS., Vol 25, No 1, 1969.

17. Spankuch, D., Dohler, W., "Statistische Charakteristika der Vertikalprofile von Temperature und Ozon und ihre Kreuzkorrelation uber Berlin," GEOD. GEOPH. VEROFF., B II, H 9, 1975.

18. Vupputuri, R. K. R., "Seasonal and Latitudinal Variations of CF_x Cly (Freons) and Cl (Cl, ClO, HCl) in the Stratosphere and Their Impact on Stratospheric Ozone and Temperature," DOWNSVIEW ATMOS. ENVIRON. SERVICE CONTR., 1976.

UDC 551.465

MODEL FOR COMPUTING THICKNESS OF THE QUASIHOMOGENEOUS LAYER IN THE OCEAN

Moscow METEOROLOGIYA I GIDROLOGIYA in Russian No 3, Mar 80 pp 59-64

[Article by T. R. Kil'matov and Candidate of Physical and Mathematical Sciences S. N. Protasov, Pacific Ocean Oceanological Institute, submitted for publication 6 June 1979]

Abstract: The authors propose a model for computing the thickness and temperature of the quasihomogeneous layer (QHL) in the ocean. By the term "lower boundary" of the QHL is meant the depth at which the energy of turbulence is extinguished by the operation of buoyancy forces. Mixing is determined from the similarity criterion. Such an approach made it possible to avoid difficulties in parameterization of the production and dissipation of turbulent energy in the QHL. The results of numerical computations are given. There is good agreement with observational data. Evaluations of the mixing coefficient in the QHL are given.

[Text] 1. Models for a mathematical description of the vertical structure of the active layer in the ocean are usually divided in the literature into integral and differential, depending on the equations used [4, 6]. These models can also be divided into two types on the basis of the method for determining the lower boundary of the upper mixed quasihomogeneous layer (QHL). The first type includes models in which by "thickness of the QHL" is meant the layer in which there is a balance between the influx of turbulent energy from the surface and its expenditure in dissipation, and also work against buoyancy forces [5, 8]. This criterion was proposed for the first time in [8]. The second type includes models in which by the term "depth of the jump layer" (lower boundary of the QHL) is meant the depth at which the kinetic energy of turbulence is small and comparable to the work of buoyancy forces [3, 4, 6]. Models of the first type are integral, whereas the second are usually differential, although this criterion has recently been used in integral models as well [4].

In models of the first type the principal difficulty is an adequate description of the production and dissipation of turbulent energy in the QHL. The second approach, based on solution of the equation for the balance of turbulent energy in a semi-empirical approximation, is complex in realization and gives excessive detail concerning turbulent structure in the QHL when computing the characteristics of the upper layer of the ocean at the scale of a season or longer.

In this study we formulate a model for describing evolution of the parameters of the QHL in which the determination of thickness of the mixing layer is made using the second approach in the above-mentioned classification and mixing in the layer is determined from similarity criteria. Such an approach makes it possible to avoid both the difficulties in parameterization of production and dissipation of turbulent energy in the QHL and solution of the equation for the balance of turbulent energy.

2. We will derive an equation for computing the thickness h and temperature T_0 of the QHL. By the term "lower boundary of the QHL" z = h we will mean the depth at which the production of turbulent energy, as a result of shearing instability of mean motion, is compensated by the operation of buoyancy forces. This criterion for discriminating the thickness of the QHL is used in the models in [3, 4, 6]. At the lower boundary of the QHL there must be satisfaction of the relationship

$$k\left(\frac{\partial \bar{U}}{\partial z}\right)^2 - \alpha g \bar{Q} = 0 \qquad \text{when } z = h. \tag{1}$$

Expression (1) is a direct corollary of the Obukhov formula [6]

$$k = (0{,}05\ h)^2 \sqrt{\left(\frac{\partial \bar{U}}{\partial z}\right)^2 + \alpha g \frac{\partial T}{\partial z}},$$

in which the right-hand side becomes equal to zero when z = h. We will neglect advection, the contribution of salinity to the buoyancy flow and penetrating radiation (as a simplification).

In (1) k is the coefficient of vertical exchange of momentum, $\bar{U}$ is the vector of horizontal current velocity, α is the coefficient of thermal expansion, g is the acceleration of free falling, $\alpha g\bar{Q}$ is the operation of buoyancy forces in the QHL.

Equation (1) determines the thickness of the QHL. We will introduce a hypothesis concerning mixing in the QHL. Taking into account the experimental fact of weak stratification in the considered layer, from considerations of the theory of dimensionality [1] we write

$$k = dv_* h \qquad \text{when } 0 < z < h, \tag{2}$$

where d is a dimensionless proportionality constant, v_* is dynamic velocity.

Expression (2) also follows from the Obukhov formula, averaged with depth in the QHL with stratification neglected. Formula (2) can be derived from the Kolmogorov hypothesis for the closing of the semi-empirical turbulence theory, where the turbulence scale is assumed proportional to the thickness of the QHL. With (2) taken into account, the production of turbulent energy from shearing instability can be rewritten as follows, using the classical Ekman relationships for an ocean with the depth z = h, $\overline{U}(h) = 0$:

$$k\left(\frac{\partial \overline{U}}{\partial z}\right)^2 = \frac{v_*^3}{dh} e^{-a}(1 + 2e^{-a}\cos a + e^{-2a})^{-1} \quad \text{when } z = h, \qquad (3)$$

where

$$a = \sqrt{\frac{2fh}{dv_*}},$$

f is the Coriolis parameter.

In order to parameterize the work of buoyancy forces in the QHL $\alpha g\overline{Q}$ we will examine the equation for thermal conductivity in the QHL

$$\frac{\partial T}{\partial t} = -\frac{\partial Q}{\partial z} \quad \text{when } 0 \leqslant z \leqslant h, \qquad (4)$$

where Q is the heat flow in the section z with $0 < z < h$, normalized for density and heat capacity. In integral models the temperature in the QHL is usually assumed to be constant with depth. Expanding temperature into a Taylor series with z = 0 and retaining two terms of the expansion, that is, taking into account weak stratification in the QHL, we obtain

$$T \approx T_0 + \left(\frac{\partial T}{\partial z}\right) z \approx T_0 - \frac{\overline{Q}}{k} z,$$

where

$$\overline{Q} = \frac{1}{h}\int_0^h Q dz.$$

Substituting into (4) the derived expression for temperature and integrating within the QHL, we obtain the equation

$$h\frac{\partial T_0}{\partial t} - \frac{h^2}{2k}\frac{d\overline{Q}}{dt} = Q_0 - Q_h, \qquad (5)$$

where Q_0, Q_h are the heat flows at the upper and lower boundaries of the QHL. Taking the double integral of equation (4)

$$\int_0^h \int_0^z$$

with (5) taken into account, we obtain a differential equation for $\overline{Q}$

$$\frac{d\overline{Q}}{dt} + \frac{12k}{h^2}\overline{Q} = \frac{6k}{h^2}(Q_0 + Q_h); \qquad (6)$$

which is an ordinary linear first-degree differential equation, whose general solution is easily written. The stationary solution (6) will have the form

$$\overline{Q} = \frac{1}{2}(Q_0 + Q_h). \tag{7}$$

The general solution of equation (6) asymptotically tends to a stationary solution (7) when $t \to \infty$. With times $t \quad t_* = h^2(12k)^{-1}$ to a high degree there is satisfaction of (7); the t_* evaluation gives the time less than which integral models cannot be used. Finally, with (3) and (7) taken into account, from (1) we obtain an equation for computing the thickness of the QHL:

$$Q_h = \frac{2v_*^3}{dh^2 g} e^{-a}(1 + 2e^{-a}\cos a + e^{-2a})^{-1} Q_0. \tag{8}$$

Since times greater than t_* are considered, from (5) for computing T_0 we have

$$h\frac{\partial T_0}{\partial t} = Q_0 - Q_h. \tag{9}$$

The system of equations (8)-(9) is similar to a system of the Kraus-Turner type for computing T_0 and h.

3. Now we will investigate the derived equations. For the middle latitudes from (3) we have approximately

$$k\left(\frac{\partial \overline{U}}{\partial z}\right)^2 \approx \frac{v_*^3}{dh} e^{-a} \approx f U_0^2 e^{-a}, \tag{10}$$

where U_0 is drift velocity at the ocean surface.

At the time of summer heating $Q_0 > 0$, the thermocline is "suppressed" [8], $Q_k = 0$. In this case, reducing (8) to logarithmic form in the approximation (10), for the thickness of the QHL we obtain the following formula:

$$h = \frac{d}{2}\frac{v_*}{f}\left(\ln\frac{2fU_0^2}{\alpha g Q_0}\right)^2. \tag{11}$$

For the time of summer heating in the middle latitudes, on the basis of statistical processing of observational data in [7], the following formula was derived:

$$h = 0{,}6\frac{v_*^{1.3}}{f^{0.85}(\alpha g Q_0)^{0.15}} = 0{,}6\frac{v_*}{f}\left(\frac{v_*^2 f}{\alpha g Q_0}\right)^{0.15}. \tag{12}$$

The good agreement of (11) and (12) in the nature of the dependence of thickness of the QHL on wind velocity, heat flow and the Coriolis parameter confirms the correctness of hypotheses (1) and (2) incorporated in the model. In particular, it follows from (11) that in summer to a high degree $h \sim v_*/f$, $k \sim v^2/f$ in the middle latitudes. Formula (11) makes it possible to estimate the unknown proportionality constant d, which is of the order of $d \approx 0.05$, which coincides with that cited in [6] in the Obukhov formula. In the equatorial zone $a \approx 0$; from (8) for the thickness of the QHL we obtain $h = v^3/2d\alpha g Q_0$, that is, h is proportional

to the Monin-Obukhov scale. With advance into the high latitudes an ever-greater influence is exerted on the thickness of the QHL by the Coriolis parameter in the middle latitudes as well; as follows from (11), h to a high degree is proportional to the scale of the Ekman length v_*/f. Since at the equator the main role in the buoyancy flux at the surface is played by salinity, with allowance for formulas (19) and (20) for the thickness of the QHL at the equator it is possible to write that

$$h = \frac{v_*^3}{2\,dg\,(\alpha Q_0 - \gamma\Gamma_0)},$$

where $g\gamma\Gamma_0$ is the buoyancy flux at the surface as a result of change in salinity as a result of evaporation and precipitation.

Substituting into the formula the characteristic scales $Q_0 = 0$, $v_* = 0.5$ cm·sec^{-1}, $\gamma g \Gamma_0 = -10^{-4}$ cm^2·sec^{-3}, with d = 0.05 for a thickness of the QHL we obtain $h = 10^4$ cm, that is, the estimates of d for the middle and equatorial latitudes coincide.

The Kraus-Turner equation for computing the thickness of the QHL from [8] has the form

$$Q_h = \frac{2\,(G - D)}{\alpha g h} - Q_0, \tag{13}$$

where G and D are the integral production and dissipation of turbulent energy in the QHL.

Subtracting (8) from (13), we obtain

$$G - D = \frac{v_*^3}{d} \cdot e^{-a}\,(1 + 2\,e^{-a}\cos a + e^{-2a})^{-1}. \tag{14}$$

On the right-hand side of (14) the only unknown dimensionless parameter is easily determined from (11). It can be seen from a comparison of equations (8) and (13) at the time of the autumn-winter cooling, when $Q_0 < 0$ and the role of wind mixing is reduced, the derived equation (8) is identical to a model of the Kraus-Turner type (13).

4. Now we will cite the results of computation of the seasonal variation of temperature and the thickness of the QHL on the basis of data on the heat flux Q_0 and wind velocity V at the ocean surface. The empirical expression $v_* = 1.3 \cdot 10^{-3}$ V was used. Since the mixing mechanism is unclear, a very simple entrainment hypothesis [8] was used:

[c = jump]
$$Q_h = \Lambda(T_0 - T_c)\ \frac{dh}{dt},$$

where Λ is the Heaviside function of the argument dh/dt, $T_0 - T_{jump}$ is the temperature drop in the jump layer, which was assumed to be constant and equal to 5°C.

The figure shows the results of computations of the thickness and temperature of the QHL on the basis of characteristic mean climatic data in the middle latitudes (50°N, 145°W) of the Pacific Ocean [5]. The model correctly describes the seasonal evolution of QHL parameters. The input parameters are stipulated by the first harmonic of a Fourier series, but for the computed T_0 and h there is a characteristic asymmetric distribution -- h in winter, but T_0 in summer have a more acute extremum, as is also observed in the ocean. The seasonal variation of the coefficient of turbulent exchange coincides in character with its estimates made on the basis of temperature waves [2] -- an increase and acute extremum in winter, a decrease and more gentle extremum in summer. This confirms the possibility of using the hypothesis (2) for parameterization of mixing in the QHL.

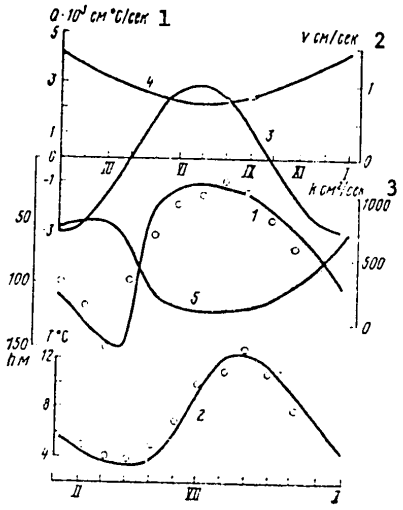

Fig. 1. Computation of the seasonal variation of thickness (1) and temperature (2) of the QHL and change in the heat flow through the water surface (3), dynamic velocity (4) and coefficient of turbulent mixing vertically (5)

KEY:

1. cm °C/sec
2. cm/sec
3. cm^2/sec

The model gives the following estimates of the coefficient of vertical turbulent exchange -- in the middle latitudes in summer $k \sim 100$ cm^2/sec, in winter 1000 cm^2/sec, in the low latitudes $k \sim 10^3$ cm^2/sec and varies little in the course of the year. This coincides with the computations in [6].

5. The model is easily generalized, taking into account advection, salinity s_0 and penetrating radiation. Using the reasonings cited in [4] and the formulation of point 2 with allowance for the enumerated factors, the total system in the QHL can be written as follows:

$$h\frac{\partial T_0}{\partial t} + \Pi_x\frac{\partial T_0}{\partial x} + \Pi_y\frac{\partial T_0}{\partial y} = Q_0 - Q_h, \tag{15}$$

$$h\frac{\partial s_0}{\partial t} + \Pi_x\frac{\partial s_0}{\partial x} + \Pi_y\frac{\partial s_0}{\partial y} = \Gamma_0 - \Gamma_h, \tag{16}$$

where Γ_0 and Γ_h are the salt fluxes at the upper and lower boundaries of the QHL.

For the equation of the flow vector Π_x, Π_y and vertical velocity w we have:

$$\Pi_x \equiv \int_0^h u\,dz = \frac{\tau_y}{f}, \quad \Pi_y = \int_0^h v\,dz = -\frac{\tau_x}{f}, \tag{17}$$

$$w = -\left(\frac{\partial \Pi_x}{\partial x} + \frac{\partial \Pi_y}{\partial y}\right). \tag{18}$$

The equation for determining thickness of the QHL is

$$g(\alpha Q_h - \gamma\Gamma_h) = \frac{2V_*^3}{dh}(e^a + 2\cos a + e^{-a})^{-1} - g(\alpha Q_0 - \gamma\Gamma_0) + 2\pi S. \tag{19}$$

Here S is the intensity of solar radiation, π is the absorption function [5],

$$\pi = \frac{1}{\beta h}(1 - e^{-\beta h}) - \frac{1}{2}e^{-\beta h},$$

where β is the sea water absorption coefficient.

The last term on the right-hand side of (19) characterizes the influx of mechanical energy of mixing as a result of heating of the water within the QHL as a result of penetrating radiation and heat loss at the surface. This effect can lead to considerable mixing in the QHL [5]. Equation (19) was derived under the condition that the equation of state of sea water was used in the linearized form

$$\rho = \rho_0[1 - \alpha T + \gamma(s - 35)]. \tag{20}$$

For the buoyancy flux at the lower boundary of the QHL it is possible to write [4]

$$g(\alpha Q_h - \gamma\Gamma_h) = \Lambda g[\alpha(T_0 - T_c) - \gamma(s_0 - s_c)]\left(\frac{dh}{dt} - w\right), \tag{21}$$

[c = seas]

where T_{seas}, s_{seas} are temperature and salinity in the seasonal thermocline.

The cited model (15)-(21) with respect to physical principles is identical to the models in [4, 6], but the averaging of the mixing coefficients with depth in the QHL made it possible to obtain simple expressions for

the computed characteristics with conservation of all the properties of behavior of the QHL. The QHL mixing is determined by the single constant d, which is easily estimated on the basis of (11). Although the cited model retains the shortcomings of integral models, such as parameterization of interaction between the QHL and the seasonal thermocline, nevertheless all the parameterization variants for integral models of the Kraus-Turner type can also be used in equation (21).

A further improvement in the model evidently is dependent on the possibility of an adequate description of mixing in the seasonal thermocline and interaction at the lower boundary of the QHL.

BIBLIOGRAPHY

1. Barenblatt, G. I., PODOBIYE, AVTOMODEL'NOST', PROMEZHUTOCHNAYA ASIMPTOTIKA (Similarity, Self-Similarity and Intermediate Asymptotic Behavior), Leningrad, Gidrometeoizdat, 1979.

2. Boguslavskiy, S. G., "Annual Variation of the Coefficients of Turbulent Thermal Conductivity Vertically in the Sea," TRUDY IGI (Transactions of the Institute of Mineral Fuels), No 13, 1958.

3. Kalatskiy, V. I., "Two-Layer Model for Computing the Thickness of the Isothermal Layer in the Ocean," METEOROLOGIYA I GIDROLOGIYA (Meteorology and Hydrology), No 11, 1973.

4. Kalatskiy, V. I., MODELIROVANIYE VERTIKAL'NOY TERMICHESKOY STRUKTURY DEYATEL'NOGO SLOYA OKEANA (Modeling of the Vertical Thermal Structure of the Active Layer in the Ocean), Leningrad, Gidrometeoizdat, 1978.

5. Kil'matov, T. R., Protasov, S. N., "Computation of the Seasonal Temperature Variation at the Ocean Surface and the Thickness of the Quasi-homogeneous Layer," METEOROLOGIYA I GIDROLOGIYA, No 8, 1978.

6. Marchuk, G. I., Kochergin, V. P., Klimok, V. I., Sukhorukov, V. A., "Mathematical Modeling of the Seasonal Variability of the Surface Turbulent Layer in the Ocean," IZV. AN SSSR, FIZIKA ATMOSFERY I OKEANA (News of the USSR Academy of Sciences, Physics of the Atmosphere and Ocean), Vol 14, No 19, 1978.

7. Filyushkin, B. N., "Thermal Characteristics of the Upper Water Layer in the Northern Part of the Pacific Ocean," OKEANOLOGICHESKIYE ISSLEDOVANIYA (Oceanological Investigations), No 9, 1968.

8. Kraus, E. B., Turner, J. S., "A One-Dimensional Model of the Seasonal Thermocline. Part II. The General Theory and its Consequences," TELLUS, Vol 19, No 1, 1967.

UDC 551.465(-062.4)

COMPUTATION OF CHARACTERISTICS OF THE QUASI-ISOTHERMAL LAYER IN THE EQUATORIAL ZONE OF THE OCEAN

Moscow METEOROLOGIYA I GIDROLOGIYA in Russian No 3, Mar 80 pp 65-72

[Article by A. B. Polonskiy, Marine Hydrophysical Institute Ukrainian Academy of Sciences, submitted for publication 23 July 1979]

Abstract: The author proposes a stationary two-layer model of a baroclinic ocean, including the equator. The model generalizes the formulation of the problem in [7] in the case of allowance for an isothermal layer. It is shown that it describes quite well the principal characteristics of distribution of parameters in the isothermal layer in the equatorial zone.

[Text] Introduction. The discovery of a system of countercurrents in the equatorial region has stimulated studies devoted to a description of the equatorial zone of the world. A review of the studies made up to 1973 was given by Philander in [17]. A concise summary of the results obtained during recent years is given in the review [9].

We note the circumstance that the purpose of the overwhelming majority of the studies, in particular, is a description of the observable features in the velocity field. Considerably lesser attention is devoted to the very important peculiarities of the temperature and density fields in the surface layer (in particular, formation of the quasihomogeneous layer (QHL) at the equator). This is probably attributable to the fact that in the equatorial zone there has been unsound use of relatively simple one-dimensional models of the QHL assuming a secondary importance of the influence of large-scale circulation on formation of the QHL [5]. Observations show [11] that the principal element in the equatorial large-scale circulation -- the subsurface countercurrent -- is closely associated with the QHL. The core of the countercurrent is concentrated in the thermocline, directly under the QHL, rising together with the latter from west to east toward the surface. On the other hand, the thickness of the thermocline at the equator decreases to 150-200 m [17] and becomes commensurable with the thickness of the QHL. Thus, in contrast to the middle

latitudes, the equatorial QHL can evidently be described only in the framework of models of large-scale circulation. It is interesting that the first attempt at computing the thickness of the QHL in the equatorial zone, undertaken by Reid [18], was essentially based on similar considerations. The objectives of this study are computation of QHL characteristics in the equatorial zone within the framework of a stationary integral model describing the principal features of large-scale circulation and clarification of the role of different factors in formation of the thermal structure in the upper layer of the ocean.

Formulation of Problem and Solution Method

We will limit ourselves to an examination of stationary circulation and we will neglect barotropic pressure gradients. The results obtained in [4, 6-8] show that this approximation works well both in the middle latitudes and in the equatorial zone. In the equations of motion we will neglect the nonlinear terms and lateral exchange will be taken into account by the introduction of dissipative terms in the Rayleigh-Stommel form. Within the framework of such an approach many results were obtained in the modeling of equatorial circulation (for example, see [10]). Then the initial system of equations is written in the following form:

$$\frac{\partial \tau_{xz}}{\partial z} - ru + fv = g\alpha \frac{\partial}{\partial x}\int_z^\infty T dz, \tag{1}$$

$$\frac{\partial \tau_{yz}}{\partial z} - fu - rv = g\alpha \frac{\partial}{\partial y}\int_z^\infty T dz, \tag{2}$$

$$u\frac{\partial T}{\partial x} + v\frac{\partial T}{\partial y} + w\frac{\partial T}{\partial z} = \frac{\partial Q}{\partial z} + k_l \Delta T, \tag{3}$$

$$\operatorname{div} \overline{v} = 0. \tag{4}$$

The Oz-axis is directed downward, the Ox-axis to the east, the Oy-axis to the north. The following notations were used in (1)-(4):

$$\tau_{xz} = -\overline{u'w'}, \quad \tau_{yz} = -\overline{v'w'}, \quad Q = -\overline{w'T'};$$

T is the temperature deviation from some standard value in the deep layers. The remaining notations are those in general use.

We note that in this formulation no assumptions are made concerning the mechanism of vertical turbulent exchange for momentum and temperature. In writing (1)-(4) we neglected the influence of salinity on density, assuming a linear correlation between density and temperature. The heat flows and frictional shearing stress are stipulated at the ocean surface. The rate of flow and temperature decrease with depth.

Then we introduce a model for temperature: at the surface there is a mixed isothermal layer of the thickness h with the temperature T_0; below the temperature decreases exponentially:

$$T = \begin{cases} T_0 \text{ when } z \leqslant h \\ T_0 \exp\left(\frac{z-h}{c}\right) \text{ when } z > h. \end{cases} \quad (5)$$

The c parameter is selected in such a way that in the temperate latitudes we obtain an expression close to the well-known Nedler solution [15, 19], but in the equatorial region the thickness of the thermocline was 150-200 m. Adhering to [7], we will assume $c = \sqrt{f^2 + \lambda^2/c_1}$, where λ and c_1 are constants characterizing the thickness of the thermocline. The introduction of λ makes it possible to avoid a singularity at the equator present in the special Nedler solution. The model (5) is a generalization for the case of presence of an isothermal layer in the thermocline model proposed in [7].

By stipulating the vertical thermal structure of the ocean we deprive ourselves of the possibility of using system (1)-(4) in differential form and can satisfy it only in an integral sense.

First we will integrate (1)-(4) within the limits of the QHL. Assuming that the QHL coincides with the friction layer, with (5) taken into account, we obtain:

$$\tau_{0x} - rS_x^h + fS_y^h = g\alpha\left[\frac{\partial T_0}{\partial x}\left(ch + \frac{h^2}{2}\right) + T_0 h \frac{\partial h}{\partial x}\right], \quad (6)$$

$$\tau_{0y} - rS_y^h - fS_x^h = g\alpha\left[\frac{\partial T_0}{\partial y}\left(ch + \frac{h^2}{2}\right) + T_0 h \frac{\partial (h+c)}{\partial y}\right], \quad (7)$$

$$S_x^h \frac{\partial T_0}{\partial x} + S_y^h \frac{\partial T_0}{\partial y} = q_0 - q_h + k_L h \Delta T_0, \quad (8)$$

$$\frac{\partial S_x^h}{\partial x} + \frac{\partial S_y^h}{\partial y} - u_h \frac{\partial h}{\partial x} - v_h \frac{\partial h}{\partial y} + w_h = 0. \quad (9)$$

Here τ_{0x} and τ_{0y} are components of wind shearing stress, q_0 is the heat flow at the surface, u_h, v_h, w_h, q_h are the three components of velocity and heat flow at the lower boundary of the QHL.

We will assume that the heat flow is continuous at the lower boundary of the QHL. Then

$$q_h = \lim_{z \to h+0}\left(-k_T \frac{\partial T}{\partial z}\right) = \frac{k_T T_0}{c}. \quad (10)$$

In (10) k_T is the coefficient of turbulent thermal conductivity at the upper boundary of the thermocline. Expression (10) was used earlier in [16].

Now we will integrate equation (3), written in divergent form, from h to ∞. Assuming that the heat flow asymptotically attenuates with depth and using the condition of continuity of velocity at the lower boundary of the QHL, with (9) taken into account we obtain:

$$\frac{\partial}{\partial x}\int_h^\infty uT\,dz + \frac{\partial}{\partial y}\int_h^\infty vT\,dz + T_0\left(\frac{\partial S_x^h}{\partial x} + \frac{\partial S_y^h}{\partial y}\right) = q_h + k_L\int_h^\infty \Delta T\,dz. \tag{11}$$

The system of equations (6)-(8), (10), (11) is closed relative to T_0, h, S_x^h, S_y^h, q_h. The velocities u and v outside the QHL are unambiguously expressed from (1)-(2) through the gradients T_0 and h.

Now we will transform the derived system. Solving (6)-(7) for S_x^h and S_y^h, we obtain

$$S_x^h = \frac{-g\alpha r\left[\frac{\partial T_0}{\partial x}\left(ch + \frac{h^2}{2}\right) + T_0 h\frac{\partial h}{\partial x}\right] + r\tau_{0x}}{r^2+f^2} - \frac{g\alpha f\left[\frac{\partial T_0}{\partial y}\left(ch + \frac{h^2}{2}\right) + T_0 h\frac{\partial (h+c)}{\partial y}\right] - f\tau_{0y}}{r^2+f^2}, \tag{12}$$

$$S_y^h = \frac{-g\alpha r\left[\frac{\partial T_0}{\partial y}\left(ch + \frac{h^2}{2}\right) + T_0 h\frac{\partial (h+c)}{\partial y}\right] + r\tau_{0y}}{r^2+f^2} + \frac{g\alpha f\left[\frac{\partial T_0}{\partial x}\left(ch + \frac{h^2}{2}\right) + T_0 h\frac{\partial h}{\partial x}\right] - f\tau_{0x}}{r^2+f^2}. \tag{13}$$

Performing integration on the right-hand side of (11) and expressing q_h by means of (10), we rewrite (8) and (11) in the following form:

$$k_L\left\{T_0\left(\frac{\partial^2 h}{\partial x^2} + \frac{\partial^2 h}{\partial y^2}\right) + c\left(\frac{\partial^2 T_0}{\partial x^2} + \frac{\partial^2 T_0}{\partial y^2}\right) + 2\left(\frac{\partial h}{\partial x}\frac{\partial T_0}{\partial x} + \frac{\partial h}{\partial y}\frac{\partial T_0}{\partial y}\right) + \frac{T_0}{c}\left[\left(\frac{\partial h}{\partial x}\right)^2 + \left(\frac{\partial h}{\partial y}\right)^2\right] + T_0\frac{\partial^2 c}{\partial y^2} + 2\frac{\partial T_0}{\partial y}\frac{\partial c}{\partial y}\right\} + \frac{k_T T_0}{c} =$$

$$= \frac{\partial}{\partial x}\int_h^\infty uT\,dz + \frac{\partial}{\partial y}\int_h^\infty vT\,dz + T_0\left(\frac{\partial S_x^h}{\partial x} + \frac{\partial S_y^h}{\partial y}\right); \tag{14}$$

$$k_L h\left(\frac{\partial^2 T_0}{\partial x^2} + \frac{\partial^2 T_0}{\partial y^2}\right) - S_x^h\frac{\partial T_0}{\partial x} - S_y^h\frac{\partial T_0}{\partial y} = -q_0 + \frac{k_T T_0}{c}. \tag{15}$$

In (14):

$$\int_h^\infty uT\,dz = \frac{g\alpha T_0 c\left[r\left(\frac{\partial T_0}{\partial x}c + T_0\frac{\partial h}{\partial x}\right) + f\left(\frac{\partial T_0}{\partial y}c + \frac{3}{2}T_0\frac{\partial c}{\partial y} + \frac{\partial h}{\partial y}T_0\right)\right]}{2(r^2+f^2)},$$

$$\int_h^\infty vT\,dz = \frac{-g\alpha T_0 c\left[r\left(\frac{\partial T_0}{\partial y}c + T_0\frac{\partial h}{\partial y} + \frac{3}{2}T_0\frac{\partial c}{\partial y}\right) - f\left(\frac{\partial T_0}{\partial x}c + T_0\frac{\partial h}{\partial x}\right)\right]}{2(r^2+f^2)}.$$

Thus, system (12)-(15) of second-degree differential equations relative to T_0 and h was derived. The unknowns S_x^h and S_y^h can be avoided by substituting (12)-(13) into (14)-(15). This gives a system of two equations of the elliptical type relative to T_0 and h. However, since the solution is sought by the successive approximations method, we will retain the derived system unchanged. This makes it possible to avoid unwieldy expressions.

After transformation to dimensionless form in (15) with higher derivatives, small parameters appear, evidence of presence of boundary temperature layers. Since S_x^h can change sign with approach to the equator, assuming a positive value due to the existence of the subsurface countercurrent, it is natural to expect that near the equator the temperature boundary layer is formed at the eastern boundary. However, in contrast to [7], this can occur only when there is an adequately accurate description of the subsurface countercurrent. Only in this case will S_x^h be a sign-variable value. Such a difference is associated, to be sure, with allowance for the QHL in our case. T_0 is determined in this case from an equation describing the heat balance within the limits of the QHL, whereas in [7] T_0 was determined from a similar equation for the thermocline, used here for determining h. Terms with small parameters also appear in (14). In principle it is possible to simplify the initial system for the inner region, neglecting terms with small parameters. But in this case as well it is not possible to obtain an analytical solution. Therefore, we will numerically solve the nonlinear system (12)-(15) in full form.

Now we will discuss the problem of boundary conditions. Observations show [13] that at the equator there is good satisfaction of the symmetry condition for T_0 and

$$h\left(\frac{\partial T_0}{\partial y}\Big|_{y=0} = \frac{\partial h}{\partial y}\Big|_{y=0} = 0\right);$$

at the western and eastern walls it is reasonable to set "nonflowthrough" conditions and the condition of absence of a heat flow; this will give two conditions for h and T_0. In this case the integral heat flow and the total flows at the northern boundary should be stipulated taking into account the integral heat balance in the entire region. However, two complications arise in this case. The first is computational in nature and is related to the type of boundary conditions at the western and eastern walls (oblique derivatives). The second is fundamental in nature and follows from the uncertainty in stipulating the boundary conditions at the northern boundary. Therefore, we will limit ourselves to solution of the problem with a stipulated distribution of T_0 and h at three boundaries. The specific types of boundary conditions will be discussed in detail below.

The problem is solved in the following way: on the basis of the stipulated h and T_0 fields we compute S_x^h, S_y^h, $\partial S_x^h/\partial x$, $\partial S_y^h/\partial y$ and the integrals on the right-hand side of (14). Then we solve (14) and (15) for h and T_0

respectively. The resulting h field is used in computing T_0. Then the entire operation is repeated until the convergence test is met. Equations (14)-(15) are solved by the stabilization method using an implicit longitudinal-transverse scheme of the first order of approximation. The relative error T_0 in two adjacent intervals of fictitious time (Δt) was selected as the stabilization test. When an error of a stipulated value ε is attained the process is considered

The problem was solved in a rectangle measuring 4,400 x 660 km. The x and y intervals were varied for checking the finite difference scheme. In the main computation variant we used a uniform grid with a 400-km interval along x and 60 km along y. The values of the principal constants are given in Table 1 (in the cgs system).

Table 1

β	λ	k_1	k_L	r	c_1	ε	Δt
$2 \cdot 10^{-13}$	$(1{,}5 \div 2) \cdot 10^{-5}$	1	10^8	10^{-6}	10^{-9}	10^{-3}	30

The value $k_T = 1$ cm^2/sec is now the generally accepted evaluation for the effective coefficient of turbulent exchange in the thermocline [3]. The cited λ and c_1 values give for the equator a thickness of the thermocline 200 m, and in the middle latitudes -- about 1,200 m, which corresponds to the generally accepted concepts [17].

The time interval is selected empirically. In most computation variants a constant heat flow $q_0 = 10^{-3}$ cal/(cm^2·sec) was stipulated at the surface, which is characteristic for the equatorial zone [2], as well as a zonal wind. The shearing stress value was varied from -0.2 dyne/cm^2 to -0.5 dyne/cm^2. An experiment with a linear increase in wind velocity from east to west from -0.2 to -0.75 dyne/cm^2 was carried out for clarifying the role of zonal nonuniformity of the wind.

Principal Results of Computations

Since the presented formulation is a generalization of the model proposed in [7], it is interesting to compare the results of numerical experiments with an identical choice of the principal parameters and boundary conditions for the purpose of clarifying the role of the QHL in the formation of large-scale thermodynamic characteristics of the equatorial zone of the ocean. [There is still another fundamental difference in this model associated with allowance for horizontal turbulent exchange of heat. However, the influence of this effect for the most part does not extend beyond the limits of the thermal boundary layers.] For this we will seek a solution of the problem with constant values stipulated at the boundaries and $T_0 = 21°C$, $h = 10$ m, $\lambda = 1.5 \cdot 10^{-5}$ sec^{-1}, $\tau = -0.2$ dyne/cm^2.

The results of the computations are given in Fig. 1 together with similar results taken from [7]. The principal peculiarity characteristic for both experiments is a well-expressed bunching of the isotherms in the western part of the basin. The eastern boundary layer in our case is absent. This is attributable to the fact that S_x^h is everywhere negative with the boundary conditions used.

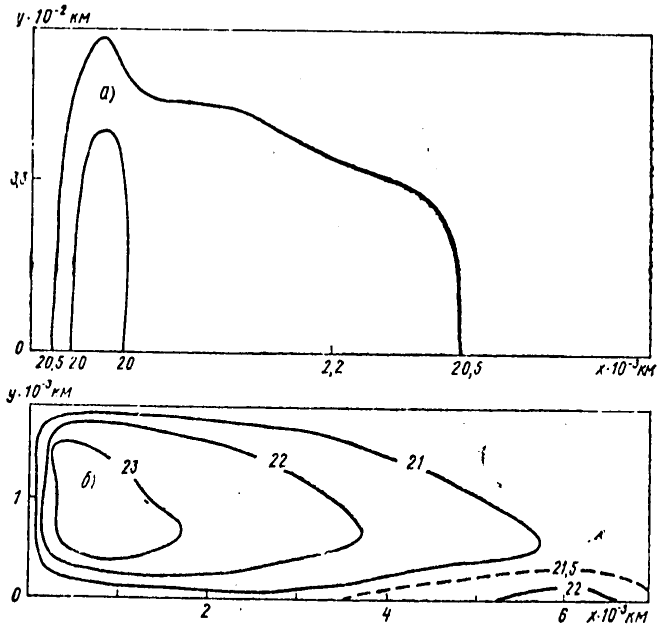

Fig. 1. T_0 distribution with stipulated constant temperature at three boundaries of basin. a) according to results of numerical experiment with allowance for h, b) from [7] (scale not maintained).

The temperature gradients in our experiment are considerably less than the values obtained in [7]. This is attributable to two factors. First, the heat flow at the lower boundary of the QHL (in [7] serving as the surface heat flow) in our variant is about 10^{-3} cal/(cm^2·sec), which is an order of magnitude less than the value adopted in [7]. In order to obtain $q_h \sim 10^{-2}$ cal/(cm^2·sec) we must increase k_T by an order of magnitude, which contradicts the generally accepted evaluations. Second, a considerable contribution to the baroclinic pressure gradient is made by the h gradient, in the absence of which the role of the T_0 gradients is exaggerated. In particular, the conclusion is drawn in [7] that there is an unambiguous relationship between the equatorial subsurface countercurrent and the T_0 gradient in a zonal direction. In our case an equally important role is played by the h gradients.

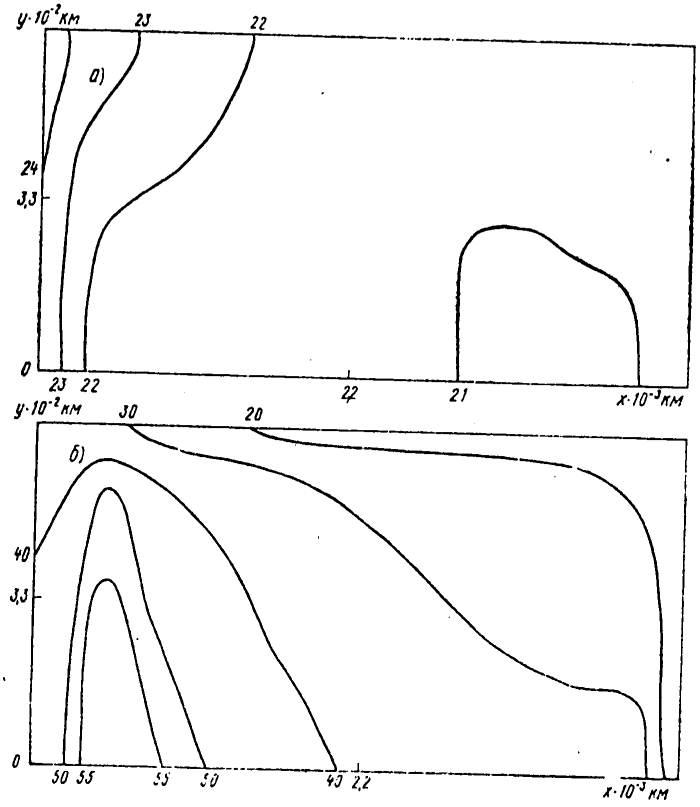

Fig. 2. Distribution of temperature (a) and thickness of QHL (b) with variable T_0 and h at boundaries.

In order to clarify the possibilities of the proposed model for adequately describing the large-scale characteristics of distribution of QHL parameters we carried out a numerical experiment with boundary conditions simulating the real T_0 and h distribution [13]. In a zonal direction there is stipulation of a temperature drop of 3.5°C and a thickness of the QHL of 35 m. Figure 2 gives the results of computations with $\tau = -0.2$ dyne/cm^2 and $\lambda = 2 \cdot 10^{-5}$ sec^{-1}. At the eastern wall a boundary layer is formed which is expressed both in the T_0 field and in the h field. S_x^h at the equator attains values $3.1 \cdot 10^5$ cm^2/sec with a QHL thickness equal to 49 m. This result agrees rather well with observational data. There is poorer description of the effect of a decrease in the thickness of the QHL and a decrease in temperature with approach to the equator. It is known [13] that the dropoff in thickness of the QHL in a meridional direction within the limits of a 2-3° zone near the equator attains tens of meters and temperature -- more than one degree. The computations give values which are an

order of magnitude less. The main reason for this is evidently the neglecting of the vertical advection of heat within the limits of the QHL. In actuality, the vertical and horizontal advection values have the same order of magnitude for the real conditions existing in the equatorial zone.

It is interesting that the local characteristics of the wind field are the main reason determining the observable peculiarities in distribution of thickness of the QHL. With any wind of an easterly direction the thickness of the QHL increases from east to west.

Conclusions

1. The characteristics of the QHL in the equatorial zone are closely related to large-scale circulation. This is manifested, in particular, in a relatively weak dependence of temperature and the thickness of the QHL on local conditions at the ocean surface.

2. Zonal nonuniformity of the wind (intensification from east to west) increases the zonal baroclinic pressure gradient and thereby intensifies the equatorial subsurface countercurrent.

3. Within the framework of this formulation the gradients of thickness of the QHL are an important factor forming the baroclinic pressure gradient.

4. The proposed model for the most part correctly describes the large-scale peculiarities of characteristics of the QHL in the equatorial zone of the ocean. The principal shortcoming of such models applicable to the equatorial zone evidently must be considered the neglecting of the vertical advection of heat in the QHL.

In conclusion I express sincere appreciation to N. B. Shapiro and A. A. Serebryakov for assistance in the work and useful comments.

BIBLIOGRAPHY

1. Aksenov, A. V., Muzylev, S. V., Fel'zenbaum, A. I., "On the Theory of Emergence of the Equatorial Deep Countercurrent at the Ocean Surface," DOKLADY AN SSSR (Reports of the USSR Academy of Sciences), Vol 245, No 3, 1979.

2. ATLAS TEPLOVOGO BALANSA OKEANOV (Atlas of the Heat Balance of the Oceans), Morskoy Gidrofizicheskiy Institut, Sevastopol', 1970.

3. Barenblatt, G. I., "Self-Similarity in the Distribution of Temperature and Salinity in the Upper Thermocline," IZV. AN SSSR, FIZIKA ATMOSFERY I OKEANA (News of the USSR Academy of Sciences, Physics of the Atmosphere and Ocean), Vol 14, No 11, 1978.

4. Gutman, L. N., "Large-Scale Currents in a Baroclinic Ocean," IZV. AN SSSR, FIZIKA ATMOSFERY I OKEANA, Vol 6, No 9, 1970.

5. Kitaygorodskiy, S. A., Filyushkin, S. N., "Temperature Jump Layer in the Ocean," TRUDY IO AN SSSR (Transactions of the Institute of Oceanology USSR Academy of Sciences), Vol 16, 1963.

6. Korotayev, G. K., Mikhaylova, E. N., Shapiro, N. B., "On the Theory of Large-Scale Circulation in a Baroclinic Ocean," SB. MGI AN UkrSSR (Collection of Papers of the Marine Hydrophysical Institute Ukrainian Academy of Sciences), No 3(70), 1975.

7. Kosnyrev, V. K., Kuftarkov, Yu. M., "On the Theory of a Baroclinic Ocean Including the Equator," SB. MGI AN UkrSSR, No 3(70), 1975.

8. Lineykin, P. S., "Solution of the Boundary Value Problem in the Theory of Ocean Currents," METEOROLOGIYA I GIDROLOGIYA (Meteorology and Hydrology), No 12, 1970.

9. Lineykin, P. S., Maderich, V. S., "Dynamics of Oceanic Circulation," OKEANOLOGIYA (Oceanology), Vol 4, 1977.

10. Mikhaylova, E. N., Shapiro, N. B., "On the Problem of the Influence of Baroclinicity on Currents in the Equatorial Zone of the Ocean," SB. MGI AN UkrSSR, No 3(49), 1969.

11. Khanaychenko, N. K., SISTEMA EKVATORIAL'NYKH PROTIVOTECHENIY V OKEANE (System of Equatorial Countercurrents in the Ocean), Leningrad, Gidrometeoizdat, 1974.

12. Khlystov, N. Z., "Structure of Waters in the Tropical Zone of the Atlantic Ocean," SB. MGI AN UkrSSR, No 3(53), 1971.

13. Shapkina, V. F., "Density and Pressure Fields in the Equatorial Zone of the Atlantic Ocean," TECHENIYE LOMONOSOVA (Lomonosov Current), Kiev, Naukova Dumka, 1966.

14. Alexander, R. C., Kim, J. W., "Diagnostic Model Study of Mixed Layer Depths in the Summer North Pacific," J. PHYS. OCEANOGR., Vol 6, 1976.

15. Nedler, G. T., "A Model for the Thermohaline Circulation in an Ocean of Finite Depth," J. MARINE RES., Vol 25, No 3, 1967.

16. Niiler, P. P., Dubbelday, P. S., "Circulation in a Wind-Swept and Cooled Ocean," J. MARINE RES., Vol 28, No 2, 1970.

17. Philander, S. G., "Equatorial Undercurrent Measurements and Theories," REV. GEOPHYS. SPACE PHYS., Vol 13, No 3, 1973.

18. Reid, R. D., "A Model of the Vertical Structure of Mass in Equatorial Wind-Driven Currents of a Baroclinic Ocean," J. MARINE RES., Vol 7, No 3, 1948.

19. Veronis, G., "On Theoretical Models of the Thermocline Circulation," DEEP-SEA RES., Suppl. to Vol 16, 1969.

UDC 551.467.3(98)

OPPOSITION IN ICE REDISTRIBUTION IN THE WATERS OF THE FOREIGN ARCTIC

Moscow METEOROLOGIYA I GIDROLOGIYA in Russian No 3, Mar 80 pp 73-77

[Article by Candidate of Geographical Sciences V. I. Smirnov, Arctic and Antarctic Scientific Research Institute, submitted for publication 12 July 1979]

Abstract: The presence of an opposition in the redistribution of ice in the western and eastern regions of waters of the foreign Arctic has been detected. This opposition is manifested in the ice coverage and areas of ice masses. The opposition is manifested with particular clarity in the displacements of the Baffin and Alaskan ice masses. The mechanism of opposition formation is described.

[Text] The "mirror reflection" in the course of ice coverage in the Chukchi and Barents Seas was discovered by V. Yu. Vize [1] at the beginning of the 1920's. Then he suggested that this property is characteristic of ice conditions in the near-Pacific Ocean and near-Atlantic Ocean parts of the Arctic Ocean. Proof of such an opposition in ice conditions later was published by V. Itin [6].

In his classical study devoted to the principles of long-range ice forecasts for arctic seas, V. Yu. Vize [2] confirmed the presence of this opposition in ice conditions of the near-Atlantic and near-Pacific parts of the Arctic Ocean. And whereas in his first study [1] in 1926 he felt that the reason for the opposition was oscillation of the arctic wind divide, later [2], in 1944, he stated that changes in the intensity of atmospheric circulation are the reason for the opposition.

The reality of existence of the opposition between ice conditions in the western and eastern regions of the Soviet Arctic after almost 30 years of accumulation of observational data on ice was mentioned in the studies of N. A. Volkov and B. A. Sleptsov-Shevlevich [3], Yu. V. Nikolayev, E. I. Sarkhanyan [7] and V. F. Zakharov [4, 5], who examined the presence of an

opposition between the near-Pacific Ocean and near-Atlantic parts of the Arctic Ocean in the examples of the variability of their ice content, ice continuity, times of onset of ice formation, quantity of pack ice and variability of its boundaries, air pressure differences at representative stations and air temperature differences. The near-Atlantic part includes the Kara Sea, Laptev Sea and the western part of the East Siberian Sea; in the near-Pacific Ocean part -- the eastern part of the East Siberian Sea and the southwestern part of the Chukchi Sea.

The opposition in the redistribution of ice conditions in the western (eastern part of the Chukchi Sea and the Beaufort Sea) and eastern (Baffin Sea, Greenland Sea and Davis Strait) regions of the foreign Arctic was for the first time discovered by the author in an analysis of displacements of ice masses [8]. It was found that in 14 of 17 cases (82%) with favorable or unfavorable displacements of the Alaskan ice mass the displacements of the Baffin ice mass were opposite in sign. For example, in 1955 the Alaskan ice mass in June-October occupied southerly positions unfavorable in navigational respects, with its southern periphery toward the shore. The total extent of the "bridges" of solid ice in this sector of the Northwestern Sea Route during the entire period attained 200 miles.

On the other hand, the displacements of the Baffin ice mass during June-September 1955 were extremely favorable. Already in the second 10-day period in June the mass was displaced to a westerly position and between its eastern periphery and the shores of Greenland there was rarefied ice or open water. The width of this zone attained 50 miles or more. Beginning in mid-June ships could sail to Lancaster Strait without assistance of an icebreaker.

During the navigation season of 1968 extremely favorable displacements of the Alaskan ice mass made the movement of ships possible at an extremely early time (from the second half of July) without the accompaniment of an icebreaker. Open water was observed most frequently before November between the shore and the southern periphery of the mass. The width of this zone was 30-100 miles or more. The displacements of the Baffin ice mass were unfavorable in 1968. The ice mass withdrew from the shores of Greenland at an extremely late time -- late in July. The navigation of ships without icebreakers became possible only in late July - early August. The difference between the times of beginning of ship navigation in this sector without icebreakers in 1955 and 1968 was about 1.5 months.

Opposition in displacements of the masses was attributed to differences in the intensity of anticyclonic drift of ice in the Arctic basin and a drift flow of ice into the strait between Greenland and Spitzbergen. It was postulated that such a variability in the directions and rates of drift does not occur in individual small sectors, but with the drift current as a whole or with the eastern or western branches of anticyclonic drift.

The mechanism of the effect of the East Greenland ice flow seemed to be as follows. With its intensification there will be unfavorable displacements of the Greenland eastern and Greenland northern ice masses and an increase in their area. Since this process is accompanied by an intensification of the East Greenland Current, there will be an intensification of the West Greenland Current, and as a result, the Canadian and Labrador Currents, which in turn leads to an unfavorable displacement of the Baffin ice mass. But the manifestation of individual elements of this process may also be asynchronous. On the other hand, with a weakening of the flow there can be favorable displacements of all the eastern ice masses.

A subsequent analysis of the redistribution of ice conditions in June-October in the western and eastern regions indicated that the opposition is also manifested in ice content, areas of the ice masses and other characteristics of ice conditions. Thus, the relationship of the ice content of the Beaufort Sea in August and the Greenland Sea in July has the opposite sign. Its guaranteed probability is 73% with an admissible error of ±20% in the amplitude of changes in the ice content of the Greenland Sea in July.

A comparison of the areas of the Alaskan ice mass in September and the Baffin ice mass in July also confirms the presence of an opposition. In 10 cases of 14 (71%) with the area of one ice mass greater than or less than the mean annual value, the area of the other had the opposite sign of the anomaly. This correlation has a guaranteed probability of 79% with an admissible error ±20% in the amplitude of the changes in the area of the Alaskan ice mass in September.

This phenomenon is most indicative in the example of the relationship of changes in the area of the Alaskan ice mass with the outward transport of ice of thousands of square kilometers from the Arctic basin into the Greenland Sea. For example, the correlation between the area of the Alaskan ice mass in July and the transport of ice into the Greenland Sea in June and July has the opposite sign with a guaranteed probability 75%. The correlation between the area of the Alaskan ice mass in August with the transport of ice in June-July has a guaranteed probability 87%, and in September -- with the mean transport during the period of the preceding October - September of the current year -- 80%.

All these correlations once again confirm that the opposition between the redistribution of ice in the western and eastern Greenland regions is a consequence of changes in the intensity of the transporting flow, and also anticyclonic drift as a whole, and not in their individual sectors and is manifested in changes in the direction and velocity of ice drift, the width of the transporting flow and other phenomena observable with synchronous movements of drifting stations, buoys and ice islands.

Such an "opposition" distribution of anomalies of ice content and the area of ice masses in the western and eastern regions occurs most frequently with some time shift, on the average equal to one or two months. In such cases the sign of the anomaly in the eastern region is formed sooner than the opposite sign in the western region.

In addition, the forming of the sign of anomalies in the eastern region is caused by atmospheric processes in the northern part of the central region. A confirmation of this is the correlations between changes in the area of the Baffin ice mass in June and July and the sums of mean monthly differences of air pressure in January-June along the line Cambridge Bay-Alert. Whereas in January-June there was a predominance of air flows of the westerly quadrant, in June and July the area of the Baffin ice mass in approximately 80% of the cases exceeded the mean long-term area by a value equal to half the positive sum of the mean monthly pressure differences for January-June. In the case of a positive sum of the pressure differences (predominance of air flows of the easterly quadrant) the area of the ice mass was less than the mean long-term area on the average equal to half this sum.

With the prevalence of colder westerly flows in January-June the Baffin ice mass increases not only in its area, but also with respect to the thickness of the ice from which it is formed. As a result, it also persists a longer time in unfavorable positions. However, the predominance of less cold flows of the easterly quadrant causes the formation of anomalies of the other sign.

As already mentioned, the Baffin ice mass consists primarily of one-year ice. The perennial ice predominating in the Canadian northern, Greenland northern and Greenland eastern ice masses replenishes Baffin ice in extremely insignificant quantities. This gives reason for assuming that the opposition in the redistribution of ice conditions in the western and eastern regions to a high degree is caused by atmospheric processes in the northern parts of the central and eastern regions.

The opposition in the redistribution of ice conditions in the western and eastern regions, in addition to all else, can also be used for prognostic purposes. The presence of a time shift in the forming of a particular sign of the anomaly makes it possible, in particular, already in June, using the known area of the Baffin ice mass, to judge the possible area of the Alaskan ice mass in July or on the basis of the ice content of the Greenland Sea in July to judge the ice content of the Beaufort Sea in August. With a high probable success the prognostic dependences for one of the regions can be used for predicting the redistribution of ice in other regions.

The ascertained reasons for the opposition in the redistribution of ice in the western and eastern regions once again confirm that the principal factor responsible for the existence of ice masses in the waters of the foreign Arctic is the outflowing cold currents, transporting ice from the Arctic Ocean or its seas. However, there are peculiarities in the formation and existence of each of the ice masses.

For example, the Alaskan ice mass is formed due to the stable runoff of ice along the eastern branch of an anticyclonic drift. According to data from observations of drift made by American stations (T-3, ARLIS-2, and

others), buoys and ice islands, the general direction of their displacement during all the years of observations in the region between 73 and 80°N was toward the southwest. The possible width of the ice flow was not less than 200 miles. In the region 72-73°N this flow turns toward the west. This turning is caused in winter by the presence of ice along the shore, and in summer by the prevailing winds of the easterly quadrant and the backwater of the Mackenzie River. Thus, the year-round existence of the Alaskan ice mass is caused by the temporal stability of the southwesterly transport of ice along the easterly branch of an anticyclonic drift. Several peculiarities of this transport can be pointed out.

It is possible that the drift velocity in winter is greater than in summer. For example, the drift of T-3 in April-September was slower in comparison with the drift in October-March. As an average for four half-years the drift velocity in April-September was 1.6 mile/day and in October-March — 2.2 miles/day. However, the velocity of the southwesterly drift of four ice islands forming near Ward Hunt Island in August 1961 - April 1962, according to data for June - September 1963-1967, on the average was the same as during the period October-May -- about 2.0 mile/day.

If the movements of individual ice islands (T-1, T-3) and stations (SP-2, 3, 11, 12, 16) are considered, in the anticyclonic drift it is possible to discriminate two ellipsoidal orbits with a common center in the region 77-78°N, 145-150°W. The longer axis of the outer orbit passes approximately along the meridian 150°W and in the case of the inner orbit -- along the parallel 78°N. On the average their extent is about 1000 and 500-700 miles respectively. The extent of the shorter axes is about 800 and 400-500 miles respectively.

A zone of unstable ice drifts in these orbits is observed in their northeastern parts. In these areas there can also be drifts of different directions. For example, during the period August 1961-April 1962 four of the five ice islands forming in the neighborhood of Ward Hunt Island began to drift toward the southwest, whereas the other (the largest, with an area of about 200 km^2) began to drift to the east and the southeast. In the northeastern parts of the orbits, bounded by 85-87°N and 90 and 140° W (outer orbit), 80 and 83°N and 120 and 150°W (inner orbit) in different years there were drifts of stations and ice islands to the northeast, east, southeast, south and southwest. In addition, these regions are more slowly moving. The mean ice drift velocities rarely exceed one mile per day.

A southeasterly branching off from the easterly branch of the anticyclonic drift causes the formation of the Canadian northern ice mass. It is situated in very extensive straits and bays in the Canadian Arctic Archipelago. The existence of this ice mass is caused by the stability of ice drift direction and velocity with time. The velocity of the southeasterly ice

flow in the northern part of the northwestern straits, according to data on the drift of ice islands during 1962-1966, is about 0.5 mile/day, whereas the velocity of the southerly flow in the southern part of the straits is 0.2-0.3 mile/day.

The Greenland northern ice mass is formed due to the presence of a branching of the transarctic ice flow directed into Lincoln Sea, and easterly drift along the northern shore of Ellesmere Island. The Greenland eastern ice mass -- this to all intents and purposes is the East Greenland ice flow. The mean velocity of ice drift is about 4 miles/day.

The formation and existence of the Baffin ice mass is influenced to an appreciable degree by the Canadian cold current, transporting ice along Baffin Island and the Labrador peninsula. With an increase in ice drift velocity during winter there is an increase in ice productivity in the mass, whereas in summer there is an increase in ice discharge. With a decrease in drift velocity in winter there is an increase in the mean thickness of the ice. In summer there is a decrease in ice discharge. The mean velocity of drift of the ice islands during 1963-1964 was about 6 miles/day.

It is characteristic that the directions and velocities of drift of ice islands agree well with the directions and velocities of cold currents which transport them. The drift velocities of ice islands, in addition, are dependent on the distribution of ice conditions in the region of their drift. With an ice continuity up to 10 units, the presence in this case of up to 7-8 units of perennial ice, as well as large fields of ice breccia (northwesterly straits), the drift velocity is minimum (averaging 0.2-0.5 mile/day). With a continuity of one-year ice of 9-10 units or less (Baffin ice mass) the velocity of its drift is maximum (averaging about 6 miles/day).

We should note the inertness in changes in the directions and velocities of currents in comparison with atmospheric processes. However, the redistribution of ice to a greater degree than currents is subject to the influence of variability of atmospheric processes and especially during summer. This must be taken into account in preparing ice forecasts.

A good indicator of ice redistributions during summer is ice navigation characteristics: rate of movement of ships, times required for their passage along individual sectors of the northwestern sea route. An analysis of ice navigation characteristics on the basis of data from ice voyages of ships in the waters of the foreign Arctic in the 16th-19th centuries and the beginning of the 20th century has shown that superanomalous redistributions of ice conditions did not occur during these periods. It can therefore be postulated that the detected mechanism of interaction between the atmosphere, ocean and sea ice has been operative in these waters for not less than 600 years.

BIBLIOGRAPHY

1. Vize, V. Yu., GIDROLOGICHESKIY OCHERK MORYA LAPTEVYKH I VOSTOCHNO-SIBIRSKOGO; MATERIALY KOMISSII PO IZUCHENIYU YAKUTSKOY ASSR (Hydrological Outline of the Laptev and East Siberian Seas; Materials of the Commission on Study of the Yakutian ASSR), No 5, Leningrad, Izd-vo AN SSSR, 1926.

2. Vize, V. Yu., OSNOVY DOLGOSROCHNYKH LEDOVYKH PROGNOZOV DLYA ARKTICHESKIKH MOREY (Principles for Long-Range Ice Forecasts for Arctic Seas), Moscow, Izd-vo Glavsevmorputi, 1944.

3. Volkov, N. A., Sleptsov-Shevlevich, B. A., "Cyclicity in Variations of Ice Content of Arctic Seas," TRUDY AANII (Transactions of the Arctic and Antarctic Scientific Research Institute), Vol 303, 1971.

4. Zakharov, V. F., "Ice Opposition," TRUDY AANII (Transactions of the Arctic and Antarctic Scientific Research Institute), Vol 320, 1976.

5. Zakharov, V. F., "Cooling of the Arctic and the Ice Cover of Arctic Seas," TRUDY AANII, Vol 337, 1976.

6. Itin, V., MORSKIYE PUTI SOVETSKOY ARKTIKI (Sea Routes of the Soviet Arctic), Moscow, Sovetskaya Aziya, 1933.

7. Nikolayev, Yu. V., Sarukhanyan, E. I., "Application of the Main Components Method in Study of Long-Term Variations in the Ice Content of Arctic Seas," TRUDY AANII, Vol 307, 1973.

8. Smirnov, V. I., LEDOVYYE USLOVIYA PLAVANIYA SUDOV V VODAKH KANADSKO-ALYASKINSKOY ARKTIKI (Ice Conditions for the Navigation of Ships in the Waters of the Canadian-Alaskan Arctic), Leningrad, Gidrometeoizdat, 1974.

UDC 556.16

METHODS FOR REGIME AND OPERATIONAL DETERMINATION OF RIVER RUNOFF

Moscow METEOROLOGIYA I GIDROLOGIYA in Russian No 3, Mar 80 pp 78-88

[Article by Doctor of Technical Sciences I. F. Karasev, State Hydrological Institute, submitted for publication 28 August 1979]

Abstract: Modern methods for determining runoff on the basis of hydrometric data are generalized and analytically interpreted. The various aspects of determination of runoff are defined as applicable to the purposeful use of the determined characteristics: for regime generalizations and operational servicing of the national economy.

[Text] Hydrometric determination of runoff is the basic source of information on water resources and the hydrological regime of rivers. Its importance has increased considerably under modern conditions as a result of introduction of the system for the state determination of waters and water inventory, broadening of operational servicing of the national economy and monitoring of the environment. In accordance with the directions in use of hydrometric data the determination of runoff is accomplished in two variants: regime and operational. Although these variants of runoff determination were established a long time ago, up to the present time there is no needed clarity as to their difference, on the one hand, and on the methodological advantages, on the other. Moreover, there is a gap between regime and operational determinations of runoff and these determinations are made in different organizations: regime determinations at data processing and storage centers and operational determinations in forecasting divisions. Operational data on runoff, as becomes clear at the end of a year, in many cases differ by 30-50% from the values published in regime publications.

As is well known, the determination of runoff at river posts is based on discrete measurements of discharges and continuous observations of water levels; this makes it possible to reproduce the runoff hydrograph as a series of daily water discharges (DWD).

In the regime variant the runoff is computed at the end of the annual cycle, so to speak at the last minute, when the entire mass of measurements is available. There are many methods for the regime determination of runoff (more than 20), which to some degree is attributable to the diversity of factors determining the channel capacity. But to a considerable degree this is attributable to the isolation of development work carried out at different times.

Operational determination is necessary for hydrological forecasts and the current monitoring of water volume in rivers. When there is a stable correlation between discharges and levels the DWD determination presents no difficulties -- it is sufficient that they be taken directly from the discharge curve Q(H). The task is considerably complicated when there is an ambiguous dependence between discharges and levels caused by a variable backwater, channel deformations, ice formation and other factors changing the hydraulic conditions for movement of the flow. In these cases the operational computation of the daily discharges requires extrapolation of the characteristics of channel capacity, registered on the basis of the results of the preceding measurement. Ill-suited for solution of such problems are the still-employed Stout, Bolster and other time curve methods in which a major role is played by subjective elements and even "aesthetic considerations" [7]. The artificiality and schematic nature of such procedures are becoming particularly obvious with a reduction (for economic reasons) in the frequency of measurements at hydrological posts. It would be improper to use these procedures, impoverished in physical content, for work with an electronic computer.

The perfection and physical soundness of models for determining runoff should be determined by the possibility of their use for both regime and operational purposes. Recently such models have been created in the Hydrometry Division of the State Hydrological Institute [3]. They are based on the capacity of the channel registered in the measurement of discharges and factors determining it in the interval between these measurements.

In the case of an unambiguous relationship between discharges and levels in a stable channel the DWD are determined on the basis of the Q(H) curve or the measured discharges by levels

$$Q = a_0 + a_1 H + \ldots + a_m H^m. \qquad (1)$$

The parameters of equation (1) are computed by the least squares method with $2 \leqslant m \leqslant 4$.

The analytical structure of models for determining runoff is substantially complicated with an increase in the number of factors taken into account. In this case it is desirable to use a multiple linear regression equation of a general form in which, in addition to the levels it is also necessary

to include other observational data characterizing the factors on which the channel capacity is dependent:

$$Y = a_0 + \sum_{i=1}^{i=N} X_i, \qquad (2)$$

where X_i represents both the directly measured values and different nonlinear functions of them. It was demonstrated in [5] that the inclusion of nonlinear terms in transformed form in the linear regression equation considerably broadens the possibilities of regression analysis.

Now we will examine some models of hydrometric determination of runoff applicable to factors creating ambiguity in the relationship between discharges and water levels, such as a change in hydraulic conditions (variable backwater and unsteady movement), channel deformation and the appearance of seasonal obstacles in it (ice formation and overgrowth).

In the case of a variable backwater, which is observed in the tail zones of reservoirs and above the inflow of large tributaries into the main river, the regression equation (2) with Y = Q includes the readings of the levels at two successive posts -- at the upper $X_1 = H_{up}$, $X_2 = H_{up}^2$ and lower $X_3 = H_{low}$ (the last factor reflects the changing slope of the free surface).

If the upper hydrometric post is the entry post for the reservoir, the flow velocities in it must exceed by at least a factor of two the initial velocity of the hydrometric current meters, that is, will be not less than 8-10 cm/sec. With respect to the lower post, insofar as possible it should be outside the zone of considerable level disturbances associated with wind-induced level rises and drops and the passage of waves from the movement of water masses related to the change in discharges at the posts at hydroelectric power stations.

A special problem is the determination of the inertial effects of unsteady flow movement. In these cases the International Standard ISO-1100-73 recommends use of the Jones formula, which applicable to equation (2) forms the variables:

$$Y = \frac{Q_p}{Q_0}, \quad X_i = \sqrt{1 + \frac{B}{I_0\left(\frac{\Delta Q}{\Delta z}\right)}\frac{\Delta z}{\Delta t}},$$

where Q_0 and I_0 are the water discharge and the slope of the free surface in the case of steady movement, B is channel width, ΔQ and Δz are the increments of discharge and level respectively during the time interval Δt.

The determination of runoff becomes especially complex in the presence of obstacles to flow movement -- ice formation and channel overgrowth.

Applicable to the peculiarities of determination of runoff during winter and transitional periods, it is necessary to distinguish four types of river regime: I -- ice formation without formation of solid ice (frazil

ice); II -- unstable ice cover; III -- prolonged stable ice cover; IV -- refreezing and ice incrustation.

One of the most commonly used methods for determining runoff in the case of a stable ice cover is based on the relative characteristic of channel capacity

$$K_{win} = Q_{win}/Q_0,$$

where Q_{win} is the measured winter water discharge with the level H, Q_0 is the water discharge in an open channel corresponding to this level.

The hydraulic dependence for K_{win} is represented by the Chezy-Manning formula

[ЗИМ = win; ЛЛ = ice]
$$K_{зим} = m_1\left(1 - \frac{\omega_л}{\omega_0}\right)^{2/3} \frac{n_0}{n_{зим}} \left(\frac{I_{зим}}{I_0}\right)^{0,5}, \quad (3)$$

where ω_{ice} is the area of the submerged ice, ω_0 and n_0 are the cross-sectional area and the roughness coefficient for an open channel, n_{win} is the generalized roughness coefficient, I_0 and I_{win} are the slopes of an open flow and a flow covered with ice, m is a coefficient taking into account the relationship of the geometrical characteristics of the cross section in the presence of ice formations.

In the absence of ice jam or overgrowth blockage it can be assumed that $I_0 = I_{win}$. If such an equality is not guaranteed, for example, at the entry posts of reservoirs, as the "control" dependence for determining K_{win} we use a regression equation in which the water discharge is set in accordance with the two levels at the conjugate posts H_{up} and H_{low}.

It is more difficult to evaluate the dynamics of changes in channel roughness under the ice: the n_{win} value varies from the maximum values during the initial period of ice formation to minimum values at its end. In the case of a free channel, both directly prior to the onset of ice phenomena and after opening-up of the river $n_0/n_{win} = 1$. These regularities in the change in n_0/n_{win} are described by the following empirical function of time:

[ЗИМ = win; ЛЛ = ice]
$$n_0/n_{зим} = 1 - m_2\beta_л e^{-5,3_л}, \quad (4)$$

where $\beta_{ice} = T/T_{ice}$ (T is the time from the onset of ice cover, T_{ice} is the duration of ice cover.

If the function (3) is expanded into a Maclaurin series, limiting ourselves to the first two terms, and the representation (4) is used, then applicable to equation (2) we obtain the following set of variables X_i, on which $Y = K_{win}$ is dependent:

-- the roughness factor, represented as a factor of time,

$$X_1 = \beta_1 e^{-5\omega_1};$$

-- the factor of restriction of the channel by ice

$$X_2 = \omega_1/\omega_0; \quad X_4 = \omega_1^2/\omega_0^2;$$

-- mixed factors

$$X_3 = \frac{\omega_1}{\omega_0}\ \beta_1 e^{-5\omega_1}; \quad X_5 = \frac{\omega_1^2}{\omega_0^2}\ \beta_1 e^{-5\omega_1}.$$

As is well known, ice thickness is not measured daily, but is dependent on the sums of the absolute values of the negative air temperatures t^0_{air}, which makes it possible in each of the complex arguments $X_2,\ldots,X_5$ in place of ω_{ice} to introduce $B_0\sqrt{|\Sigma t^0_{air}|}$. The structure of the hydraulic-meteorological model for the determination of winter runoff was so determined (its idea was proposed for the first time by A. V. Ogiyevskiy).

In the case of unstable ice formation and ice jam-overgrowth blockage, when the river levels in many cases are above the spring-summer levels, the coefficient K_{win} loses its definiteness. In these cases it is feasible to rely directly on the Chezy-Manning formula, which after reduction to logarithmic form makes it possible to obtain the following composition of variables of equation (2):

$$Y = \lg Q; \tag{5}$$

$$X_1 = \lg \omega_{зим}; \quad X_2 = \lg h_{зим}; \quad X_3 = \sqrt{|\Sigma t_0|}.$$

[B = air; ЗИМ = win]

The regression equations are computed separately for each period of ice formation.

In addition to the hydraulic dependences, in creating models of hydrometric determination of runoff it is also possible to use general physical laws for the water regime of rivers during winter. One of the peculiarities of the hydrograph in stable winters without thaws is a dropoff in water discharge with a decrease in moisture reserves in the basin. The exhaustion - hydrograph dropoff curve is effectively described by the Boussinesq formula, used in directly establishing the analytical basis of the model for determining runoff

$$\frac{Q_0}{Q} = a_0 + a_1 T + a_2 T^2. \tag{6}$$

Here Q_0 is the last of the discharges measured with an open channel, a_1 and a_2 are regression coefficients expressing the regularities in dropoff of water supply, in particular, exhaustion of ground water supply.

A model based on the regularities of decrease in winter runoff was especially effective for mountain watercourses carrying frazil ice and refreezing rivers with ice encrustations. In the latter case, in addition to the

dependence for the decrease in water discharges, it was necessary to introduce the time function expressing the runoff loss in ice formation and the formation of ice encrustations. The model for determining runoff became more complex and assumed the form

$$[\text{c = dropoff}] \quad Q = \frac{Q_0}{(1 + a_0 T)^3} \left| a_0 + a_1 \frac{T}{T_c} + a_2 \left(\frac{T}{T_c}\right)^2 + \ldots + a_m \left(\frac{T}{T_c}\right)^m \right|, \quad (7)$$

where $T_{dropoff}$ is the duration of the period of the hydrograph dropoff branch. The second term on the right-hand side takes into account the losses of runoff on ice formation.

We will emphasize an important merit of models (6) and (7): they rest on the discharges Q_0, measured with a still-open channel, which are more precise than the results of subsequent measurements, especially when there is frazil ice, ice encrustations and refreezing of the channel.

After the renewal of runoff in the prespring period the DWD are computed on the basis of an exponential approximation of the ascending branch of the hydrograph

$$Q = Q_{min} e^Y, \quad (8)$$

where Y expresses the regularity of change in discharges with time T, reckoned from the onset of rise in water volume

$$Y = \ln Q/Q_{min} = a_0 + a_1 T.$$

The hydrochemical model of runoff determination is especially effective in the service for monitoring water quality in winter. It uses the inverse relationship between mineralization S and water discharges Q with H levels in a channel covered by ice. From the conditions of balance of dissolved substances we can obtain

$$Q = a_0 + \frac{a_1}{H} + a_2 \frac{H}{S}. \quad (9)$$

The model (9) would not be rational for use in computing the DWD: this would require time-consuming analyses of the daily water samples. But if equation (9) was obtained using data from earlier measurements, its merit is that it makes it possible to determine discharges in each sampling for monitoring the quality of water at posts where regular runoff observations are not made.

During the warm season of the year additional resistances to the movement of flow are created by water-loving vegetation. As is well known, in evaluating the channel capacity when it is overgrown use is made of the coefficient

$$K_{over} = Q_{over}/Q_0,$$

where Q_{over} and Q_0 are the discharges in the overgrown and free channels with one and the same level H.

In this case as well the analytical structure of the model for determining runoff follows from the Chezy-Manning formula, taking into account the changing channel resistances as the biomass develops. Its growth is proportional to the root of the sum of mean daily water temperatures t° and begins after their transition through some threshold value (10°C for the middle zone of the European USSR). At the same time there is an aging and dying-out of first a part, and then the entire mass of water-loving plants. Accordingly, in addition to determination of the thermal factor in flow restriction it is necessary to introduce some empirical function of time in order to describe the influence of "development-aging" of biomass on the roughness coefficient n_{over}:

$$n_{over} = n_0(1 - \beta + \beta^{4/3}),$$

where $\beta = T/T_{over}$ (T is time from the onset of overgrowth, T_{over} is the total period of existence of vegetation in the flow).

The complex of variables, established from the Chezy-Manning formula, applicable to equation (2), is as follows:

$$Y = K_{over};$$

$$X_1 = \beta; \quad X_2 = \beta^{4/3}; \quad X_3 = \frac{B_0\sqrt{T}}{\omega_0}; \qquad (10)$$

$$X_4 = \frac{\beta B_0\sqrt{\Sigma t}}{\omega_0}; \quad X_5 = \frac{\beta^{4/3} B_0\sqrt{\Sigma t}}{\omega_0}.$$

The general regression equation (2) with the considered complexes of determining factors gives only a first approximation to the DWD values. They can be substantially refined if we also take into account the so-called "regression residuals" which characterize the relative deviations of the discharges $Q_{meas\ j}$ from the $Q_{comp\ j}$ values obtained using equation (2) on the measurement date:

[м = meas; p = comp]

$$\tilde{q}_j = \frac{Q_{м_j} - Q_{p_j}}{Q_{p_j}}. \qquad (11)$$

An example of refinement of the model for determining runoff, based on the general regression equation (2), will be examined applicable to one of the most complex cases -- an easily deformed river channel of the Amu-dar'ya type, where the scatter of the Q(H) correlation is 25-30%.

A series of measured discharges makes it possible to obtain a chronological sequence of discrete values qj, which within the limits of an individually taken phase of the hydrological regime can be considered a realization of a quasistationary random process $\tilde{q}(t)$. Its statistical characteristics are: mathematical expectation $m_q = 0$, dispersion $D_{\tilde{q}} = \sigma_q^2$ (the

line at top is the symbol for averaging of the set $\tilde{q}_j$) and the autocorrelation function $r_q(t)$. These characteristics are obtained on the basis of measurements of water discharges, made with an increased frequency, carried out in the course of phase-homogeneous (high- and low-water) periods.

The $\tilde{q}_j$ values by one method or another must be interpolated in the interval between measurements τ_{meas}. It is best to use the so-called optimum interpolation of elements developed by L. S. Gandin applicable to meteorological fields and processes [2]. The $\tilde{q}_{int}$ value on any date in the interval between the measurements is represented in the form of the sum of the weighted results of measurements of the $\tilde{q}_j$ values:

$$\tilde{q}_{int} = \sum_{j=2}^{j=N} P_j \tilde{q}_j. \tag{12}$$

The weighting factors P_j are dependent on the discreteness interval τ_{meas} and the time at which the interpolation is carried out. The formulas for determining P_j also include the above-mentioned statistical characteristics [2, 3]. The number of terms in the sum (9) is limited to the two successive values $\tilde{q}_j$ and $\tilde{q}_j + 1$.

Thus, the refined model for hydrometric determination of runoff assumes the form

[K = int]
$$Q = \left(a_0 + \sum_{i=1}^{i=N} X_i\right)(1 + \tilde{q}_K), \tag{13}$$

A peculiarity of the operational determination of runoff is that the DWD is computed in the absence of a full set of measurements for a particular year. Under these conditions, in addition to the current measurements, it is natural to base the computations on the long-term characteristics of channel capacity, that is, on regression equations in the form (2) for the totality of discharges measured over a series of characteristic years.

The simplest model for operational determination of runoff, based on refinement of equation (2) for a long series of years using data from current measurements, is

$$Q = a_{0_j} + \sum_{i=1}^{i=N} X_i, \tag{14}$$

where a_{0_j} is determined on the basis of the last of the measured discharges

$$a_{0_j} = Q_j - \sum_{i=1}^{i=N} X_i.$$

The a_{0_j} values are used for determining DWD in the entire time interval prior to the next measurement of water discharge. With respect to the variables X_i (water levels, mean daily water temperature or air temperature), as is well known, they are measured daily.

A considerably more complex model for the operational determination of runoff is based on the optimum extrapolation of the deviation $\tilde{q}_j$ [3]. Its peculiarity is a decrease in the weighting factor P_j with an increase

Table 1

Parameters of Regression Equations and Errors in Hydrometric Determination of Runoff

Regime conditions and nature of correlation	Y	Computation periods and parameters of regression equation r/σ_{sc}, %	Characteristic of closeness of correlation	$\tilde{\sigma}_{int_{op}}$ %
Ob' River - Belogor'ye				
Unambiguous correlation Q(H)	Q	1971-1973 1791; 28; 46; 0.00065	0.98 6.6	14.0
Volga River Volga River - Cheboksary H_{up} - Cheboksary hydrometric post H_{low} - V. Uslon hydrometric post				
Variable backwater	Q	1969 10034; 16.07; 0.0096; -19.96	$\frac{0.99}{5.7}$	12.0
Suur River - Emayygi - Tartu H_{up} - Tartu hydrometric post H_{low} - Praaga hydrometric post				
	Q	1962 47.106; 0.250; 0.0016; -0.276	$\frac{0.99}{4.0}$	10.0
Ob' River - Belogor'ye				
Unsteady movement	Q	1971 184; 0.989 1971-1973 -265.34; 1.0096	$\frac{0.97}{5.2}$ $\frac{0.97}{7.3}$	12.0

Regime conditions and nature of correlation	Y	Computation periods and parameters of regression equation r/σ_{sc}, %	Characteristic of closeness of correlation	$\sigma_{int_{op}}$%
Naryn River - Naryn				
Ice formation without ice cover (frazil ice)	$\frac{Q_Q}{Q_T}$	1966-1967 water volume decrease 0.706; 0.026; -0.00013	$\frac{0.91}{6.4}$	13.3
		water volume rise -0.014; 0.004	$\frac{0.98}{1.7}$	8.3
Venta River - Kuldiga				
Unstable ice cover	lg Q	1965-1966 -1.155; 1.441; -0.317; 0.0078; 0.194	$\frac{0.98}{17.4}$	32.0
Oka River - Gorbatov				
Stable ice cover	K_{win}	1973-1974 1.007; 13.97; 0.065; 8.431; -0.014; 0.793	$\frac{0.97}{6.6}$	8.1
Vetluga River - Vetluzhskiy post				
	Q	1965-1975 60.87; -20132; 119.55	$\frac{0.95}{37.5}$	--

Regime conditions and nature of correlation	Y	Computation periods and parameters of regression equation r/σ_{sc}, %	Characteristic of closeness of correlation	$\sigma_{int_{op}}$ %
Tok River - Nikolayevskiy station				
Refreezing and ice encrustations	Q	1968-1969 $Q_0 = 38.1; \alpha = 0.034$ 16.371; -84.617; 160.87; -99.79	$\frac{0.95}{19.9}$	32.0
Issa River - Vizgi village				
Overgrown channels	K_{over}	1958 1.173; -3.748; 3.17; -0.019; 0.065; -0.044	$\frac{0.98}{4.5}$	24.1
Amudar'ya River - Kerki				
Deforming channels	Q	Optimum interpolation $\tilde{q}_j$ in combination with equation (2) 1966 high water: 4604.7; -6.47; 0.303	$\frac{0.94}{16.2}$	25.0
		low water: 409.3; -3.77; 0.106	$\frac{0.95}{9.2}$	15.0

extrapolation interval τ_{ex}, so that $P_j \to 0$ with $\tau_{ex} \to \infty$.

The examined models for determining runoff were applied in the Hydrometry Division at the State Hydrological Institute in experimental computations with a "Minsk-32" electronic computer (more than 50 hydrological posts in different zones of the Soviet Union). Models for the winter and transitional periods were subjected to particularly extensive checking. Some of these, under the direction of V. S. Ryazanov (Upper Volga Administration of the Hydrometeorological Service), on an experimental basis were used in operational determination of the runoff of rivers in the Volga basin. The table gives sample data for characteristic hydrometric posts -- the parameters of the regression equations and the characteristics of closeness of the correlation -- scatter σ_{sc} and the correlation coefficients r.

The error in regime determination of runoff σ_{int}, characterizing the accuracy in determining DWD, is evaluated directly by the mean square scatter of the regression equation σ_{sc} for an individually taken year. In a rigorous sense this evaluation relates to cases when the scatter of the correlation (2) is caused by predominantly hydraulic factors. The small difference σ_{sc} from the measurement error σ_{meas} substantially increases the accuracy in computing DWD: in the case of a large number of measurements as a result of statistical smoothing of their random errors the σ_{int} value becomes negligible. In the case of a sufficiently small measurement frequency (not more than 2-3 per month) the errors in σ_{sc} assume a systematic character. Accordingly, also in the case of the correlation (2), close to an unambiguous dependence, it is recommended that it be assumed that $\sigma_{int} \approx \sigma_{sc}$.

It is more difficult to evaluate the accuracy in operational determination of runoff. Its error is some fraction of the scatter σ_{sc} characterizing the closeness of the correlation (2) over a period of many years. In our numerical experiments the errors in operational data were evaluated directly using the difference between the water discharges measured and computed on the measurement date. Taking into account the totality of the investigated hydrometric posts the error in operational determination of runoff was 1.5-2 times greater than in the regime variant, that is, $\sigma_{int_{op}} = (1.5\text{-}2)\,\sigma_{int_{reg}}$.

Applicable to equation (2), the use of additional characteristics of channel capacity q_j makes it possible to extract useful information from the "regression residual." The figure shows a comparison of hydrographs for Kerki hydrometric post for the high-water period 1973: using data from the hydrological yearbook (1), on the basis of operational data from the Administration of the Hydrometeorological Service with the use of time discharge curves (2), on the basis of models of regime (3) and operational (4) determination of runoff. This reveals an unreliability of regime and operational data from the Administration of the Hydrometeorological Service during individual periods: the computed hydrograph deviates from the measured discharges (5), whereas it should smooth their chronological

series. The computation of DWD using the scheme (13) ensures a close correspondence between the hydrograph and the measured discharges and a virtual coincidence of the regime and operational data.

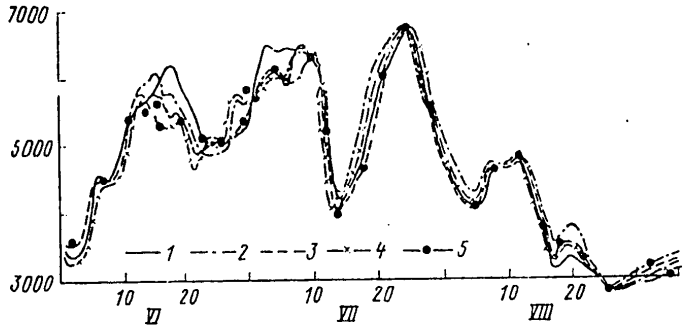

Fig. 1. Comparison of measured discharges and runoff hydrograph by variants of its computation (see text for an explanation of the notations).

The use of the proposed models considerably (by 30-50%) decreases the errors in regime and operational determination of runoff in comparison with presently used methods. An exception is a model based on the Jones equation. It is applicable only for rivers with an insignificant slope, but allowance for the inertial term virtually does not reduce the usual scatter of the Q(H) correlation.

Despite the diversity of the models of hydrometric determination of runoff considered above, their common basis is the interpolation of measurement data with the use of hydraulic dependences for channel capacity and determining its additional factors. A set of the latter virtually always can be limited to the most informative part, taking into account how significant is the difference of the dispersions σ^2_{sc} with complete and reduced sets of variables X_i (the Fisher test can be used for this purpose).

Evaluations of the accuracy in computing DWD from the totality of the considered models are close to the values cited in the official publication [4]. With respect to discharges averaged for a 10-day, monthly and seasonal period, their accuracy is dependent on the frequency of measurement of discharges and the statistical properties of errors in computing DWD. According to our data, the errors in determining the mean 10-day and mean monthly discharges will be less by a factor of 1.5 and 2-3 respectively than the DWD, and in any case, are almost an order of magnitude below the values which can be found in [1]. In this study there was an inadmissible use of the autocorrelation functions of the DWD series taken from hydrological yearbooks in place of autocorrelation functions relating to the characteristics of channel capacity. This fact is extremely

characteristic. In many cases different methodological investigations for the development of algorithms and evaluation of the accuracy in computation of runoff on an electronic computer are carried out on the basis of data from hydrological yearbooks, although this indirect information does not reflect the variations in channel capacity filtered in DWD computation. All the experience from experimental computations shows that the use of an electronic computer not only does not reduce, but on the contrary increases the accuracy in determination of runoff. However, this is attained only in a case if the search for the best computation model is carried out on the basis of an adequate quantity and high quality of field data. After the development of a rational method the number of measurements can be reduced in dependence on the required accuracy of the computed characteristics.

Models of hydrometric determination of runoff are being developed for phase-homogeneous periods which are first discriminated by the methods of hydrological analysis [6]. Not all the operations carried out in this process can be described mathematically -- much is dependent on intuition and the experience of the worker. In the future it is necessary to formalize the objective criteria for discriminating the regime and data-checking phases in order for it to be possible to carry out this operation on an electronic computer.

We note in conclusion that the proposed models for determining runoff still do not constitute a finalized programming-computation complex. The creation of a packet of applied programs is the next stage in further research and development.

BIBLIOGRAPHY

1. Alekseyev, G. A., METODY OTSENKI SLUCHAYNYKH POGRESHNOSTEY GIDROMETEOROLOGICHESKOY INFORMATSII (Methods for Evaluating Random Errors in Hydrometeorological Information), Leningrad, Gidrometeoizdat, 1975.

2. Gandin, L. S., Kogan, R. L., STATISTICHESKIYE METODY INTERPRETATSII METEOROLOGICHESKIKH DANNYKH (Statistical Methods for the Interpretation of Meteorological Data), Leningrad, Gidrometeoizdat, 1976.

3. Karasev, I. F., "Mathematical Models of Hydrometric Determination of River Runoff," TRUDY GGI (Transactions of the State Hydrological Institute), No 256, 1978.

4. NABLYUDENIYA NA GIDROMETEOROLOGICHESKOY SETI SSSR. OPREDELENIYE PONYATIY GIDROLOGICHESKIKH ELEMENTOV I OTSENKA TOCHNOSTI NABLYUDENIY (Observations in the USSR Hydrometeorological Network. Definition of Terms for Hydrological Elements and Evaluation of Accuracy of Observations), edited by O. A. Gorodetskiy, Leningrad, Gidrometeoizdat, 1970.

5. Rumyantsev, V. A., Zorin, M. V., "Some Peculiarities in Use of the Multiple Linear Regression Approach in Constructing Nonlinear Models," TRUDY IV VSESOYUZ. GIDROLOGICHESKOGO S"YEZDA (Transactions of the Fourth All-Union Hydrological Congress), Vol 7, Leningrad, Gidrometeoizdat, 1976.

6. Flerova, R. A., GIDROLOGICHESKIY ANALIZ REZUL'TATOV NABLYUDENIY NA RECHNYKH STANTSIYAKH (Hydrological Analysis of Results of Observations at River Stations), Leningrad, Gidrometeoizdat, 1957.

7. Coesperlein, A., Muller, S., "Anwendung elektronischer Rechner zur Ermittlung von Abflussen aus Wasserstanden," WASSER UND BODEN, Bd 2, 1976.

UDC 556.06

OBJECTIVE METHOD FOR EVALUATING THE PROBABLE SUCCESS OF AN INDIVIDUAL HYDROLOGICAL FORECAST

Moscow METEOROLOGIYA I GIDROLOGIYA in Russian No 3, Mar 80 pp 89-92

[Article by Candidate of Technical Sciences G. N. Ugreninov, Leningrad Hydrometeorological Institute, submitted for publication 20 June 1979]

Abstract: A new statistically valid test for evaluating an individual forecast is proposed. The results of application of the proposed test are given and an example of evaluation of the forecasts is presented.

[Text] The method for evaluating the effectiveness of the forecasting method presently used by the hydrological forecasting service [2] corresponds to an adequate degree to the stochastic essence of precomputation of hydrological phenomena. The procedure for evaluating an individual forecast is less sound. It involves a comparison of the error of an i-th forecast ($\Delta \hat{y}_i = \hat{y}_i - y_i$) with the admissible error, equal to $\delta = 0.674\,\sigma_y$, where σ_y is the standard deviation. A prediction is considered successful when its error $|\Delta \hat{y}_i|$ is less than or equal to the admissible error, that is, $|\Delta \hat{y}_i| \leqslant \delta$.

The arbitrariness of such an approach was already mentioned in the introduction to the Instructions now in force [2] for the practical work of operational subdivisions in the hydrological forecasting service [3]. The experience of 1 1/2 decades of use of the method for evaluating forecasts has confirmed its inadequate soundness. The success of the forecasts is usually maximum at the time of low water. Periods of increased water level are the least favorable time with respect to precomputation success. The reason for this phenomenon is that the mean square errors of specific forecasts $s_{y,i}$ vary in dependence on the anomaly of the argument, usually increasing in the case of positive anomalies [2, 3].

The probabilities of the anticipated value falling in a rigorously stipulated admissible interval $p(\hat{y}_i \pm \delta)$ vary. Hence the nonidentical success of the forecasts. In principle use should be made of the variable value of the admissible interval

$$\left(\hat{y}_i \pm 0{,}674\ \sigma_y \frac{s_{y,i}}{s_y}\right),$$

where s_y is the standard error of forecasts. Then the probability of successful precomputation using a specific dependence is always identical, and for example, with an effectiveness of the method $s_y/\sigma_y = 0.80$ is $p(\hat{y}_i \pm 0.843\ s_{y,i}) \approx 0.60$.

The proposed evaluation method affords specialists preparing forecasts by one and the same method identical chances for a successful result independently of the initial conditions. However, the proposed evaluation scheme is also far from being objective. The choice of the admissible interval of variation of the anticipated value is inadequately sound.

The purpose of any forecast is an increase in certainty of our ideas concerning the future state of an object. Every forecast foreseeing the phenomenon which occurs with a greater probability than would be possible on the basis of statistical generalizations concerning the regime of the object during the past period must therefore be considered successful.

In order to clarify the problem of the probable success of an individual forecast it must be remembered that like the anticipated value, the determined value of a hydrological phenomenon is only an approximate evaluation of the actual state of a water body. Any hydrological measurement is made with some error; strictly speaking, with a stipulated probability it is possible to confirm only realization of the interval $(y_i \pm \beta)$. If it is assumed that $\beta = 0.674\ \sigma_{\Delta_y}$, where σ_{Δ_y} is the standard measurement error, the probability of the true value of the determined hydrological phenomenon falling in the interval $(y_i \pm \beta)$ is 50%, that is, $p(y_i \pm 0.674\ \sigma_{\Delta y}) = 0.50$. It should be noted that in many cases the mean square errors in measurement are dependent on the anomalies of the measured parameter, that is, $\sigma_{\Delta y,i} = f(y_i)$ [1]. For uniformity we will adopt the interval $(y_i \pm 0.674\ \sigma_{\Delta y,i})$ as an evaluation of the determined hydrological conditions predicted by the i-th forecast.

The probable success of an individual forecast is checked in the following way:

1. One of the methods recommended by the Instructions [2] is the plotting of a conditional probable success curve with the forecast $\hat{y}_i$.
2. The conditional probability of the anticipated value falling in the interval $(y_i \pm 0.674\ \sigma_{\Delta y,i})$ is computed:

$$p\left[(y_i \pm 0{,}674\ \sigma_{\Delta y,i}) \mid \hat{y}_i\right] = P\left[(y_i - 0{,}674\ \sigma_{\Delta y,i}) \mid \hat{y}_i\right] - P\left[(y_i + 0{,}674\ \sigma_{\Delta y,i}) \mid \hat{y}_i\right]. \quad (1)$$

3. Using the long-term unconditional probable success curve, the probability of realizing the Y value in this same interval is determined:

$$p\ (y_l \pm 0{,}674\ \sigma_{\Delta y,\ l}) = P\ (y_l - 0{,}674\ \sigma_{\Delta y,\ l}) - P\ (y_l + 0{,}674\ \sigma_{\Delta y,\ l}). \tag{2}$$

The conditional and unconditional probabilities are compared. Two cases are possible:

$$a)\ p\ [(y_l \pm 0{,}674\ \sigma_{\Delta y,\ l}) | \hat{y}_l] > p\ (y_l \pm 0{,}674\ \sigma_{\Delta y,\ l}),$$

in this case the forecast is successful (evaluation 1);

$$б)\ p\ [(y_l \pm 0{,}674\ \sigma_{\Delta y,\ l}) | \hat{y}_l] \leq p\ (y_l \pm 0{,}674\ \sigma_{\Delta y,\ l})$$

in this case the forecast is unsuccessful (evaluation 0).

The set of forecasts is evaluated using the ratio

$$N = \frac{m}{n}\ 100\%, \tag{3}$$

where m is the sum of evaluations of individual forecasts and n is the number of forecasts prepared.

The checking of the proposed scheme for evaluation of the forecast was made using a whole series of both linear and nonlinear prognostic dependences. As the predictable elements we considered water level, runoff, useful and river (general) inflow into lakes and reservoirs, the dates of onset of different phases of the hydrological regime. A comparison of the results of these investigations is a simple task as a result of the different closeness of the relationships, nonidentical laws of distribution of hydrometeorological elements and other factors. The limitation on the volumes of homogeneous samples of initial data makes particularly difficult a reliable quantitative analysis of the aspects of forecasting examined in this article.

Some general conclusions are the following:

1. The probable success of the method when using the proposed test of prediction success on the average is 5-10% greater than when using the test given in the Instructions [2]. This result should be expected, since a correct prediction of at least the sign of an anomaly of the phenomenon within the framework of the proposed evaluation scheme is an important prerequisite for a successful forecast. In the case of a clearly expressed "isogenic" correlation [3], the differences in the values of the probable successes N and P are relatively small. The probable success N is computed using formula (3) and the probable success P is equal to

$$P = \frac{l}{n}\ 100\%, \tag{4}$$

where l is the number of successful forecasts according to the test in the Instructions [2].

2. All the tests carried out on the basis of more extensive samples (n > 60) unambiguously indicate the virtual nondependence of the success of forecasts on the anomaly of the phenomenon (if the proposed evaluation criterion is used). The probability of successful precomputation in this case is always identical and is equal to m/n, and the mean number of successful forecasts in the case of the predictable parameter falling n_j times into the j-th interval is

$$\hat{m}_j = m \frac{n_j}{n}. \tag{5}$$

A statistical analysis of this phenomenon was made using the χ^2 test [4]. We considered the deviations of the number of successful forecasts m in the realization of the j-th interval from the mathematical expectation $\hat{m}_j$. In this case, if the sum

$$\sum_{j=1}^{j=d} \frac{(m_j - \hat{m}_j)^2}{\hat{m}_j} = \sum_{j=1}^{j=d} \frac{(\Delta \hat{m}_j)^2}{\hat{m}_j} \tag{6}$$

is greater than the critical value u_1, with some stipulated reliability of the conclusion it can be admitted that the number of successful forecasts m_j is not proportional to the number of times the predictable value falls in the j-th interval. The critical value u_1 is a function of the reliability of the conclusion P_1 and the number of degrees of freedom k = d - 1.

As an illustration of what we have said above we will cite an example of forecasts of April inflow into the Kamskoye Reservoir. The prognostic dependence has the form

$$\hat{Q}_{IV} = 84\ x + 30\ y + 136, \tag{7}$$

where x and y are indirect characteristics of atmospheric processes in the prespring period.

The long-term range of change of the Q_{IV} parameter was broken down into d = 6 intervals. The number n_j of occurrences of the actual Q_{IV} values in the j-th interval was calculated and then we determined the number of successful forecasts in the realization of each interval of the predictable parameter: l_j is the number of forecasts successful according to the criterion given in the Instructions [2], m_j is the same according to the proposed test. The results of evaluation of the forecasts using dependence (7) are given in Table 1.

With a reliability of the conclusion P_1 = 0.90 and the number of degrees of freedom k = 5 the critical value u_1 = 9.24. Accordingly, the success in precomputation in an evaluation of forecasts in accordance with the Instructions [2] is essentially dependent on the anomaly of the phenomenon. The proposed evaluation scheme is free of this shortcoming. It must be noted that with allowance for the used volume of the sample (n = 78) the resulting conclusion can be regarded only as a preliminary evaluation of the phenomenon.

Table 1

Results of Evaluation of Test Prediction of April Inflow into Kamskoye Reservoir

Объем выборки, n 1	$^{s}Q_{IV}$	$^{g}Q_{IV}$	$^{g}\Delta Q_{IV}$	Обеспеченность 2		$\sum_l \frac{(\Delta \hat{l}_j)^2}{\hat{l}_j}$	$\sum_l \frac{(\Delta \hat{m}_j)^2}{\hat{m}_j}$
	$м^3/сек$ 3			P	N		
78	847	1060	263	69	81	9,94	1,46

KEY:

1. Volume of sample, n
2. Probable success
3. m^3/sec

The proposed method for evaluation of an individual forecast, in our opinion, is more acceptable from the scientific and psychological points of view than the scheme used at the present time [2]. The introduction of the proposed method into forecasting practice will encourage operational workers to penetrate more deeply into the stochastic essence of prediction and at the requests of the serviced organizations to make more extensive use of the stochastic form of representation of prognostic information -- conditional probable success curves. It is important to emphasize that only in stochastic form can forecasts be used in full measure in the optimization of economic decisions. When hydrological forecasters have a clearer idea about the accuracy of hydrological measurements there will be assurance of a more correct evaluation of the current status of water bodies. This should also favor an increase in the quality of hydrological support of the national economy.

BIBLIOGRAPHY

1. NABLYUDENIYA NA GIDROMETEOROLOGICHESKOY SETI SSSR (Observations in the USSR Hydrometeorological Network), Leningrad, Gidrometeoizdat, 1970.

2. NASTAVLENIYE PO SLUZHBE PROGNOZOV (Instructions for the Forecasting Service), Razdel 3, Chast' 1 (Section 3, Part 1), Leningrad, Gidrometeoizdat, 1962.

3. Popov, Ye. G., VOPROSY TEORII I PRAKTIKI PROGNOZOV RECHNOGO STOKA (Problems in the Theory and Practice of River Runoff Forecasts), Moscow, Gidrometeoizdat, 1963.

4. Rumshinskiy, L. Z., ELEMENTY TEORII VEROYATNOSTEY (Elements of the Theory of Probabilities), Moscow, Nauka, 1970.

UDC 551.465

DISTRIBUTION OF CURRENT VELOCITY AND TURBULENT FRICTION NEAR THE WATER-AIR INTERFACE

Moscow METEOROLOGIYA I GIDROLOGIYA in Russian No 3, Mar 80 pp 93-97

[Article by Candidates of Physical and Mathematical Sciences N. K. Shelkovnikov and L. A. Bukina, P. V. Mironov, Moscow State University, submitted for publication 20 July 1979]

Abstract: The paper gives the results of an investigation of the structure of the turbulent flow of water in an open rectangular channel and data on the structure of the accompanying air flow arising as a result of the effect of the moving water surface on the adjacent air layers. Data are given on the vertical distribution of current velocity and the velocity of the accompanying air flow near the water-air interface. It is shown that in the region of relative distances from the bottom $\eta = 0.91$ the current velocity gradient and turbulent friction assume negative values, which makes it possible to conclude that negative viscosity is absent in this flow region.

[Text] This paper gives the results of a detailed investigation of the structure of a turbulent water flow in an open rectangular channel at Reynolds numbers $Re = 2 \cdot 10^5 - 1.2 \cdot 10^6$, and also data on the structure of the accompanying air flow arising as a result of the effect of the moving water surface on the adjacent air layers.

The measurements were made in the axial part of a channel measuring 60 x 50 x 2,500 cm^3 at a distance of 50 depths from the intake in the region of relative distances from the bottom $\eta = 0.1$-0.95 ($\eta = z/H$, H is flow depth, z is the distance from the bottom to the measurement point). The mean flow velocity was measured with a Kh-6 microcurrent meter.

Registry of the longitudinal u' and vertical w' components of velocity fluctuations was with a V-shaped thermohydrometer [1] with subsequent registry of signals using a H010-M oscillograph. The instrument was calibrated using

the fluctuation method [1]. The response of the thermohydrometer to change in the longitudinal velocity component in the water was 0.7 cm/sec per 1 mm of recorder scale and response to vertical variations of the sensor angle of attack was 0.013 rad/mm. The measurement channel inertia was determined by the time constant of a platinum thermohydrometer attachment and did not exceed 0.02 sec. The measurements of the averaged and fluctuation characteristics were made each 0.5 cm with a total flow depth of 20 cm.

The measurement of the mean velocity of the accompanying air flow was made by the fluctuation method in which two single-component thermohydrometers were spaced along the flow at 13 cm. The flow velocity was determined from the ratio of the distance between the sensors to the value of the time shift of the maximum of the cross-correlation function of the longitudinal components of fluctuations of velocity relative to the origin of reading [4].

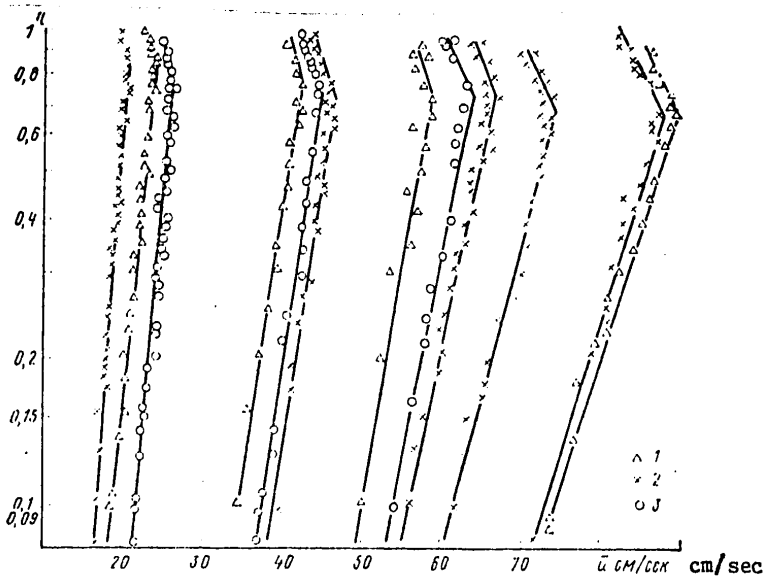

Fig. 1. Vertical profiles of water current velocity at semilogarithmic scale. 1) H = 10 cm; 2) H = 20 cm; 3) H = 30 cm.

Fluctuations of the accompanying air flow u'_{air} and w'_{air} were measured using a two-component thermoanemometer with a platinum attachment such as used in the thermohydrometer. The thermoanemometer was calibrated in a special calibration flume by moving the sensor. The thermoanemometer response to a change in the longitudinal velocity component was 1.4 cm/sec per 1 mm of recorder scale; its response to variations of sensor angle of attack was 0.35 rad/mm.

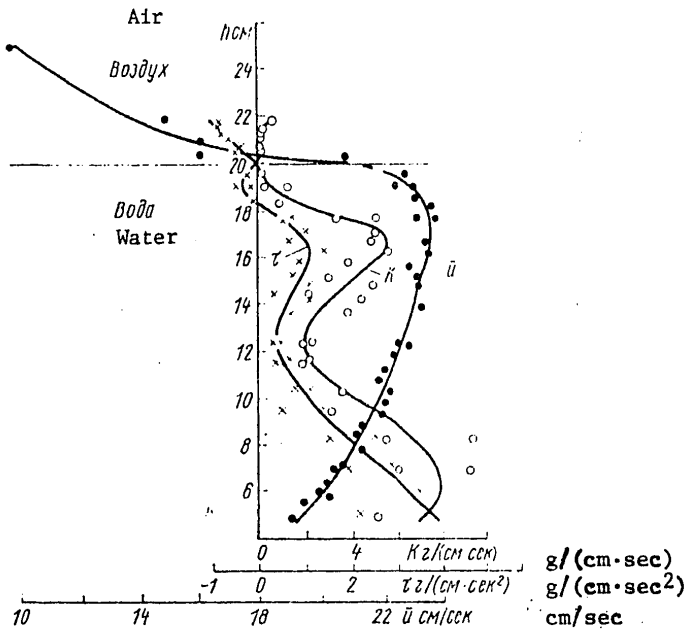

Fig. 2. $\bar{u}$ -- matched curve of vertical distribution of water current velocity and velocity of the accompanying air flow; τ, K -- distribution of coefficient of turbulent friction and coefficient of turbulent viscosity in water and in accompanying air flow.

Figure 1, at a semilogarithmic scale, shows water current velocity curves in a channel. These show that in the subsurface region of the flow there is a decrease in current velocity, so that the flow has a maximum velocity below the free boundary. The depth at which the flow velocity attains a maximum increases with an increase in flow velocity. The graph also shows that the mean velocity profile can be approximated by two logarithmic dependences for the subsurface region and for the nucleus of the flow. The tangent of the slope of these dependences, characterizing the dynamic flow velocity

$$u_* = \sqrt{\frac{\tau_0}{\rho}},$$

increases with an increase in current velocity. It should be noted that although Nikuradze [5] already mentioned a decrease in current velocity near the free boundary, nevertheless this fact has not yet received further confirmation and it is assumed that the velocity of a flow with an open water surface up to the upper boundary conforms to the same logarithmic law (excluding the bottom layer). The large number of measurements which we made indicated that in the range of velocities from 15 to 80 cm/sec there is a tendency to a decrease in velocity in the subsurface region. The results of measurement of water flow velocity with Re = 380-110, carried out

using a laser Doppler hydrometer [2], also indicated that u_{max} is below the free boundary. It can therefore be concluded that in a broad range of Reynolds numbers (from 110 to 10^6) the maximum value of the averaged fluid velocity in an open rectangular channel is not at the free boundary, as is frequently assumed, but at relative distances from the bottom η = 0.9-0.7, depending on the mean current velocity of the water.

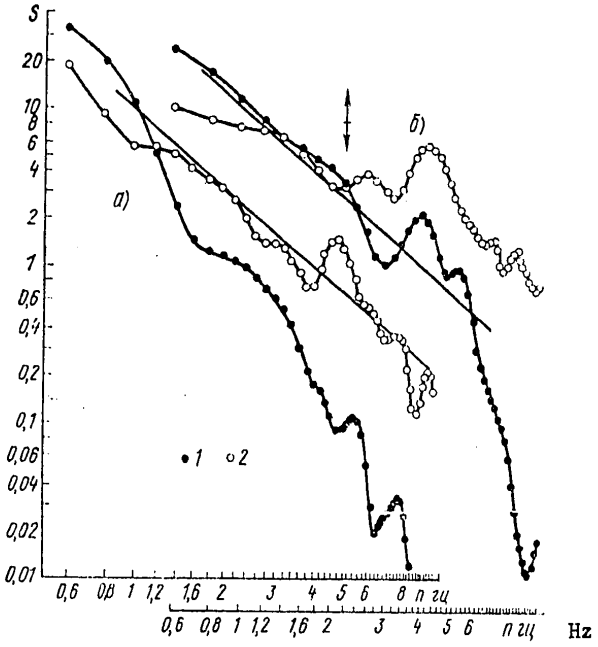

Fig. 3. Curves of spectral density of longitudinal (a) and vertical (b) velocity components near the water-air interface.

One of the possible reasons for the decrease in current velocity near the water-air interface is the dynamic effect of a moving fluid on adjacent air layers, as a result of which an accompanying air movement arises and water current velocity in the surface layer decreases.

Figure 2 shows a matched curve of the vertical distribution of water current velocity and the velocity of the accompanying air flow. The figure shows that with migration of the interface there is a smooth change in velocity. This gives basis for assuming that at the water-air interface the velocities of the fluid and air are identical, that is, the attachment condition is observed.

It should be noted that although the decrease in velocity which we registered in the subsurface region of the flow is small and cannot exert a significant influence on the discharge of fluid in the channels, nevertheless this fact is of fundamental importance for understanding the exchange mechanism at the free boundary. Thus, in accordance with [3], in the region $\eta \geqslant 0.91$ a negative viscosity was noted. Such a conclusion was drawn on the basis of data on the vertical profiles of the flux of momentum $\tau(z) = \rho\, u'\overline{w}'$ and the current velocity u(z), according to which $\tau(z)$ in the region $\eta \geqslant 0.91$ assumes a negative value, and du/dz -- a positive value, that is, the velocity in the surface layer increases. Taking into account the opposite signs on $\tau(z)$ and du/dz, the conclusion is drawn that the coefficient of turbulent viscosity has a negative value.

According to our data (Fig. 2), there is also a change in the sign on $\tau(z)$ at a distance from the bottom $\eta \geqslant 0.9$ (for u_{max} = 24 cm/sec). However, in contradiction to [3], in the region $\eta \geqslant 0.9$ the gradient of averaged current velocity has a negative value and therefore it follows that the coefficient of turbulent viscosity has a positive value. With passage through the water-air interface both turbulent friction and the velocity gradient retain negative values and accordingly the coefficient of turbulent exchange in the accompanying air flow is positive, which is evidence of energy transfer from the moving fluid to the accompanying air flow.

It is interesting to compare the spectral characteristics measured in the subsurface layer of fluid and in the surface layer of the accompanying air flow. Figure 3 shows spectral density curves for the longitudinal and vertical velocity components, computed using data from measurements of velocity fluctuations along both sides of the water-air interface at a distance of 5 mm (for the air) and 10 mm (for the water) from the water-air interface. This figure shows that the spectral density function in the subsurface flow region is characterized by the presence of a maximum in the region 4-5 Hz. For the longitudinal component of velocity fluctuations the spectral density function in the frequency region from 1 to 4 Hz on the average is close to the law $S = n^{-5/3}$. For the velocity transverse component this law does not apply. The nature of the distribution of spectral density of the longitudinal and vertical components of velocity fluctuations of the accompanying air flow differs somewhat from the similar curves for the water flow: here there is a more rapid decrease in the energy of velocity fluctuations with an increase in frequency and the Kolmogorov-Obukhov 5/3 law is not satisfied. The maximum in the frequency region 4-5 Hz is observed only for the transverse component of flow velocity. For the longitudinal component this maximum is very poorly expressed and falls within the limits of the confidence interval.

BIBLIOGRAPHY

1. Bukina, L. A., Shelkovnikov, N. K., Mironov, P. V., "Method for Calibrating Thermohydrometers Using the Absolute Value and Angular Component of the Velocity Vector," VESTNIK MGU, FIZIKA, ASTRONOMIYA (Herald of Moscow State University, Physics, Astronomy), Vol 14, No 5, 1974.

2. Gusev, A. M., Rozanov, V. V., Solntsev, M. V., Shelkovnikov, N. K., "Investigation of Open Flows Using a Laser Doppler Hydrometer," TEZISY DOKLADOV NA VSESOYUZNOY KCNFERENTSII "OKEANOTEKHNIKA-78" (Summaries of Reports at the All-Union Conference "Oceanic Equipment-78"), Leningrad, 1978.

3. Nikitin, I. K., "Peculiarities of the Structure of a Turbulent Flow at its Free Boundary," GIDROTEKHNIKA I GIDROMEKHANIKA (Hydroengineering and Hydromechanics), Institut Gidromekhaniki AN UkrSSR, Kiev, 1964.

4. Shelkovnikov, N. K., "A Method for Investigating the Structure of Turbulent Flows," VESTNIK MGU, FIZIKA, ASTRONOMIYA, Vol 14, No 2, 1974.

5. Shlikhting, G., TEORIYA POGRANICHNOGO SLOYA (Boundary Layer Theory), Moscow, 1974.

UDC 551.463.5

METHOD FOR MEASURING THE THICKNESS OF A PETROLEUM FILM ON THE SURFACE OF A WATER BASIN

Moscow METEOROLOGIYA I GIDROLOGIYA in Russian No 3, Mar 80 pp 98-101

[Article by Candidates of Technical Sciences T. Yu. Sheveleva and M. A. Kropotkin, N. B. Leus, Leningrad Electrical Engineering Institute, submitted for publication 31 August 1979]

Abstract: The article gives the dependence of the intensity of optical radiation transmitted through a film on the thickness of the film, the variety of petroleum product and the radiation wavelength. The authors describe an apparatus which makes it possible, under field conditions, to measure the thickness of petroleum films at discrete points of an oil slick. The range of measured thicknesses is from several micrometers to several millimeters.

[Text] In order to estimate the volume of surface petroleum contaminations of water basins it is necessary to detect a petroleum slick, measure its area and determine the distribution of film thickness in the slick. Whereas the methods for detecting and measuring the extent of petroleum films have been adequately developed [1, 3], there are virtually no methods for routine measurement of the thickness of films. For this reason at the present time, in order to determine the thickness of the petroleum slick, the time-consuming method usually employed is based on sampling with subsequent chemical analysis in station laboratories.

This article describes an optical method for routine determination of the thickness of a petroleum film on the surface of a water basin. The physical basis of the method is the dependence of the intensity of optical radiation transmitted through the film on the thickness of the film, the variety of petroleum product and radiation wavelength. We made an investigation of transmission by crude petroleums and petroleum products which differed with respect to density, viscosity and color, in the ultraviolet (UV), visible and infrared (IR) spectral regions. Table 1 gives the characteristics of

some investigations of petroleum products. The spectral transmission curves obtained using a SF-23 spectrophotometer and an IKS-21 spectrometer are shown in Fig. 1 for two kinds of petroleum, diesel fuel and cylinder oil. The results of the measurements indicated that most of the investigated petroleums and petroleum products with a thickness less than 10μ m transmit radiation well in the visible and near-IR ranges.

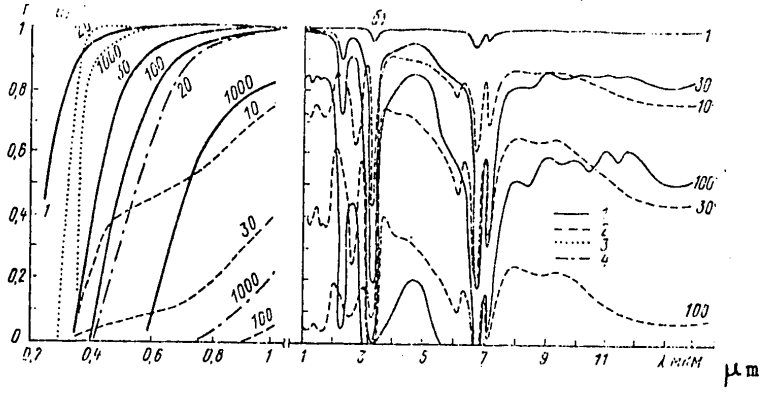

Fig. 1. Transmission of UV, visible (a) and IR (b) radiation by petroleum and petroleum product films of different thickness.

Table 1

Physical Characteristics of Investigated Petroleum Products

Petroleum product	Density at 22°C, g/cm^2	Viscosity, cst	Color
Diesel fuel	0.75	4 at 20°C	colorless
Kerosene KO-20	0.83	2.3 at 20°C	colorless
Oil AS-8	0.88	8 at 50°C	light yellow
Petroleum of deposits:			
Neftyanyye Kamni	0.85	5.1 at 50°C	black
Sangachaly-sea	0.88	53 at 25°C	brown
Surakhany	0.85	13.3 at 20°C	black
Peschanyy Peninsula	0.88	28 at 20°C	bright brown
Kyursangya	0.89	156 at 30°C	black
Cylinder oil	0.95	28 at 100°C	reddish brown

The computations indicate that the intensity of the light flux entering the water through the film decreases primarily as a result of reflection at the interfaces water-petroleum (reflection coefficient about 4%) and petroleum-water (reflection coefficient 0.5%). It follows from the collected data that the transparency of the films is essentially dependent

on their thickness and the spectral composition of the incident radiation. Films of dark-colored petroleums with thicknesses greater than 100 μm almost completely absorb the blue-green part of the spectrum. In the region of wavelengths 0.6-1 μm all the petroleum products absorb poorly. Petroleums and petroleum products, including colorless ones, extremely strongly attenuate radiation with a wavelength $\lambda < 0.4\,\mu$m (UV and violet parts of the spectrum). In the IR part of the spectrum all petroleums have strong absorption bands at wavelengths 2.3-2.4, 3.4-3.5, 6.8 and 7.2 m, and also several weaker bands in the wavelength region 8-15 μm.

For measuring the thickness of petroleum films on a water surface it is most convenient to use the wavelength range from 0.3 to 0.8 μm, in which the water has a high transparency. An analysis of the registered experimental values of the indices of attenuation by petroleum and petroleum products, and also their comparison with the attenuation indices for water [2] show that the indices of attenuation by petroleum and petroleum products are several orders of magnitude higher than for water. Accordingly, the thickness of the petroleum film on a water surface can be determined from the attenuation of radiation with a wavelength λ in it using the expression

$$I_\lambda = k_1 k_2 I_{0\lambda} e^{-\varkappa d},$$

where $I_{0\lambda}$ and I_λ are the intensities of the incident radiation and the radiation transmitted through the petroleum film, d is the thickness of the film, k_1 and k_2 are correction factors whose values are dependent on the losses of radiation on reflection at the air-petroleum-water interfaces and the design of the sampler, and also petroleum viscosity, $\varkappa$ is the absorption index for petroleum at the wavelength λ.

The k_2 and $\varkappa$ values are determined in preliminary experiments. It is interesting to note that light-colored petroleum products (diesel fuel, benzine, kerosene, etc.) have substantially lower values of the absorption indices and a different shape of the spectral dependence $\varkappa = f(\lambda)$ than dark-colored petroleums. For example, with $\lambda = 0.4\,\mu$m the absorption indices for petroleum in the Neftyanyye Kamni deposit, DZ diesel fuel and pure water are equal to $5 \cdot 10^{-2}$, $2 \cdot 10^{-4}$ and $9 \cdot 10^{-6}\,\mu m^{-1}$ respectively. Computations and experiments indicated that the ratio of intensities of radiation at two wavelengths transmitted through a film makes it possible to make a rough identification of the petroleum products (division into dark-colored and light-colored varieties) and determine film thickness. Figure 2 shows the dependences I_{red}/I_{UV} on the film thickness for a typical petroleum (petroleum of the Neftyanyye Kamni deposit) and diesel fuel, where I_{red} and I_{UV} are the intensities of radiation with $\lambda = 0.63\,\mu$m and $\lambda = 0.36$-$0.38\,\mu$m transmitted through the film. The figure shows that with film thicknesses greater than 5 μm the value of the parameter I_{red}/I_{UV} fully characterizes the variety of petroleum product.

The recorded data were used in developing an apparatus for measuring the thickness of a petroleum film on the surface of a water basin. The apparatus, whose diagram is shown in Fig. 3, on the holder D is submerged

into the water from over the side of the ship and at the point of measurement of film thickness is raised a little above the water surface. At the time of submergence the detector B2 is covered by a lid for protecting the entry window against the entry of petroleum and at the time of measurements it is opened. The design of the double vessel makes it possible to cut out on the surface of the water basin a film which is situated on the water surface. The water level contaminated by the petroleum film is registered in the vessel by the upper edge of the outer cylinder. In such a double vessel there is virtual elimination of the influence of waves on the measurement results. The detector B1, measuring the intensity of the light flux incident on the film, is situated in the immediate neighborhood of the petroleum film. Thus, the influence of water turbidity was made minimum. The detectors B1 and B2 are supplied with a set of filters overlapping the range of wavelengths from the UV to red. The choice of the filters is dependent on the thicknesses to be measured and on the type of petroleum product. For example, for the petroleums of the Neftyanyye Kamni deposits the optimum choice is blue-green when measuring the thicknesses of films less than 100μm and yellow-orange radiation for thicknesses 100-1000μm. Films with a thickness greater than 1 mm must be measured with the use of red radiation.

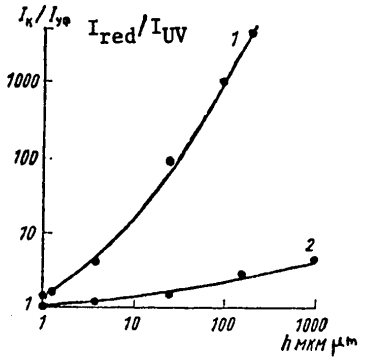

Fig. 2. Dependence of ratio of intensities of red and UV radiations passing through film on film thickness for Neftyanyye Kamni deposit (1) and diesel fuel (2).

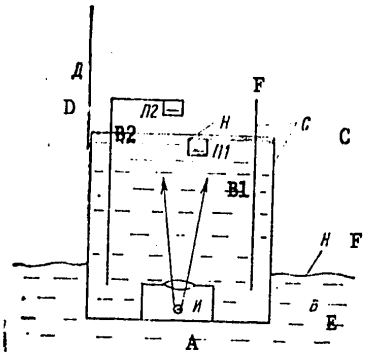

Fig. 3. Diagram of optical apparatus. A) radiation source, B1, B2) radiation detectors, C) double vessel, D) holder, E) water, F) petroleum film

Figure 4 shows the dependences of attenuation of a light flux with λ = 0.45-0.48μm (blue color) and λ = 0.63μm (red color) in films of petroleum and diesel fuel of different thickness. It should be noted that with extraction of the vessel from the water a part of the film settles on the lateral surface of the inner cylinder. The effect is dependent on the geometrical

dimensions, material of the vessel and also the viscosity of the petroleum; its influence is reduced by the optimum choice of vessel design and by the introduction of a correction factor k_2 into the measurement results.

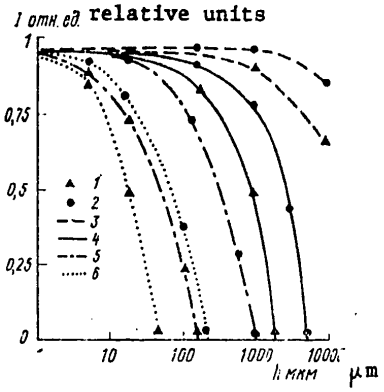

Fig. 4. Dependence of intensity of blue (1) and red (2) light transmitted through films on thickness of films of diesel fuel (3) and petroleums of Peschanyy Island deposit (4), Neftyanyye Kamni deposit (5) and Kyursangya deposit (6).

In a series of laboratory experiments the described optical method was used in measuring the thickness of films of different types of petroleums in the range of thicknesses from 1μm to several millimeters. The film thickness was checked by the weight method by pouring a carefully measured quantity of petroleum onto the water surface. It has been established that the error in measuring film thickness is dependent for the most part on the accuracy in determining the $\varkappa$ and k_2 values. This error does not exceed 20% in a case when $\varkappa$ and k_2 are known (determined in preliminary laboratory experiments) for the investigated type of petroleum product. In the case of petroleums and petroleum products not investigated in the laboratory the measured (by the optical method) film thickness can differ from the true thickness by a factor of 2-3.

The described apparatus was successfully tested in the laboratory and also under field conditions from aboard a vessel on the Volga River and on the Black Sea, as well as from a trestle in the Caspian Sea. The time required for making one measurement does not exceed 3 min.

BIBLIOGRAPHY

1. Bogorodskiy, V. V., Kropotkin, M. A., Sheveleva, T. Yu., METODY I TEKHNIKA OBNARUZHENIYA NEFTYANYKH ZAGRYAZNENIY VOD (Methods and Techniques for Detecting Petroleum Contamination of Waters), Leningrad, Gidrometeoizdat, 1975.

2. Kopelevich, O. V., "Optical Properties of Pure Water in the Spectral Region 250-600 nm," OPTIKA I SPEKTROSKOPIYA (Optics and Spectroscopy), Vol 41, No 4, 1976.

3. Estes, J. E., Senger, L. W., "The Multispectral Concept as Applied to Marine Oil Spills," REMOTE SENSING OF ENVIRONMENT, Vol 2, No 3, 1972.

UDC 631.559:633.11

COMPUTATION OF MEAN OBLAST YIELD OF WINTER WHEAT

Moscow METEOROLOGIYA I GIDROLOGIYA in Russian No 3, Mar 80 pp 102-105

[Article by Professor A. R. Konstantinov and D. N. Peradze, Leningrad Hydrometeorological Institute, submitted for publication 11 October 1979]

Abstract: The authors investigated the possibility of computing the mean oblast yield of winter wheat for specific years for a long time in advance (prior to sowing). The following determining factors were selected as the basis for the investigations (by the residual statistical analysis method in graphic and computer variants): yield, determined from the trend, potential yield (read from maps characterizing the soil-climatic resources for the potential yield of a particular crop) and the mean oblast yield of the preceding year. The closeness of the correlation between the actual and computed yields is characterized by a correlation coefficient higher than 0.8; in extremal years its value is somewhat decreased.

[Text] Among all the types of agrometeorological predictions the one of the greatest practical value is a prediction of the yield before sowing.

There is a scientific basis for making such a prediction. Attempts at long-range and superlong-range yield predictions have been undertaken before [2 and others]. They are now becoming more and more common [1, 3, 5-7, 10, 12, 13 and others]. These studies are based primarily on allowance for trends, weather anomalies, and also cyclic solar activity and give basis for hoping for their successful development in the future.

In this paper we outline a method for predicting the mean oblast yield before sowing which takes into account the trend Y_{tr}, soil-climatic resources Y_{sc} and yield cyclicity. The method is developed in the example of winter wheat, an important food crop, the time of whose sowing is more remote from the time of harvesting than is true of other crops.

The basis for the analysis was post-war data on mean oblast yields (582 cases), collected over the area of the European USSR together with other necessary characteristics. One of the principal predictors is a parameter determined by the trend of crop yield for a particular oblast or farm. As is well known, this curve smoothes the yield variations caused by changes in weather conditions in a specific year and characterizes its gradual increase, related to the improvement in the level of agricultural techniques and equipment (including the influence exerted on the yield by mechanization, the application of chemical fertilizers and the melioration of agricultural production).

The results are analyzed by the residual method [4, 9, 11, 14], which makes it possible to take into account not only the direct relationships with crop yield, but also the possible interrelationships among the factors determining crop yield, exerting an indirect influence on the yield. This method is based on allowance for and successive exclusion of the influence of the determining arguments (factors or predictors) on the function (crop yield). In this method it is not the function itself which is related to each successive argument, but its residual value after allowance for and exclusion of the influence of the preceding argument. This analytical method is completely acceptable for developing a method for computing crop yield for such a long time in advance. For greater reliability and objectivity of computations in this article the residual statistical analysis method is used parallely in two variants: by means of manual construction of two-parameter graphic regressions and by use of an electronic computer.

The correlation between the actual mean oblast crop yield and its value during the same year, taken from the trend Y_{tr} with a year (and possibly greater) advance time, is closest ($r = 0.71$), because the trend in this case, together with the improvement in agricultural techniques and equipment, characterizes the peculiarities of climate (including its long-period changes), soil and regionalization of the crop varieties used in this oblast.

Thus, at the scale of the European USSR the trend in itself gives fair possibilities for estimating the future crop yield prior to sowing. For individual regions the closeness of these correlations with time (for example, during the period from 1952 through 1973) is reduced to $r = 0.62$-0.70 due to the constancy of Y_{scr} [soil-climate resources] (here only the trend and the cyclicity of crop yield "work" to a full degree).

The trend curve for each succeeding year is drawn extremely formally; it does not fully take into account the possible increase in crop yield (in the range from the actual to the potential yield) due to incomplete allowance for the soil-climatic resources of the particular oblast or field. As the potential yield we use the magnitude of the crop yield determined by the soil and climatic conditions at the level of the agricultural techniques and equipment used at seed testing stations.

This quantity can be read from a map given in [9]. In some cases the actual crop yield is far lower than the potential yield and the trend curve can be drawn with a steep slope of the crop yield increase during the year. In other cases, where the limited soil-climatic resources for crop yield and the high level of agricultural techniques and equipment have brought the actual crop yield close to the potential yield, a great increase in crop yield for the year (under average weather conditions) must not be expected. In this case the slope of the trend curve is reduced. Allowance for this circumstance should somewhat strengthen the closeness of the correlation between the trend and the actual crop yield.

The closeness of the correlation of mean oblast crop yields for the European USSR for a specific year with the potential crop yield of a particular oblast Y_{scr} is characterized by a value of the correlation coefficient $r = 0.55$. Allowance for the joint influence exerted on crop yield by the trend Y_{tr} and the soil-climatic resources Y_{scr} increases the closeness of their graphic correlation with the final crop yield to $r = 0.79$; the probable deviation is $\sigma_E = 4.2$ tsentners/hectare. The correlations in Fig. 1 show that the value of the crop yield Y_{comp} computed before sowing increases together with an increase in the trend Y_{tr} and the potential crop yield Y_{scr}; the correlation between Y_{comp} and Y_{tr} is stronger.

In computing the crop yield before sowing we took into account the soil-climatic conditions of the oblast and the influence of a gradual increase in the level of agricultural techniques and equipment. These values are only in part characteristics of the conditions for the growing of wheat in a specific computation year and do not carry information on possible variation of the crop yield caused by variations of soil fertility in this year.

It is known that plant mass is created in the process of photosynthesis at a definite level of mineral nutrition received from the soil. The reserves of nutrients in the soil (nitrogen, phosphorus, potassium, etc.), as well as the trace elements governing its fertility, are limited. With an increase in yield their removal from the soil is increased and as a result remaining soil fertility is reduced. Accordingly, in the years after high yields, all other conditions being equal, the crop yield will be reduced somewhat, whereas after low crop yields it will increase. This circumstance has found partial experimental confirmation and is the fundamental reason for the two-year cyclicity of crop yield noted in a number of studies [3, 8, 13 and others].

For taking this fact into account we constructed a curve (Fig. 2). Along the horizontal axis we have plotted the difference in crop yields during the last year Y_n (before the computed Y_{n+1} year) and the year preceding it Y_{n-1}, and along the vertical axis -- the "residual" crop yield ΔY_1, read from Fig. 1 (as the difference between the actual mean oblast crop yield Y_{act} and the crop yield determined from the curve Y_{curve}, obtained by interpolation between the isolines of the curves plotted in the graph).

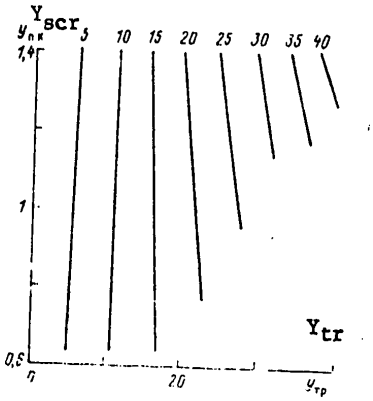

Fig. 1. Correlation between mean oblast yield of winter wheat during a specific year and soil-climatic resources Y_{scr} and trend Y_{tr}.

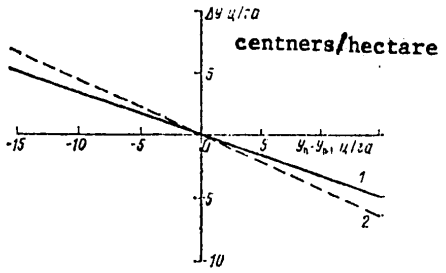

Fig. 2. Dependence of "residual" yield $\Delta Y^{curve}_{tr,\,scr}$ (after allowance for influence of Y_{tr} and Y_{scr}) on difference in yields of preceding year and year preceding that n - 1. 1) manual construction of graphic regressions; 2) computer computation

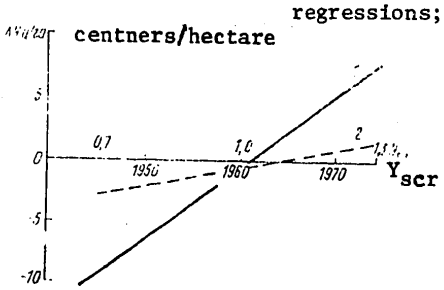

Fig. 3. Graphic representation of correlations constructed by BESM-6 electronic computer. 1) general trend of yield of winter wheat for all oblasts (the deviation of the initial sample from the mean crop yield Y_{mean} $13.98 \approx 14$ centners/hectare). The analytical expression of the trend is $Y_1 = 0.6\ (t - 1944) + 3.6$, where t is the calendar year; 2) is the dependence of ΔY on Y_{scr}. The analytical expression of the correlation is $\Delta Y(Y_{scr}) = 11.5\ Y_{scr} - 13.1$.

This difference is caused by the influence exerted on Y_{act} by other (in addition to Y_{tr} and Y_{scr}) factors not taken into account. One of these is the year-to-year variation in soil fertility. The difference in crop yields during the preceding years relative to the computation year $\Delta Y_n = Y_n - Y_{n-1}$ to some degree characterizes the cyclicity of soil fertility and

is expressed by an inverse dependence between the ΔY_n and ΔY_1 values.

The tendency of this dependence $\Delta Y_n = f(Y_n - Y_{n-1})$ is traced extremely clearly ($r = -0.23$) at the 99% significance level, which makes it possible to take into account its influence on the magnitude of the future crop yield with the selected advance time.

The general closeness of the correlation between the actual mean oblast crop yield of winter wheat for the entire territory of the European USSR with that computed before sowing, in accordance with the residual method is determined from the expression

$$Y_{comp} = Y^{curve}(Y_{tr}, Y_{scr}) + \Delta Y_1^{curve}(\Delta Y_n). \qquad (1)$$

Allowance for cyclicity through $\Delta Y_1^{curve}(\Delta Y_n)$ makes it possible to increase the general correlation coefficient between Y_{act} and the crop yield computed using (1) to the value $r = 0.81$, $\sigma = 3.2$ centners/hectare. Such an accuracy can be adequate for a practical estimate of the crop yield with a long (up to a year) advance time by the administrative and planning organizations in the country.

This closeness is somewhat reduced when estimating the crop yield before sowing for specific regions, but in this case also remains quite high ($r = 0.63$-0.74). The distribution curve for the difference between the actual Y_{act} and computed Y_{comp} crop yields has a symmetric character. This is evidence of absence of systematic error in predicting crop yield before sowing and the reciprocal compensation of computation errors for oblasts when predicting the gross grain harvest for the country as a whole before sowing.

It is of special interest to analyze the results of prediction of the yield of winter wheat before sowing in years with extremal weather conditions (for example, 1972 and 1975 with a low crop yield and 1974 with a high crop yield). In such years both the weather forecast and the prediction of crop yield lose their accuracy; the proposed method also gives, naturally, the maximum errors. For example, for 1972, a severely dry year, the computation method gave exaggerated crop yields in comparison with the actual crop yields -- by an average of 19%, and the r value decreased from 81 to 64%. However, this error is substantially less than that which would be obtained when taking into account only the first curve $Y_{tr,scr}$ (Fig. 1), that is, in computations on the basis of the mean long-term weather conditions, for which the corresponding decrease for r was to 53%, whereas for yield as an average for the European USSR the exaggeration was approximately 30%. Thus, allowance for the mean oblast crop yield of the preceding year with a good or poor crop yield substantially increases the accuracy in predicting crop yield before sowing, which affords a possibility for obtaining more precise preliminary information on the impending low or high harvests of winter wheat for the country as a whole.

Similar results were also obtained using computations of crop yield before sowing using an electronic computer with a special algorithm, the basis for which is the residual statistical analysis method. Thus, after allowance for the correlation between crop yield and the trend, constructed by computer (Fig. 3), the value of the correlation coefficient, as in the first case, was equal to 0.71. After additional allowances (for soil-climatic resources) it increased to $r = 0.77$, and after further allowance for the cyclicity of crop yield -- to $r = 0.82$.

These data confirm the conclusions drawn above concerning the possibility of first-approximation prediction of the yield of winter wheat a long time in advance (up to the time prior to sowing).

BIBLIOGRAPHY

1. Aksarina, Ye. A., Pasov, V. M., "Features of Summer Atmospheric Circulation Over the Northern Hemisphere in Years of Extremal Yield of Spring Wheat in Kazakhstan," METEOROLOGIYA I GIDROLOGIYA (Meteorology and Hydrology), No 2, 1976.

2. Brounov, P. I., "Dependence of Grain Yields on Sunspots and Meteorological Factors," Address at the Solemn Meeting of the Imperial Enfranchised Economic Society, 31 October 1898, St. Peterburg, 1899.

3. Dekhtyareva, G. V., "Prediction of the Yield of Spring Wheat Before its Sowing on the Basis of Inertial Factors," METEOROLOGIYA I GIDROLOGIYA, No 4, 1973.

4. Yezikiyel, M., Foks, K. A., METODY ANALIZA KORRELYATSIY I REGRESSIY LINEYNYKH I NELINEYNYKH (Methods for Analysis of Linear and Nonlinear Correlations and Regressions), translated from English, Moscow, Statistika, 1966.

5. Knyagnichev, N. I., "Results of Long-Term Prediction of the Yield of Grain Crops Determined from the Correlation With Solar Activity," NAUCHNYYE TRUDY OMSKOGO S.-Kh. INSTITUTA, No 99, 1972.

6. Kogan, F. N., "Weather, Agricultural Techniques and Variability of the Yield of Grain Crops," METEOROLOGIYA I GIDROLOGIYA, No 7, 1977.

7. Kogan, F. N., "Yield of Grain Crops in the Nonchernozem Zone of the European USSR and the Possibility of its Prediction on the Basis of Data on Weather," TRUDY GIDROMETTSENTRA SSSR (Transactions of the USSR Hydrometeorological Center), No 174, 1977.

8. Koloskov, P. I., KLIMATICHESKIY FAKTOR SEL'SKOGO KHOZYAYSTVA I AGROKLIMATICHESKOYE RAYONIROVANIYE (Climatic Factor in Agriculture and Agroclimatic Regionalization), Leningrad, Gidrometeoizdat, 1971.

9. Konstantinov, A. R., POGODA, POCHVA I UROZHAY OZIMOY PSHENITSY (Weather, Soil and Yield of Winter Wheat), Leningrad, Gidrometeoizdat, 1978.

10. Manelya, A. I., et al., DINAMIKA UROZHAYNOSTI SEL'SKOKHOZYAYSTVENNYKH KUL'TUR V RSFSR (Dynamics of Yields of Agricultural Crops in the RSFSR), Moscow, Statistika, 1972.

11. Panovskiy, G. A., Brayer, G. V., STATISTICHESKIYE METODY V METEOROLOGII (Statistical Methods in Meteorology), translated from English, Leningrad, Gidrometeoizdat, 1967.

12. Parshin, V. N., Pasov, V. M., Kogan, F. N., "Influence of Weather Conditions on the Yield of Grain Crops," METEOROLOGIYA I GIDROLOGIYA, No 6, 1974.

13. Pasov, V. M., "Two-Year Cyclicity in the Yields of Grain Crops," METEOROLOGIYA I GIDROLOGIYA, No 11, 1974.

14. Solomon, S., "Statistical Correlations Between Hydrological Variables," translated from English, STATISTICHESKIYE METODY V GIDROLOGII (Statistical Methods in Hydrology), Leningrad, Gidrometeoizdat, 1970.

UDC 551.521.(18+3)

COMPUTATION OF ATMOSPHERIC COUNTERRADIATION

Moscow METEOROLOGIYA I GIDROLOGIYA in Russian No 3, Mar 80 pp 107-108

[Article by Candidate of Geographical Sciences N. I. Rudnev, Forestry Laboratory USSR Academy of Sciences, submitted for publication 23 May 1979]

Abstract: New data are presented on the constant coefficients in the Brent formula for computing the flux of atmospheric IR radiation. The cited materials were obtained as a result of experimental investigations in the central wooded steppe and computations using the formula cited in this article.

[Text] Many investigations have been devoted to methods for computing the flux of IR (long-wave) atmospheric radiation (counterradiation) incident on the earth's surface, F, and the balance of IR radiation of the atmosphere and the underlying surface (effective radiation with the opposite sign) B_d. The initial data used in these investigations are the vertical air temperature and humidity profiles for the entire thickness of the troposphere. Such data are available for a small number of stations in the territory of the Soviet Union, which makes difficult the use of the theoretical formulas employed by K. Ya. Kondrat'yev, M. Ye. Berlyand and T. G. Berlyand, F. N. Shekhter, Kh. Yu. Niylisk and others for computing F and B_d.

Investigations of recent years have indicated that stratification of the middle and upper troposphere exerts little influence on the magnitude of the flux F at the level of the earth's surface and for computing F and B_d it was possible to use typical standard models of the atmosphere (at present several models are used). It was demonstrated in the studies of M. Ye. Berlyand and T. G. Berlyand, and by K. Ya. Kondrat'yev, that for the earth's surface it is possible to compute F and B_d using mean stratification values and surface data for air temperature t and humidity in the meteorological booth and the theoretical formulas in this case can be reduced to a dependence coinciding with a formula of the Brent type [1].

These formulas for computing F and B_d can be represented in the form

$$F = aE(T) + b[E(T)\,p^{0,5}], \tag{1}$$

$$B_u = b[F(T)\,p^{0,5}] - (1-a)\,E(T) + 4[E(T) - E(T_n)]. \tag{2}$$

[П = underlying surface] Here $E(T) = 0.814 \cdot 10^{-10}\ T^4$ cal·cm^{-2}·min = $5.669 \cdot 10^{-12}\ T^4$ W/cm^2; T = (273.1 + t); t is air temperature, °C; T_{under} is the temperature of the underlying surface, K; E(T) is stipulated in a table or on a graph; p is water vapor elasticity in the air, mb; a and b are empirical coefficients taking tropospheric stratification into account.

The constants a and b, cited in the summary of K. Ya. Kondrat'yev [1], and also determined by other researchers, vary in a wide range. Modern instruments, making it possible to carry out reliable measurements of IR fluxes at nighttime and during the daytime, and also the modern theories of K. Ya. Kondrat'yev and K. Yu. Niylisk [2], afford a possibility for more precise determination of the values of the constants a and b for a cloudless sky during different seasons of the year, for nighttime and daytime (Table 1).

Table 1

Values of the Constants in the Brent Formula

Сезон 1	a			b		
	сутки 2	день 3	ночь 4	сутки 2	день 3	ночь 4
5 Зима	0,71	0,69	0,74	0,05	0,056	0,044
6 Весна	0,62	0,58	0,66	0,07	0,077	0,064
7 Лето	0,55	0,50	0,61	0,08	0,087	0,073
8 Осень	0,63	0,62	0,64	0,07	0,072	0,068

KEY:

1. Season
2. 24-hours
3. Daytime
4. Nighttime
5. Winter
6. Spring
7. Summer
8. Autumn

The values of the coefficients a and b for summer and autumn were determined using S. P. Malevskiy-Malevich and B. P. Kozyrev radiometers in Kurskaya Oblast and were determined more precisely using radiosonde data for the European territory of the USSR. For winter and spring the coefficients a and b were computed using radiosonde data. The F value was computed using the K. Ya. Kondrat'yev formula [1]

$$F = \Sigma a_j p_j \int_0^{m_\infty} E(T) \exp(-\alpha_j \cdot \eta)\, d\eta, \tag{3}$$

where $m_\infty = \int_0^\infty a(z)\,dz$

j is the part of the spectrum; α_j is the IR radiation absorption coefficient; p_j is the fraction of E(T) attributable to the j-th set of parts of the spectrum, $\sum p_j = 1$; a is water vapor density in the air;

$$m_\infty = \int_0^\infty a(z)\,dz$$

is the integration variable.

In order to simplify the computations, in accordance with the investigation of Ye. D. Kovaleva, we took into account the distributions of air temperature and humidity only in the lower layer of the troposphere.

Table 2

Mean Daily and Monthly Long-Term Sums of Fluxes (Cal/cm^2) of Atmospheric IR Radiation F and Total Solar Radiation Q for Different Seasons of the Year in the Central Wooded Steppe Region

Сезон 1	Q		F	
	сутки 2	месяц 3	сутки 2	месяц 3
4 Зима	0,12	3,6	0,48	14,5
5 Весна	0,29	8,6	0,57	17,1
6 Лето	0,41	12,1	0,68	20,9
7 Осень	0,09	2,8	0,55	16.7

KEY:

1. Season
2. Day
3. Month
4. Winter
5. Spring
6. Summer
7. Autumn

As an example, Table 2 gives the results of computations (using the Brent formula) for the mean daily and mean monthly long-term sums F for the central wooded steppe (Kurskaya Oblast). The quantity of total solar radiation Q was determined using data from actinometric stations. The influence of cloud cover on the magnitude of the Q and F fluxes was taken into account by the method usually employed.

BIBLIOGRAPHY

1. Kondrat'yev, K. Ya., LUCHISTYY TEPLOOBMEN V ATMOSFERE (Radiant Heat Exchange in the Atmosphere), Leningrad, Gidrometeoizdat, 1956.

2. Kondratiew, K. Y., Niilisk, H. J., "The New Radiation Chart," GEOFISICA PURA E APPLICATA, Vol 49, 1961.

UDC 551.521.3

NEPHELOMETRIC METHOD FOR DETERMINING LIGHT ATTENUATION IN THE UV AND VISIBLE SPECTRAL REGIONS

Moscow METEOROLOGIYA I GIDROLOGIYA in Russian No 3, Mar 80 pp 109-111

[Article by Candidate of Physical and Mathematical Sciences T. P. Toropova, Astrophysical Institute, submitted for publication 25 June 1979]

Abstract: In order to validate the nephelometric method for determining light attenuation the author made an analysis of variability of shape of the scattering indicatrix in the surface air layer in the spectral region from 304 to 710 nm. The errors in determining attenuation when using an indicatrix measured at different angles are evaluated. It is shown that with use of the nephelometric method in the entire considered spectral region it is better to use measurements of the indicatrix made in the range of angles 40-50°; the mean error in measuring attenuation does not exceed 10-15%, whereas in the backscattering region it exceeds 70%, and sometimes 100%.

[Text] The essence of the nephelometric method is determination of light attenuation when measuring the coefficient of directed light scattering σ at some one scattering angle φ.

There are many studies which discuss the possibility of using the nephelometric method. However, all these studies relate to the visible region of the spectrum and sometimes contain contradictory conclusions. This relates in particular to a discussion of the possibility of determining attenuation from backscattering [1-6]. However, in connection with the development of laser technology and the use of lidar apparatus the problem of light scattering at great angles has recently acquired special interest.

The purpose of this study is a validation of the nephelometric method for the surface atmospheric layer, detection of the optimum scattering angle, evaluation of the possible errors in determining attenuation σ when using the indicatrix $\mu(\varphi)$, measured at different angles φ, including backscattering,

and also clarification of applicability of the method for different places in the spectral region from 304 to 710 nm.

In order to validate the nephelometric method it is necessary to analyze the variability of shape of the scattering indicatrix for the surface layer.

If the composition of the scattering particles does not change, only their number changes; for each scattering angle the following expression should be correct

$$I(\varphi) = \frac{\mu(\varphi)}{\sigma} = \text{const.}$$

In this case the light attenuation in the medium can be determined unambiguously on the basis of scattering intensity for any φ.

Thus, in order to analyze the applicability of the nephelometric method it is necessary to evaluate the variability of the ratio (1) for different scattering angles. For this purpose it is sufficient to know the relative (normalized) scattering indicatrices; they are measured with considerably greater accuracy than the absolute indicatrices. When determining $\mu(\varphi)$ in fractions of the flux illuminating the scattering volume there is a great brightness drop (by a factor of about 10^6). Errors in the standardization of measurements can lead to errors in the correlation coefficient between σ and $\mu(\varphi)$, especially in those cases when attenuation σ is determined by integration of indicatrix data. However, in a direct determination of the correlations between σ and $\mu(\varphi)$ it is customary to use absolute measurements.

The observational data which we used in the analysis contained a total of 240 atmospheric surface layer scattering indicatrices measured on days without fog, in large part during the summer-autumn period, in the region of scattering angles 10-175°.

The measurement method and instrumentation have been described in detail earlier [5] and they will not be described here.

The total set of indicatrices was broken down into three subsets by wavelengths (710, 405 and 304 nm), each of which contained 94, 78 and 68 individual cases respectively. Each subset included scattering indicatrices measured in five places with different climatic conditions (Mountain Observatory near Alma-Ata, shore of the Black Sea in the neighborhood of Odessa and Gelendzhik, semidesert near the village of Kirbaltabay in Kazakhstan and Alma-Ata city).

As a result of processing of the observational data it was possible to analyze the variability of the shape of the scattering indicatrix. For this purpose the observed indicatrices were normalized using the condition

$$2\pi \int_0^{\pi} \mu(\varphi) \sin\varphi \, d\varphi = 1.$$

where φ is the scattering angle.

Thus, by the term "relative scattering indicatrix" $I(\varphi)$ we will mean here the ratio of the coefficient of directed light scattering $\mu(\varphi)$ to the volumetric attenuation coefficient σ.

$$I_i(\varphi_k) = \frac{\mu_i(\varphi_k)}{2\pi \int_0^{\pi} \mu_i(\varphi_k) \sin\varphi \, d\varphi} = \frac{\mu_i(\varphi_k)}{\sigma}.$$

For validation of the nephelometric method we determined the mean value of this ratio (1) and its variation for each scattering angle:

$$\bar{I}(\varphi_k) = \frac{1}{n}\sum_{i=1}^{n} I_i(\varphi_k); \quad \Delta(\varphi_k) = \frac{\delta(\varphi_k)}{\bar{I}(\varphi_k)},$$

where the standard deviation is

$$\delta = \sqrt{\frac{\sum_{i=1}^{n} [I_i(\varphi_k) - \bar{I}(\varphi_k)]^2}{n}}.$$

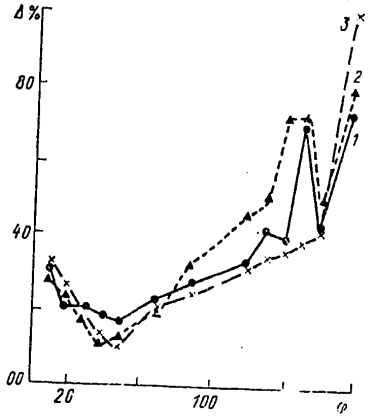

Fig. 1. Variations of the normalized scattering indicatrix for the atmospheric surface layer for different scattering angles. 1) 710 nm, 2) 410 nm, 3) 304 nm.

Figure 1 shows the angular parameters of variations in percent, obtained as a result of processing of observational data. The data in the figure show that for all three wavelengths (304, 405 and 710 nm) the curves have a clearly expressed minimum in the region of scattering angles falling between 40 and 50°. Here the variability of the normalized scattering indicatrix $I(\varphi_k)$ is minimum. The standard deviation of the ratio $\mu(\varphi)/\sigma$ is 10-15%. It therefore follows that for the UV and visible spectral regions

when applying the nephelometric method it is better to use measurements made with a scattering angle falling in the interval from 40 to 50°; in this case the mean error in measuring attenuation will not exceed 10-15%. The error becomes considerably greater if measurements of the scattering indicatrix made at other angles are used for the nephelometric determination of attenuation. For example, with a decrease in the angle to 10° the error in determining attenuation increases to 30%, whereas in the region of large scattering angles it exceeds 70%, and sometimes even 100%. Thus, a change in the shape of the scattering indicatrix can lead to errors in determining attenuation from backscattering exceeding 70-100%, but with respect to scattering at $\varphi = 40$-$50°$ -- to errors of only about 10-20%. However, under ordinary natural conditions the attenuation of light by atmospheric haze sometimes changes by one or two orders of magnitude (for example, the interval of change in visibility can be from 1 to 100 km). This circumstance evidently explains the high correlation coefficients which are frequently obtained between σ and $\mu(\varphi)$, including between attenuation and backscattering, a fact which at first glance contradicts the results obtained above. However, it can be explained if it is assumed that the decisive factor in variations of light attenuation in the atmospheric surface layer is a change in the number of scattering particles, against whose background the change in the properties of the particles determining the shape of the indicatrix does not significantly impair the correlations between σ and $\mu(\varphi)$.

The errors in determining attenuation by the nephelometric method are nevertheless determined by variations in the ratio $\mu(\varphi)/\sigma$, whose evaluation was the purpose of this study. The results which we obtained in determining the optimum scattering angle, used for the nephelometric method for determining attenuation, are in good agreement with the data published by O. D. Barteneva [1]. At the same time, according to the estimates made in [2, 3 and 6], the error in determining visibility from backscattering averages 25%, which contradicts both our results and the conclusions drawn in [1]. The following must be remembered when explaining the reasons for such a disagreement. V. A. Gavrilov [2], on the basis of his own data, and also the results obtained by other authors [2, 6], pointed out that there is a linear dependence (with a deviation from the mean straight line by 25%) between the intensity of backscattering of light and the meteorological range of visibility in a logarithmic coordinate scale. He notes the constancy of this scatter for a broad change in turbidities and defines it as the objective limit of accuracy of the backscattering method. Then he mechanically transfers this scatter evaluation, obtained for logarithms of the values, to a visibility scale. However, it is easy to demonstrate that variations in the logarithms of the measured parameters, attaining 25%, can lead to a considerable change in the values themselves. For example, if visibility varies from 20 to 10 km, the logarithms of these values change by only 30%.

BIBLIOGRAPHY

1. Barteneva, O. D., Dovgyallo, Ye. N., Polyakova, Ye. A., EKSPERIMENTAL'NYYE ISSLEDOVANIYA OPTICHESKIKH SVOYSTV PRIZEMNOGO SLOYA ATMOSFERY (Experimental Investigations of Optical Properties of the Atmospheric Surface Layer), Leningrad, Gidrometeoizdat, 1967.

2. Gavrilov, V. A., VIDIMOST' V ATMOSFERE (Atmospheric Visibility), Leningrad, Gidrometeoizdat, 1966.

3. Gol'berg, M. A., "Principal Results of Delivery Tests for the M-71 Backscattering Nephelometric Apparatus," TRUDY NAUCHNO-ISSLEDOVATEL'SKOGO INSTITUTA GIDROMETEOROLOGICHESKOGO PRIBOROSTROYENIYA (Transactions of the Scientific Research Institute of Hydrometeorological Instrument Making), No 13, 1965.

4. Gorchakov, G. I., Isakov, A. A., "Some Results of Investigation of Light Scattering in the Range of Sounding Angles," 1 VSESOYUZNOYE SOVESHCHANIYE PO ATMOSFERNOY OPTIKE: TEZISY DOKLADOV, CHAST' 1 (First All-Union Conference on Atmospheric Optics: Summaries of Reports, Part 1), Tomsk, 1976.

5. Toropova, T. P., Kos'yanenko, A. V., Ten, A. P., Tokarev, O. D., "Light Attenuation in the Surface Layer and Atmospheric Aerosol," POLE RASSEYANNOGO IZLUCHENIYA V ZEMNOY ATMOSFERE (Field of Scattered Radiation in the Earth's Atmosphere), Alma-Ata, Nauka, 1974.

6. Curcio, J. A., Knestrick, C. L., "Correlation of the Atmospheric Transmission with Backscattering," JOSA, Vol 48, No 10, 1958.

UDC 551.521:581.131

TRANSMISSION OF INTEGRAL SOLAR RADIATION BY A GRASS COVER

Moscow METEOROLOGIYA I GIDROLOGIYA in Russian No 3, Mar 80 pp 111-113

[Article by T. Kh. Tammets, Estonian Agrometeorological Laboratory, submitted for publication 30 May 1979]

Abstract: The article gives the results of measurement of the transmission of radiation by a field of Galega orientalis. The author employed an experimental Yanishevskiy band pyranometer of a new design. It was found that the coefficient of radiation transmission a_T is little dependent on solar altitude. The dependence of a_T on the relative assimilation surface L_A can be approximated by a simplified Tooming-Ross formula.

[Text] The yield of agricultural crops is frequently limited by an unfavorable radiation regime within the field. Accordingly, the need arises for a quantitative study of the function of transmission of integral solar radiation by the field and photosynthetically active radiation PAR.

For corn, sorghum, cotton and barley the transmission function is described by a semi-empirical formula proposed by Tooming and Ross [1-4]. Until now the literature has contained virtually no data on the radiation regime in fields of grass. As a first attempt at study of the radiation regime of perennial grasses we carried out measurements of integral radiation in a field of Galega orientalis. The measurements were made in the flowering phase, with a maximum assimilation surface of the field.

The fields were high (up to 120 cm), uniform, with a stand density in 1976 of 218 stems, and in 1977 -- 308 stems per square meter. The yellowing lower leaves in such a field are evidence of an inadequacy of light in the depth of the field. The radiation penetrating into the field was measured using a Yanishevskiy band pyranometer during the first 10 days in July 1976 and 1977 when there was a cloudless sky and with different solar altitudes. The differences from the readings of a Yanishevskiy M-115 pyranometer were insignificant. The band pyranometer with a diameter of 18 mm and a length of the sensing component of 290 mm made it possible, without

disrupting the structure of the field, to average radiation in a horizontal direction.

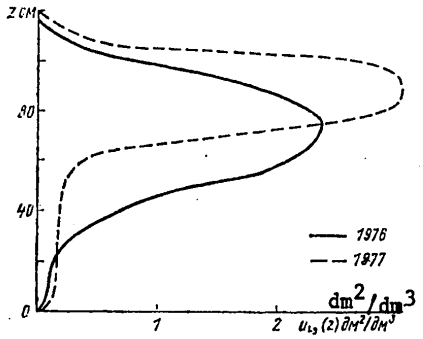

Fig. 1. Vertical distribution of area of the assimilation surface u_{L_A} (z).

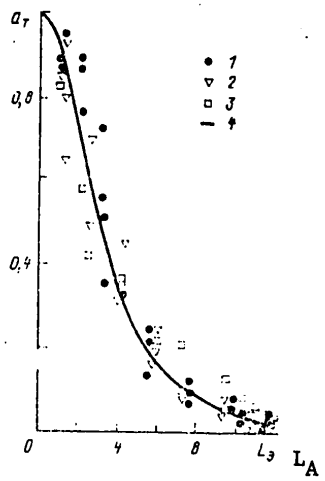

Fig. 2. Dependence of coefficient of transmission of total radiation a_T on effective assimilation area L_A for field of Galega orientalis on the basis of experimental data. 1) $h_{\odot\,mean}$ = 50°, density 218 stems/m^2; 2) $h_{\odot\,mean}$ = 50°, density 308 stems/m^2; $h_{\odot\,mean}$ = 38°, density 308 stems/m^2; 4) using Tooming-Ross formula.

A number of indices of the field were determined at the measurement sites:

1) Vertical distribution of the area of the effective assimilation surface (Fig. 1) per unit volume of the field at the height z - $u_{L_A}(z)$ dm^2/dm^3. This value was determined as the sum of the area of the leaves and the vertical projection of the stems with approximation of the latter by cylinders;
2) Relative area of the effective assimilation surface above a particular level. This value was determined by integrating the value $u_{L_A}(z)$ for z from the particular level to the upper boundary of the field;

[E = A]
$$L_э(z) = \int_z^{z_0} u_{L_э}(z)\, dz,$$

where z is the height of the particular level; z_0 is the height of the upper boundary of the field;
3) The total effective assimilation surface L_{0A}. This parameter was obtained by the integration of $u_{L_A}(z)$ from the soil surface to the upper boundary of the field. The $u_{L_A}(z)$, L_{0A} and L_A values were determined by fourfold measurements in plots measuring 0.5 x 0.5 m by the weighting method. The plots were selected near the sites where radiation was measured. A field of Galega orientalis was characterized by a high density, especially in the upper horizons (Fig. 1), as a result of which the assimilation surface attains 11.2 m^2/m^2. As a result, the total radiation within the field is greatly attenuated (Fig. 2). On the average only 3% of the radiation incident on the field penetrates to the soil surface. If we use a method for conversion from integral radiation to PAR [3], it is found that the coefficient of transmission for Galega orientalis for PAR is less than 0.002. Three-four times less total radiation and ten times less PAR penetrates under a field of Galega orientalis than under the other investigated crops (corn, sorghum, barley, cotton).

It was found that the dependence of the transmission coefficient a_T on L_A has little dependence on the density in the field for equal L_A (Fig. 2). We can only point out a somewhat reduced attenuation of radiation in the uppermost layers of the thinner field of 1976; this is evidently attributable to the incomplete coverage of the field. It was also found that the transmission of radiation by a field of Galega orientalis has little dependence on solar altitude. An analysis of the experimental data shows that the dependence of a_T on L_A for fields of Galega orientalis can be approximated by the Tooming-Ross semiempirical formula proposed for fields of corn, sorghum and cotton

[Э = A]
$$a_T(L_э, h_\odot) = \frac{Q(L_э, h_\odot)}{Q(h_\odot)} = e^{-\frac{c_1 L}{\sin h_\odot}} + c_2\left(e^{-\frac{c_1 c_3 L}{\sin h_\odot}} - e^{-\frac{c_1 L}{\sin h_\odot}}\right),$$

where $a_T(L_A, h_\odot)$ is the coefficient of transmission of integral radiation by a layer of a field with the assimilation surface L_A with a solar altitude $h_\odot$, $Q(h_\odot)$ is the flux density of total radiation incident on a

field with a solar altitude $h_\odot$, $Q(L_A, h_\odot)$ is the flux density of integral solar radiation after passing through the layer of a field with the assimilation surface L_A, c_1, c_2, c_3 are empirical coefficients. According to our data, c_1 is dependent on solar altitude and the assimilation surface:

$$c_1 = 0.09\ L_A \sin h_\odot, \text{ if } L_A \leqslant 11.1 \text{ and}$$

$$c_1 = \sin h_\odot, \text{ if } L_A > 11.1;$$

$$c_2 = 0.2;\ c_3 = 0.15.$$

Summary

In practical computations of productivity in a field of Galega orientalis the simplified Tooming-Ross formula with the proposed empirical coefficients ensures an adequate accuracy with an error 10-15%.

The author expresses appreciation to Yu. Yanishevskiy for supplying the new band pyranometer.

BIBLIOGRAPHY

1. Abashina, Ye. V., Sirotenko, O. D., "Computation of the Coefficient of Attenuation of Integral Radiation by Barley Fields," TRUDY IEM (Transactions of the Institute of Experimental Meteorology), No 3(40), 1973.

2. Ross, Yu. K., Tooming, Kh. G., "Attenuation of Direct and Total Radiation Within Fields of Agricultural Crops and the Semiempirical Formulas Describing It," AKTINOMETRIYA I OPTIKA ATMOSFERY (Actinometry and Atmospheric Optics), Tallin, Valgus, 1968.

3. Tooming, Kh. G., SOLNECHNAYA RADIATSIYA I FORMIROVANIYE UROZHAYA (Solar Radiation and Yield Formation), Leningrad, Gidrometeoizdat, 1977.

4. Tooming, Kh. G., Ross, Yu. K.. "Radiation Regime of a Corn Field by Levels and its Descriptive Approximation Formulas," ISSLEDOVANIYA PO FIZIKE ATMOSFERY (Investigations of Atmospheric Physics), No 6, 1964.

UDC 551(521.3+576)

OPTICAL PROPERTIES OF CRYSTALLINE CLOUDS

Moscow METEOROLOGIYA I GIDROLOGIYA in Russian No 3, Mar 80 pp 114-121

[Article by Doctor of Physical and Mathematical Sciences O. A. Volkovitskiy, Candidate of Physical and Mathematical Sciences L. N. Pavlova and A. G. Petrushin, Institute of Experimental Meteorology, submitted for publication 13 June 1979]

Abstract: On the basis of published investigations the authors examine the principal optical characteristics of crystalline clouds: attenuation indices, scattering indicatrices and also some results of measurements of transmission and scattering of solar radiation by crystalline clouds.

[Text] It is well known that at negative temperatures the atmosphere contains clouds with different phase composition: droplet, mixed and crystalline. The crystalline phase in clouds is already observed at a temperature 0-5°C and in some regions of the earth the frequency of recurrence of crystalline clouds is predominant [10, 17]. Some idea concerning the phase state of clouds at different latitudes is given in Table 1 from [10]. In clouds in the tropical latitudes the crystals appear at a higher temperature, but with advance toward the Arctic an increasingly deeper supercooling is encountered [10]. In all regions the crystalline phase predominates in clouds of the middle and upper levels. At the middle level nimbostratus and altostratus clouds stand out, usually combined in a single Ns-As formation. The phase composition of these systems is inhomogeneous; the liquid and solid phases are frequently encountered in different vertical sequences. In upper-level clouds, cirrus (Ci), the liquid phase was discovered only in the eastern zone of the Tropical Atlantic [10, 25].

Crystalline clouds and fogs, as a result of their great frequency of recurrence, exert an influence on many atmospheric processes, including those associated with radiation transfer. This explains the appearance of a great many studies in which the optical characteristics of crystalline media are investigated. It is necessary to know these characteristics in order to solve a number of problems in meteorology, such as radiative heat exchange,

prediction of visibility, remote investigation of the composition of terrestrial clouds and clouds on the other planets.

The purpose of the theoretical studies, and also investigations carried out under laboratory conditions, is a study of the laws of radiation transmission in media with ice particles of spherical and aspherical configuration and search for the elements of an optical model of a crystalline cloud. Due to the technical difficulties in measuring the microphysical and optical characteristics of crystalline clouds under natural conditions the experimental investigations have for the most part been made in artificially created crystalline fogs. For this purpose an ice-forming reagent (such as AgI) is usually introduced into a chamber with a supercooled fog; ice crystals of the same configuration as in clouds are formed on the nuclei of this reagent.

The particles in crystalline clouds consist of ice with a hexagonal crystal lattice whose properties differ from the properties of water, especially in the IR spectral region [29, 43]. In addition, cloud crystals are characterized by a great diversity of shapes and a broad range of sizes [17, 25]. The joint influence of all these factors results in the optical properties of the crystalline clouds differing from the properties of droplet clouds. Below, on the basis of published data, we will examine the principal optical characteristics of crystalline cloud media: attenuation indices, scattering indicatrices and also some results of measurements of transmission and scattering of solar radiation by a crystalline cloud.

Radiation Attenuation

The attenuation of radiation as a result of absorption and scattering by its particles is one of the principal optical characteristics of clouds. There are very few quantitative data on the attenuation of radiation in crystalline and mixed clouds. Some information on the values of the attenuation index for visible radiation is contained in [10, 18, 37] and is cited in Table 2. In [10] the values $\alpha \geqslant 7$ km^{-1} for Sc, As relate to clouds of the mixed phase.

Measurements of spectral transmission in [18], made in the atmosphere in the presence of crystals in the form of needles, indicated that attenuation in the region of wavelengths $\lambda = 0.5\text{-}12\,\mu$m is close to neutral, although in some spectra there is a weak minimum at $\lambda = 9.2\text{-}10\,\mu$m. It is reported in [38] that the attenuation of IR radiation with $\lambda = 10.6\,\mu$m in crystalline clouds is somewhat greater than in the case of visible radiation. On the basis of these data it can be concluded that in contrast to droplet clouds, attenuation of radiation in the range $\lambda = 0.5\text{-}12\,\mu$m by crystalline clouds is approximately identical. Therefore, Table 2 gives some idea concerning the attenuation indices of crystalline clouds in the IR spectral region as well.

In order to compute the attenuation of radiation by crystalline clouds it is important to know whether it is possible to approximate crystals of different configuration by ice spheres. At present there is no universal agreement on this subject. Computations [15, 16] of the factors involved in the effectiveness of attenuation $K_0(10.6)$ for radiation with $\lambda = 10.6\,\mu m$ by ice spheres, cylinders and platelets show that the influence of configuration is manifested for particles with sizes $\rho = 2\pi r/\lambda < 6$ (where r is the radius of a sphere or cylinder and the half-thickness of the platelet). The authors of [3, 36] compare the measured $K_0(10.6)$ values with the computed values for ice spheres and come to the conclusion that regardless of the configuration of the crystals, in computations of attenuation at $10.6\,\mu m$ it is possible to use a model of ice spheres of an equivalent section. In [15], on the basis of a comparison of the results of their measurements of spectral transparency in crystalline fogs and computations for large water droplets, the conclusion is drawn that a model of spherical particles cannot be used in computing spectral attenuation. However, the authors of this study neglected the difference in the optical constants of water and ice. Accordingly, further investigation is required for answering the formulated question.

Radiation Scattering by Ice Crystals

One of the distinguishing characteristics of the scattering properties of crystalline clouds is manifested most clearly in observation of a number of optical phenomena accompanying the transmission of solar radiation through a veil of cirrostratus clouds (less frequently, cirrus, cirrocumulus and altocumulus). These include large and small halos, false suns, tangential and circumzenith arcs, light pillars, etc. These phenomena have long attracted the attention of researchers and have been described in detail in [11, 30 and in a number of other studies]. All these phenomena are caused by the reflection of light rays from plane surfaces or by light refraction in a crystal, which occurs the same as in a prism [11]. An ice crystal, having the configuration of a regular hexagonal platelet or pillar, for the rays constitutes a prism with refracting angles 60 and 90°. A ray, entering a prism, emerges from it after double refraction, forming small and large halos in the direction of angles 22 and 46°. Due to light dispersion during the transmission of rays in the prism the halos must be brightly colored (inner edge -- red, outer edge -- violet), in contrast to the phenomena caused by reflection (for example, a horizontal circle). However, the color of a halo is frequently not pure or is totally absent. In this case there is a "white" halo. The reasons for this may be both oscillations or rotation of the crystals about their axes and the superposing of reflected, refracted and diffracted rays [11, 30].

All the enumerated phenomena arise only when clouds contain crystals and for observers serve as one of the methods for determining the phase state of cloud cover. Moreover, the appearance of most of them indicates that in clouds conditions sometimes arise for the predominant orientation of crystal axes [11]. The process of radiation scattering by particles of

any configuration is described by a transformation matrix (scattering matrix), by means of which it is possible to express the Stokes parameters of the scattered wave through the Stokes parameters of an incident wave [19]. The Stokes parameters characterize the intensity and polarization of radiation. In a general case the scattering matrix has 16 components. Spherical particles of an optically inactive substance have a scattering matrix of the simplest type (the transformation matrix contains only three independent parameters). The asphericity of particles exerts an influence on all the light scattering matrices. The predominant orientation of aspherical particles can cause linear and circular refraction effects in combination with dichroism, even if the particles are not optically active [19]. Due to the great mathematical difficulties no expression has been derived for computing the components of the scattering matrix, but in [33] a study was made of the theoretical principles for their experimental determination.

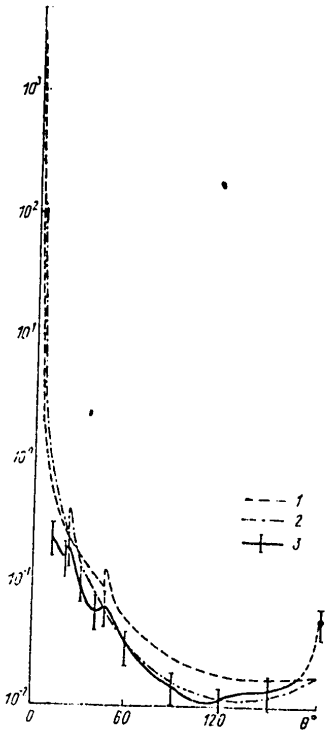

Fig. 1. Scattering indicatrices for radiation with $\lambda = 0.63\mu$m. 1) computed for prism and horizontal scattering plane, 2) same for vertical scattering plane; 3) measured in a crystalline medium (data from [1]).

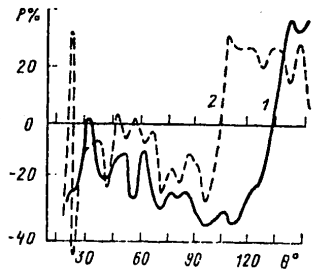

Fig. 2. Polarization of light scattered by crystals -- cylinders (1) and platelets (2) according to data in [35].

Table 1

Phase Structure of Clouds in Different Regions of the Earth

Cloud form	Eastern zone of tropical Atlantic	Temperate latitudes	Arctic
Cu	droplet	--	--
St	--	droplet, mixed	mixed, droplet
Sc	droplet	droplet, mixed	mixed, droplet
Ns	--	mixed	mixed
Ac	droplet	droplet, mixed	mixed, droplet
As	mixed, droplet	mixed, crystalline	crystalline, mixed
Cs	mixed, crystalline	crystalline	crystalline
Ci	crystalline	crystalline	crystalline

Table 2

Values of Attenuation Index in Clouds of Different Forms, km^{-1}

Cloud form	Eastern zone of tropical Atlantic	Temperate latitudes	Arctic
Sc	--	--	25
As	7-20	25	4
Cs, Ci sp	8.3	2.5	2.5
Crystalline fogs	--	0.5-1.2	2.3-32

Until recently the attention of researchers has been concentrated only on measurement of the components f_{11} and f_{12}, which characterize the intensity and degree of polarization of scattered light. The angular dependence of f_{11} (scattering indicatrix) in crystalline fogs [27], measured for the first time, did not exhibit intensity maxima in the range of halo angles, which in [28] is attributed to an inadequate angular resolution of the instrument. Later maxima of different intensity were noted at scattering angles of about 22° and 46° [4, 8, 9, 34, 35], corresponding to the small and large halo circles observed in nature, and also with $\theta \cong 142°$ [35] --

-- Bouguer halos [11]. A halo with $\theta \cong 46°$, also under natural conditions, was observed considerably less frequently. In addition, in these investigations greater scattering in the region of angles close to 90° was observed in comparison with droplet clouds (for the first time in [12, 27]).

However, the scattering indicatrices measured by different authors reveal a substantial scatter of values, especially in the region of lateral scattering angles. An analysis of the data indicated that this scatter cannot be attributed to a difference in the shape and size of particles. The reason for the discrepancy in the experimental data was explained in [13, 14], where it was demonstrated that the presence of droplets or ice spheres in the medium, together with crystals, exerts an influence on the angular distribution of scattered radiation. With a clear identification of the phase state and discrimination of cases of a purely crystalline medium the scatter of scattering indicatrices for crystals of different shape and size in the range of angles 10-180° was ±30%. In [1, 14] the authors also demonstrated that an increase in scattering by crystals in the region of lateral angles occurs due to a decrease in the region of angles $2° \lesssim \theta \lesssim 40°$. These data were obtained when measuring scattering in a single plane. However, as demonstrated in [2, 8, 9, 36, 44], the predominant orientation of crystals leads to an asymmetric distribution of the scattered radiation in different scattering planes, although in the range of angles 10-180° the difference in $f_{11}(\theta)$ for different planes does not exceed the discrepancy in the intensity values measured in a single plane. Figure 1 shows the averaged scattering indicatrix from [1, 13], and Figure 2 shows the degree of plane polarization of scattered light [35].

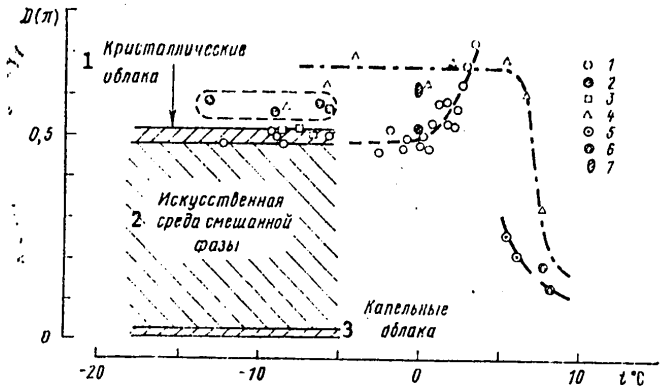

Fig. 3. $D(\pi)$ values for clouds of different phase state according to data from [41]. 1) snowflakes, 2) snowflakes covered with hoarfrost, 3) falling snow, 4) graupel, 5)-6) thawing particles, 7) freezing droplets of aspherical configuration.

KEY:

1. Crystalline clouds
2. Artificial medium of mixed phase
3. Droplet clouds

Measurements of the angular variation of other matrix components have been made only in [7], whose basic conclusion is that the matrix of light scattering by crystals is characteristic for asymmetric particles with a random orientation. In addition, it is noted that measurement of its components can become a means for the remote study of clouds, for example, study of the depolarization of scattered light.

The conclusion that it is possible to identify the phase state of clouds on the basis of the depolarization ratio $D(\pi)$ was drawn earlier in [20]. $D(\pi)$ is determined as the ratio of the perpendicular and parallel components in the backscattering signal in the case of irradiation of particles by plane-polarized radiation. The experiments revealed that for water droplets with a diameter up to 5.5 mm the depolarization ratio $D(\pi) \leq 0.03$ [40], whereas in crystalline clouds and snowfalls -- from 0.5 to 1.0 [20, 41]. However, it is difficult to characterize clouds of different composition by any definite $D(\pi)$ values. It is only possible to establish some limits of these values in dependence on the phase state of clouds at different temperatures, as is demonstrated by Fig. 3 from [41].

Thus, the singularity of the light scattering matrix for a crystalline medium is caused for the most part by the configuration of the crystalline particles. Therefore, the use of the scattering indicatrices in computations as the model of a crystalline cloud, as models of ice spheres [24, 39] or circular cylinders [31] does not give a satisfactory result.

In [1] there was a study of light scattering by hexagonal ice prisms of finite length in the approximation of geometrical optics and diffraction and analytical expressions were derived for computing the scattering indicatrix. Figure 1 shows the computed scattering indicatrices in the horizontal and vertical planes for prisms oriented in the horizontal plane (the radiation beam is propagated in this same plane) [1]. The considered case makes it possible to evaluate the maximum possible asymmetry of light scattering because all other cases of orientation should lead to its decrease. The agreement with the experimental data in [13] can be considered satisfactory. The discrepancy in the computed and experimental [1, 42] indicatrices in the region of backscattering angles can be attributed to the fact that in the computations no allowance was made for a number of effects, such as surface waves [19].

Thus, the scattering indicatrices shown in Fig. 1 can evidently characterize the angular distribution of apparent radiation scattered by a crystalline cloud with $\theta > 10°$.

Interrelationship Between Backscattering and Optical Thickness

In interpreting the results of lidar sounding of clouds at different wavelengths it is of interest to study the interrelationship between backscattering σ_π and the optical thickness τ_λ. Experimental investigations [3,

13, 14] have shown that this interrelationship for $\lambda = 0.63\mu m$, independently of the phase composition of the medium, is described by a regression equation with identical coefficients. For $\tau_{0.63} \lesssim 0.4$ the interrelationship between σ_π and optical thickness can be considered linear. The deviation from linearity in the case of large $\tau_{0.63}$ is attributable to the increasing contribution of multiple scattering. The equality of the regression coefficients means that the value of the backscattering indicatrix for $\lambda = 0.63\mu m$ in a crystalline medium is the same as in a droplet medium: $f_{11}(\pi) \simeq 0.05$ (±30%). Measurements [6, 42] for wavelengths $\lambda = 0.57$, 0.63 and 10.6 μ m, the same as in [3, 14], did not reveal σ_π differences in droplet and crystalline fogs with identical τ_λ. Investigations were not made at other wavelengths.

Thus, from the backscattering signal for $\lambda = 0.63$, 0.57 and $10.6\mu m$ it is evidently impossible to determine the phase composition of cloud cover. This requires that measurements of polarization, such as $D(\pi)$, be made.

Transmission and Scattering of Radiation by a Crystalline Cloud

Crystalline clouds, the same as droplet clouds, constitute an optical medium which is quite dense in which single scattering is accompanied by multiple scattering processes. The problem of the propagation of radiation in cloud media in which multiple scattering occurs and with allowance for absorption by atmospheric gases and aerosol has not been solved at all. In theoretical investigations it has been special methods for solving this problem which for the most part have been developed and the results of computations of the fluxes of solar radiation reflected, absorbed and transmitted by layers of droplet clouds are given. Individual characteristics of radiation transfer were also examined for crystalline clouds, a layer of ice spheres or circular cylinders being used as the model [23, 24, 31, 32, 39]. It was noted earlier that these models cannot be regarded as satisfactory for computations of the indicatrix of light scattering by ice crystals. However, the results of some theoretical and experimental studies give basis for assuming that a model of ice spheres can be employed in computing the characteristics of radiation transfer. For example, it was demonstrated in [32] that the computed values for radiation and transmission in the window $\lambda = 8.3$-$12.5\mu m$ for layers of different thickness containing ice cylinders and spheres of equivalent cross section differ insignificantly. Measurements of the reflectivity of artificial crystalline fogs in the near-IR spectral region were made in [45]. The author of [24] demonstrated that the results of these measurements agree well with the computed reflectivity values for spherical ice particles.

The transmission and reflection of solar radiation by clouds is dependent both on the optical properties of droplets and crystals and on the characteristics of radiation absorption in and outside a cloud [21, 22, 26]. The influence of absorption by atmospheric gases in the range $\lambda = 2.4$-3.0 μm is illustrated by Fig. 4, which shows the solar radiation spectra

for radiation transmitted by crystalline clouds Ci [21]. The solar spectrum was measured in a clear sky at the same altitude (6.2 km) at which in another flight the base of Ci clouds with a thickness from 0.5 to 3 km was situated.

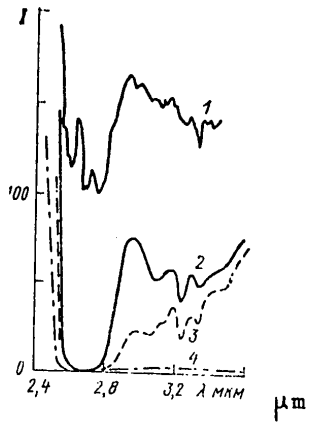

Fig. 4. Transmission of solar radiation by the pure atmosphere at an altitude of 6.2 km (1) and by Ci clouds -- thin (about 0.5 km), (2) intermediate thickness (3) and dense (about 3 km) (4).

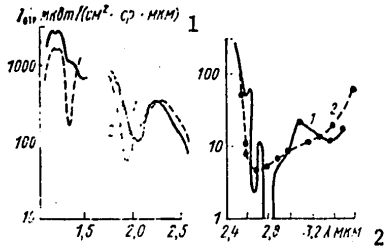

Fig. 5. Reflectivity of solar radiation by dense Ci (1) and dense Cu (2).

KEY:
1. I_{refl}, $\mu W/(cm^2 \cdot sr \cdot \mu m)$
2. μm

The influence of absorption by atmospheric gases is also manifested in the spectra of reflectivity of solar radiation. There are reflectivity minima corresponding to the absorption bands of oxygen $\lambda = 0.76$ and $1.26 \mu m$, the strong bands of water vapor $\lambda = 0.95$, 1.13, 1.38, 1.47, 1.86, 1.9 and 2.58 μm, as well as the H_2O and CO_2 bands with $\lambda = 2.01$, 2.06 and $2.68 \mu m$. In addition, there are minima corresponding to the water or ice absorption bands [21, 22].

The latter is attributable to the fact that the absorption of radiation by particles decreases scattering. Figure 5 shows the averaged reflectivity spectra for crystalline Ci and droplet Cu clouds from [21]. In some intervals of wavelengths the reflectivity of these clouds is different. The difference is maximum where the complex refractive indices of water and ice are most different.

Thus, the measurement of reflectivity in the IR spectral region can be used in identifying the phase state of clouds. This conclusion was later confirmed by computations for plane-parallel layers of the medium containing spherical particles of water and ice [24, 29, 39].

Summary

Thus, the optical properties of crystalline clouds at present have not been fully studied. Some components of the scattering matrix of visible radiation, especially the scattering indicatrix with $\theta > 10°$ and the polarization of scattered radiation for angles 15-150°, can be considered known.

An analysis of published investigations shows that the singularity of the scattering properties of crystalline clouds, distinguishing them from droplet clouds, includes:
1) manifestation of such optical phenomena as halos, light pillars, false suns, different arcs, etc., caused by refraction, reflection or diffraction of light on ice crystals in the case of a random or predominant orientation;
2) an increase in the fraction of radiation scattered in lateral directions in comparison with drops;
3) the partial depolarization of backscattered radiation.

All these effects are caused by a difference in the shape of the crystals from spherical and therefore cannot be precisely modeled by means of polydisperse ice spheres or cylinders. In computations of the scattering indicatrix for visible radiation it is possible to use the analytical expressions proposed in [1]. These were derived for a model medium consisting of ice hexagonal prisms.

In addition, the spectral variation of reflectivity of IR radiation by crystalline and droplet clouds is different. This is evidently attributable for the most part to the influence of the optical constants of water and ice. Accordingly, for computing the spectral variation of reflectivity of crystalline clouds it is possible to use a model of ice spheres of corresponding size.

The characteristics of the optical properties of crystalline clouds given above give basis for remote determination of the presence of the crystalline phase in clouds and the relative content of crystals and droplets.

BIBLIOGRAPHY

1. Volkovitskiy, O. A., Pavlova, L. N., Petrushin, A. G., "Light Scattering by Ice Crystals," IZV. AN SSSR, FIZIKA ATMOSFERY I OKEANA (News of the USSR Academy of Sciences, Physics of the Atmosphere and Ocean), Vol 16, No 2, 1980.

2. Volkovitskiy, O. A., Pavlova, L. N., Snykov, V. P., "Asymmetry of the Scattering Properties of a Crystalline Cloud Medium," IZV. AN SSSR, FIZIKA ATMOSFERY I OKEANA, Vol 11, No 7, 1975.

3. Volkovitskiv, O. A., Nikiforova, N. K., Pavlova, L. N., Petrushin, A. G., Snykov, V. P., "Model Investigations of the Optical and Aerodynamic Properties of Ice Crystals," VOPROSY FIZIKI OBLAKOV (Problems in Cloud Physics), Gidrometeoizdat, Leningrad, 1978.

4. Dugin, V. P., Golubitskiy, B. M., Mirumyants, S. O., Paramonov, P. I., Tantashev, M. V., "Experimental Investigations of the Optical Characteristics of Artificial Ice Clouds," IZV. AN SSSR, FIZIKA ATMOSFERY I OKEANA, Vol 7, No 8, 1971.

5. Dugin, V. P., Volkovitskiy, O. A., Maksimyuk, V. S., Mirumyants, S. O., Snykov, V. P., "Spectral Transmission of Artificial Crystalline Cloud Formations," IZV. AN SSSR, FIZIKA ATMOSFERY I OKEANA, Vol 12, No 4, 1976.

6. Dugin, V. P., Mirumyants, S. O., Pavlova, L. N., "Experimental Investigations of Backscattering at Wavelengths 10.6 and 0.57 μm by Artificial Cloud Formations," TRUDY IEM (Transactions of the Institute of Experimental Meteorology), No 13(58), 1976.

7. Dugin, V. P., Mirumyants, S. O., "Scattering Matrices of the Light of Artificial Crystalline Clouds," IZV. AN SSSR, FIZIKA ATMOSFERY I OKEANA, Vol 12, No 9, 1976.

8. Dugin, V. P., Volkovitskiy, O. A., Mirumyants, S. O., Nikiforova, N. K., "Anisotropy of Light Scattering by Artificial Crystalline Cloud Formations," IZV. AN SSSR, FIZIKA ATMOSFERY I OKEANA, Vol 13, No 1, 1977.

9. Dugin, V. P., Maksimyuk, V. S., Mirumyants, S. O., Nikiforova, N. K., "Anisotropy of Light Scattering by Artificial Crystalline Cloud Formations (Vertical Illumination of Medium)," TRUDY IEM, No 13(58), 1976.

10. Kosarev, A. D., Mazin, I. P., Nevzorov, A. N., Potemkin, V. G., Shugayev, V. F., "Comparison of Some Microphysical Characteristics of Clouds in Different Geographical Regions," VOPROSY FIZIKI OBLAKOV, Leningrad, 1978.

11. Mindart, M., SVET I TSVET V PRIRODE (Light and Color in Nature), Moscow, Nauka, 1969.

12. Nikiforova, N. K., "Experimental Study of Light Scattering by Droplet and Crystalline Fogs," TRUDY IEM, No 10, 1970.

13. Pavlova, L. N., "Investigation of the Scattering of Visible Radiation in Cloud Media Containing Crystals," IV VSESOYUZNYY SIMPOZIUM PO RASPROSTRANENIYU LAZERNOGO IZLUCHENIYA V ATMOSFERE (Fourth All-Union Symposium on the Propagation of Laser Radiation in the Atmosphere), Summaries, Tomsk, 1977.

14. Pavlova, L. N., "Measurement of the Coefficients of Directed Light Scattering in Droplet and Crystalline Cloud Media," IZV. AN SSSR, FIZIKA ATMOSFERY I OKEANA, Vol 14, No 9, 1978.

15. Petrushin, A. G., "Attenuation, Scattering and Absorption of Radiation at 10.6 m by a Model Cloud Medium Containing Ice Circular Cylinders of Infinite Length," TRUDY IEM, No 11(54), 1975.

16. Petrushin, A. G., "Attenuation of IR Radiation in Crystalline Cloud Media," TEZISY DOKLADOV NA IV VSESOYUZNOM SIMPOZIUME PO RASPROSTRANENIYU LAZERNOGO IZLUCHENIYA V ATMOSFERE (Summaries of Reports at 4th All-Union Symposium on the Propagation of Laser Radiation in the Atmosphere), Tomsk, 1977.

17. FIZIKA OBLAKOV (Cloud Physics), edited by A. Kh. Khrgian, Leningrad, Gidrometeoizdat, 1961.

18. Filippov, V. L., Ivanov, V. P., Makarov, A. S., "Variations of Aerosol Attenuation of Radiation Under Conditions of an Ice Fog," TEZISY DOKLADOV NA IV VSESOYUZNOM SIMPOZIUME PO RASPROSTRANENIYU LAZERNOGO IZLUCHENIYA V ATMOSFERE, Tomsk, 1977.

19. Van de Khyulst, G., RASSEYANIYE SVETA MALYMI CHASTITSAMI (Light Scattering by Small Particles), Moscow, IL, 1961.

20. Shupyatskiy, A. B., Shlyakhov, V. I., Kravets, V. V., Tyabotov, A. Ye., "Use of Laser Technology in Polarization Investigations of Meteorological Formations," METEOROLOGIYA I GIDROLOGIYA (Meteorology and Hydrology), No 2, 1967.

21. Blau, H. H., Espinola, R. P., Reifenstein, E., "Near-IR Scattering by Sunlit Terrestrial Clouds," APPL. OPTICS, Vol 5, No 4, 1966.

22. Blau, H. H., Espinola, R. P., "Spectral Property of Clouds from 2.5 to 3.5 Microns," APPL. OPTICS, Vol 7, No 10, 1968.

23. Dave, J. V., "Intensity and Polarization of the Radiation Emerging from a Plane-Parallel Atmosphere Containing Monodispersed Aerosols," APPL. OPTICS, Vol 9, No 12, 1970.

24. Hansen, J. E., Cheynay, H., "Theoretical Spectral Scattering of Ice Clouds in the Near Infrared," JGR, Vol 74, No 13, 1969.

25. Heymsfield, A. J., Knollenberg, R., "Properties of Cirrus Generating Cell," J. ATMOS. SCI., Vol 29, No 7, 1972.

26. Hovis, W. A., Blaine, L. R., Forman, M. L., "Infrared Reflectance of High-Altitude Clouds," J. APPL. OPTICS, Vol 9, No 3, 1970.

27. Huffman, P. J., Thursby, W. R., "Light Scattering by Ice Crystals," J. ATMOS. SCI., Vol 26, No 5, 1969.

28. Huffman, P. J., "Polarization of Light Scattering by Ice Crystals," J. ATMOS. SCI., Vol 27, No 8, 1970.

29. Irvine, W. W., Pollack, J. B., "Infrared Optical Properties of Water and Ice Spheres," ICARUS, Vol 8, 1968.

30. Lenggenhager, K., "Eine Meteorologische Erscheinung. Z. Erklarung der "unchten" Spektralfarben des Sonnenhalos von 22° Radius," UNIVERSUM, Vol 30, No 3, 1975.

31. Liou, K. N., "Transfer of Solar Irradiance Through Cirrus Cloud Layers," JGR, Vol 78, No 9, 1973.

32. Liou, K. N., "On the Radiative Properties of Cirrus in the Window Region and Their Influence on Remote Sensing of the Atmosphere," J. ATMOS. SCI., Vol. 31, No 3, 1974.

33. Liou, K. N., "Theory of the Scattering Phase-Matrix Determination for Ice Crystals," JOSA, Vol 65, No 2, 1975.

34. Liou, K. N., Baldwin, R., Kaser, T., "Preliminary Experiments on the Scattering of Polarized Laser Light by Ice Crystals," J. ATMOS. SCI., Vol 33, No 3, 1976.

35. Morita, Y., "Scattering Cross Section of Freely Suspended Ice Crystals for Visible Light," TENKI, Vol 20, No 3, 1973.

36. Nikiforova, N. K., Pavlova, L. N., Petrushin, A. G., Snykov, V. P., Volkovitskiy, O. A., "Aerodynamic and Optical Properties of Ice Crystals," J. AEROSOL. SCI., Vol 8, No 3, 1977.

37. Ohtake, T., Huffman, P. J., "Visual Range in Ice Fog," J. APPL. METEOROL., Vol 8, 1969.

38. Pembrook, J. D., Gryvnak, D. A., Burch, D. B., "Attenuation of Solar Radiation by Natural Clouds at Several Wavelengths in the Visible and Infrared," JOSA, Vol 61, No 4, 1971.

39. Plass, G. N., Kattawar, G. W., "Radiative Transfer in Water and Ice Clouds in the Visible and Infrared Region," J. APPL. OPT., Vol 10, No 4, 1971.

40. Sassen, K., "Depolarization of Laser Light Backscattered by Artificial Clouds," J. APPL. METEOROL., Vol 13, No 8, 1974.

41. Sassen, K., "Laser Depolarization 'Bright Hand' from Melting Snowflakes," NATURE, Vol 255, 1975.

42. Sassen, K., "Backscattering Cross Sections for Hydrometeors: Measurements at 6328 A," J. APPL. OPT., Vol 17, No 5, 1978.

43. Schaaf, I. W., Williams, D., "Optical Constants of Ice in the Infrared," JOSA, Vol 63, No 6, 1973.

44. Thuman, W. C., Brown, A. G., "Preliminary Studies of Intensity of Light Scattering by Water Fogs and Ice Fogs," SCIENCE, Vol 120, No 3128, 1954.

45. Zander, R., "Additional Details on the Near-Infrared Reflectivity of Laboratory Ice Clouds," JGR, Vol 73, No 20, 1968.

SIXTIETH BIRTHDAY OF SOLOMON MOISEYEVICH SHMETER

Moscow METEOROLOGIYA I GIDROLOGIYA in Russian No 3, Mar 80 p 122

[Article by personnel of the Central Aerological Observatory]

[Text] Solomon Moiseyevich Shmeter, a well-known scientist in the field of atmospheric physics, a Doctor of Physical and Mathematical Sciences, head of the Division of Cloud Physics and Atmospheric Dynamics of the Central Aerological Observatory, marked his 60th birthday on 10 March 1980.

Solomon Moiseyevich came to meteorology after graduating from the Mechanics-Mathematics Faculty of Moscow State University and then Khar'kov Hydrometeorological Institute. During the period 1944-1947 he worked at the Yakutsk Geophysical Observatory, first as an aerological engineer and then as head of the aerology division. In 1947 he undertook graduate studies at the

Central Aerological Observatory. S. M. Shmeter was the first graduate student at the observatory and after then all his scientific activity over a period of 32 years has been closely associated with the Central Aerological Observatory.

S. M. Shmeter dealt with a very broad range of problems during these years. Original investigations of the chemical composition of clouds were the subject of his Candidate's dissertation, which he successfully defended in 1951. During 1951-1957 he carried out a series of important theoretical and experimental studies devoted to an improvement in aerological measurements. Since 1957 the scientific activity of Solomon Moiseyevich for the most part has been concentrated on experimental investigations of atmospheric turbulence and cloud physics. His many years of investigations of the dynamics and mesostructure of convective clouds later served as a basis for his doctoral dissertation, successfully defended in 1968. The book by S. M. Shmeter, entitled FIZIKA KONVEKTIVNYKH OBLAKOV (Physics of Convective Clouds), received broad international recognition.

S. M. Shmeter repeatedly headed flight expeditions and participated in flights carried out under highly complex meteorological conditions. During these flight expeditions he created a new method for aircraft investigations of the atmosphere and obtained unique materials substantially enriching our concepts concerning turbulence, convection, and especially the physics of convective clouds.

The results of the studies of S. M. Shmeter have been published in more than 60 scientific articles. He is the author and coauthor of six monographs on cloud physics and atmospheric turbulence. Three of his monographs have been translated and published abroad. The rich experience of this working aerologist and at the same time his excellent mastery of theory assisted him in creating a text for use in the aerology course (1965), he being the coauthor.

Solomon Moiseyevich devotes great attention to teaching work. Under his direction several Candidate's dissertations were prepared on different aspects of atmospheric physics.

S. M. Shmeter is engaged in much public and political work. A member of the CPSU since 1945, he devotes much time and energy to the indoctrination of young scientists.

Now S. M. Shmeter is at the height of his creative forces and we wish him good health and retention of the same vigorous activity and further creative successes.

AT THE USSR STATE COMMITTEE ON HYDROMETEOROLOGY AND ENVIRONMENTAL MONITORING

Moscow METEOROLOGIYA I GIDROLOGIYA in Russian No 3, Mar 80 pp 122-123

[Article by V. N. Drozdov and V. M. Voloshchuk]

[Text] A regular session of the Scientific Council of the State Committee on Hydrometeorology and Environmental Monitoring on the problem "Study of the Oceans and Seas" was held on 28 November 1979.

A report entitled "Preliminary Results of an Interdepartmental Expedition in the Baltic Sea and Prospects for its Hydrometeorological Investigation" was presented by I. N. Davidan. In his report he noted that the Leningrad Division of the State Oceanographic Institute and the Northwestern Administration of the Hydrometeorological Service, within the framework of the Commission "Study of Hydrology and Water Contamination of the Baltic Sea," during 1978-1979 carried out much work for bringing together the efforts of different departments in the field of organization and implementation of comprehensive investigations of the Baltic Sea, a generalization of the results of two interdepartmental expeditions. The expeditions were carried out to study the most timely problems of the Baltic Sea (processes on a synoptic scale, variability and spatial nonuniformity of contamination fields) in accordance with programs developed at the Leningrad Division of the State Oceanographic Institute.

Due to the close contacts between the Leningrad Division of the State Oceanographic Institute, the Northwestern Administration of the Hydrometeorological Service and the Arctic and Antarctic Scientific Research Institute, the following organizations became involved in the expeditions: Baltic Scientific Research Institute of Fisheries, Central Scientific Research Institute of Geodesy, Aerial Mapping and Cartography, All-Union Scientific Research Institute of Marine Geology and the TEF and GS DKBF [expansions unknown]. The expeditions were carried out successfully and made it possible to obtain new, original results, important for study of the Baltic Sea.

Then the speaker discussed in detail the results obtained from the observations and those preliminary conclusions which have been drawn. In conclusion he analyzed the principal directions in hydrometeorological investigations in the Baltic Sea.

The Council noted that the results obtained from the interdepartmental expeditions in the Baltic Sea and also the results of intradepartmental expeditions in Tallinn Gulf, in which several ships and aircraft participated simultaneously, make it possible to consider such an organization of field investigations to be the most rational in light of new tasks for preservation of the environment.

In its resolution the Council approved the organization and implementation of such work and recommended that the Leningrad Division of the State Oceanographic Institute prepare materials on the organization and implementation of such expeditions for extending the experience to other basins. The council also decided to consider an interdepartmental program for investigations of the Baltic Sea as a unified geographical feature over the extended period of 15-20 years (Project "Baltika").

A representative of the State Oceanographic Institute, A. N. Ovsyannikov and a representative of the Arctic and Antarctic Scientific Research Institute, A. T. Bozhkov reported on the second problem "Status and Prospects of Development of the Sea Coastal Network."

After hearing and discussing the reports, the Council noted that the marine administrations of the Hydrometeorological Service are devoting great attention to supporting the normal work of the marine hydrometeorological network. The quality of observations in the marine network on the whole is good.

The State Oceanographic Institute and the Arctic and Antarctic Scientific Research Institute are carrying out a systematic checking of operation of the marine network and are rendering the necessary assistance.

During 1980 the State Oceanographic Institute, in collaboration with the Arctic and Antarctic Scientific Research Institute, Far Eastern Scientific Research Hydrometeorological Institute and hydrometeorological observatories of marine administrations of the Hydrometeorological Service will carry out scientific research work on the theme "Development of a Scheme for the Distribution of the Marine Coastal Hydrometeorological Network in the Seas of the USSR," which will make possible a scientific validation of the prospects for development of the marine network.

V. N. Drozdov

An unofficial conference of experts on statistical planning of the Precipitation Enhancement Project was held at the State Committee on Hydrometeorology during the period 29 October-2 November 1979. It was devoted to the International Precipitation Enhancement Project being carried out in the basin of the Douro River (Spain). The scientific objectives of this project were defined by the 28th Session of the Executive Committee WMO in 1976. There have already been a series of unofficial conferences of experts at

which there was a discussion of different aspects of the Precipitation Enhancement Project. The materials of these conferences were given in different WMO bulletins and reports (Weather Modification Programme. Precipitation Enhancement Project).

At the conference of experts on statistical planning of the Precipitation Enhancement Project there was discussion of the present status of work on the project, the specialists analyzed the aspects of statistical planning and evaluation of field experiments with artificial modification for the purpose of obtaining additional precipitation and formulated recommendations for further preliminary investigations which must be made for the purposes of the Precipitation Enhancement Project in the Douro basin.

The Soviet delegation familiarized the foreign specialists with the problems involved in the planning of field experiments for enhancing precipitation in the steppe region of the Ukraine and in the basin of Lake Sevan, with the results of experiments already carried out, and also with plans for further improvement of statistical evaluations of the results of field experiments being carried out at the present time in the USSR under the direction of Academician A. N. Kolmogorov. Foreign specialists presented concise information on studies discussed at the Sixth Conference on the Use of Probabilistic and Statistical Methods in the Atmospheric Sciences held by the American Meteorological Society during the period 9-12 October 1979 in Canada. The conference materials will be published in the next WMO bulletin (Weather Modification Programme. Precipitation Enhancement Project).

V. M. Voloshchuk

CONFERENCES, MEETINGS AND SEMINARS

Moscow METEOROLOGIYA I GIDROLOGIYA in Russian No 3, Mar 80 pp 124-128

[Article by L. S. Speranskiy, K. Ya. Vinnikov, N. F. Dement'yev and V. D. Komarov]

[Text] An All-Union Conference on "Hydrodynamic and Statistical Methods for Local Weather Forecasting and Problems in Mesometeorology" was held in Novosibirsk during the period 15-19 October 1979. The conference was attended by representatives of 15 scientific institutes and colleges in the country. A total of 36 reports were presented.

A large group of reports was devoted to hydrodynamic methods for local weather forecasting. Here, in particular, we should mention a report by Academician G. I. Marchuk, V. V. Penenko, A. Ye. Aloyan and G. L. Lazriyev (Computation Center Siberian Department USSR Academy of Sciences) on numerical modeling of the microclimate of cities, with anthropogenic factors taken into account. Individual aspects of this problem were examined in reports by A. Ye. Aloyan, D. L. Iordanov and V. V. Penenko, entitled "Numerical Modeling of Transport of Passive Admixtures," A. Ye. Aloyan, G. L. Lazriyev and V. V. Abramenko, "Methods for Taking the Turbulent Energy Equation into Account," and A. Ye. Aloyan and G. V. Isayev, "Propagation of an Admixture in the Surface Layer from Fixed and Moving Sources."

A series of reports presented by specialists of the USSR Hydrometeorological Center was devoted to studies for creating a local forecasting model on the basis of deep convection equations. A numerical algorithm for integrating a system of deep convection equations and investigating the properties of this system was discussed by V. Z. Kisel'nikov, Ye. M. Pekelis and D. Ya. Pressman. A report by M. Alautdinov and N. P. Vel'tishchev presented a method for computing radiation heat influxes and gave the results of modeling of the diurnal variation of meteorological elements under moist deep convection conditions. A. A. Zhelnin and A. A. Bregman told of an algorithm for the parameterization of microphysical processes related to the formation of clouds and precipitation. V. M. Losev reported on computation of stationary mesoscale temperature and wind fields on the basis of synoptic information using linearized deep convection equations.

P. Yu. Pushistov, L. S. Speranskiy, T. A. Toloknova and Ye. G. Sementsova (West Siberian Regional Scientific Research Hydrometeorological Institute) reported on a model of local forecasting for a lowland territory and presented some results of forecasts made on the basis of this model. V. K. Arguchintsev (Irkutsk State University) told about a two-dimensional model for investigating breeze effects, constructed without the simplification of quasistatics. B. G. Vager (Leningrad Institute of Construction Engineers) reported on allowance for horizontal diffusion in a model of the surface layer intended for calculation of the heat and moisture transfer regime in the presence of inhomogeneities of a small linear scale (canal in the desert, flight strip). His second report was devoted to experience in the use of splines in boundary layer problems. M. S. Akhmetov (Pskov State University) told of some aspects of interaction between open pit mines and the atmosphere.

A number of reports were devoted to an investigation of convection and turbulence. R. S. Pastushkov and S. A. Vladimirov told about numerical modeling of the convective cloud cover accompanying a squall. G. G. Goral' and O. I. Chapovskaya (High-Mountain Geophysical Institute) reported on experimental investigations of convective processes accompanied by squalls. The synoptic and thermodynamic conditions determining the localization and intensity of convection in the Northern Caucasus were examined by L. M. Fedchenko and V. A. Belentsova (High-Mountain Geophysical Institute). The report of A. N. Koval'chuk and T. N. Terskovoy (High-Mountain Geophysical Institute) was devoted to an investigation of the dynamics of cumulonimbus clouds and the conditions for the formation of well-developed hail cells. An investigation of a model of a cloud ensemble on the basis of GATE data was presented by A. I. Fal'kovich (USSR Hydrometeorological Center). The subject of two reports by P. Yu. Pushistov, V. M. Mal'bakhov and S. M. Kononenko was the numerical modeling of penetrating convection in the boundary layer and an investigation of two-level convective ensembles and the mechanism of formation of cumulus clouds.

A report by A. S. Gavrilov (Leningrad Hydrometeorological Institute) was devoted to an investigation of the convective boundary layer using a different tool: systems of Fridman-Keller moment equations. In this report, as in the communication of the above-mentioned authors, great attention was devoted to the problem of antigradient heat transfer. A. G. Tarnopol'skiy (State Oceanographic Institute) and V. A. Shnaydman (Odessa Hydrometeorological Institute) made a comparative investigation of the characteristics of turbulence obtained employing two closing methods: on the basis of an equation for the rate of dissipation of turbulent energy and using the generalized Karman hypothesis. An investigation of the structure of vertical movements in the boundary layer on the basis of experimental data was the subject of a report by Yu. P. Perevedentsev and Yu. G. Khabutdinov (Kiev State University). The results of experimental investigations and methods for computing turbulence in the layer 50-500 m were reported by V. N. Barakhtin and E. A. Morozov (West Siberian Regional Scientific Research Hydrometeorological Institute).

A report by B. N. Sergeyev (Central Aerological Observatory), telling about a two-dimensional model of an atmospheric front, devoted great attention to the parameterization of phase transitions and the formation of precipitation. A model of formation of a frontal zone, taking into account nonadiabatic factors, was examined by B. Ya. Kutsenko (Central Aerological Observatory). A report by Z. N. Kogan and N. Z. Pinus (Central Aerological Observatory) was devoted to an evaluation of the budget of the principal types of energy in a middle-latitude cyclone. The subject of a second communication by Kogan was a study of the kinetic characteristics of a cyclone on the basis of radiosonde data. Investigations of the interaction between the boundary layer and the free atmosphere for processes on a subsynoptic scale were reported by V. A. Shlychkov and P. Yu. Pushistov.

Two reports were devoted to problems involved in flow around barriers: "Lee Wave Resistance Exerted by a Real Mountain System" -- V. N. Kozhevnikov, N. N. Zidlev and N. N. Pertsev (Moscow State University), "Numerical Modeling of the Problem of Flow Around Obstacles by an Incompressible Fluid" -- I. G. Granberg (Institute of Physics of the Atmosphere).

A number of reports examined models of prediction of local phenomena on the basis of statistical methods.

The methods for ordering and sampling of parameters in local alternative models were investigated in a report by T. A. Anikina, G. M. Vinogradova and L. N. Romanov (West Siberian Regional Scientific Research Hydrometeorological Institute). One statistical forecasting method, based on the expansion of the fields of meteorological elements into series in a system of linearly independent functions, was discussed by V. V. Kostyukov (West Siberian Regional Scientific Research Hydrometeorological Institute). A model of prediction of the frequency of recurrence of breezes was examined in a report by E. A. Burman and F. Ya. Stupina (Odessa Hydrometeorological Institute). The following reports of specialists of the West Siberian Regional Scientific Research Hydrometeorological Institute were also devoted to the prediction of individual weather phenomena: M. Ya. Kogan and L. N. Romanov -- "Quasilinear Models for Prediction of Diurnal Temperature Variation," G. G. Polyakov and Z. V. Torbina -- "Prediction of Precipitation Using a Piecewise-Linear Model," D. I. Zenkevich -- "Prediction of Visibility in Snowfalls," I. P. Prokop'yev -- "Prediction of Significant Snowfalls in the Southeastern Part of Western Siberia."

L. S. Speranskiy

A bilateral Soviet-American symposium on the modeling of climate, climatic changes and the statistical processing of climatic data was held at Tbilisi during the period 15-22 October 1979.

It was the sixth of a series of symposia held during 1976-1979 within the framework of project 02.08.11 -- "Effect of Changes in the Heat Balance on Climate" of Working Group VIII ("Effect of Environmental Change on Climate");

of the Soviet-American Commission on Scientific Cooperation in the Field of Preservation of the Environment.

The project is headed on the Soviet side by Corresponding Member USSR Academy of Sciences M. I. Budyko, and on the American side -- Professor W. L. Gates.

Well-known American scientists participated in the symposium: W. L. Gates, E. N. Lorenz, R. D. Sess, R. M. Chervin, S. Esbensen, M. Halem, I. M. Held, R. D. Jenne, R. Madden, G. R. North, A. Robock, M. J. Suarez, J. M. Wallace, E. R. Reiter and E. W. Bierley. On the Soviet side there were about 30 specialists, for the most part from the institutes of the State Committee on Hydrometeorology and the USSR Academy of Sciences.

The symposium program included 37 reports, including 20 reports of Soviet scientists and 16 reports of scientists of the United States delegation. One report was presented jointly by the scientists of the USSR and the United States.

The most general problems were considered in the reports of M. I. Budyko and E. N. Lorenz.

The report of M. I. Budyko contained a synthesis of modern concepts concerning impending changes in global climate and the biosphere under the influence of anthropogenic change in the content of carbon dioxide in the atmosphere. The report expressed the assurance that already at the present time it is possible to prepare forecasts of climatic change necessary for working up long-range economic development plans.

The problem of the predictability of behavior of a climatic system was discussed in a report by E N. Lorenz. Touching upon the problems involved in prediction of climatic changes in relation to the increase in content of atmospheric CO_2, E. N. Lorenz surmises that this is precisely the type of climatic problem whose solution will be most feasible by application of the numerical modeling method.

Empirical evaluations of recent changes in the thermal and ice regimes of the northern hemisphere were examined in a joint report of specialists of four institutes of the State Committee on Hydrometeorology: K. Ya. Vinnikov, G.V. Gruza, V. F. Zakharov, N. P. Kovyneva, K. M. Lugina and E. Ya. Ran'kova. It was demonstrated in the report that beginning from the middle 1960's there has been a warming of the northern hemisphere with a mean intensity 0.1-0.2° C/10 years. This warming is accompanied by a substantial reduction in the total ice content in the Arctic Ocean.

In a report by A. Robock, on the basis of an analysis of empirical data characterizing the change in the mean temperature of the northern hemisphere during the last 400 years, carried out using a numerical zonal model of a climatic system with parameterized dynamics, the author

refuted the hypothesis that "solar activity" is one of the important factors in change in global climate.

Empirical data on recent changes in climate and the results of a statistical analysis and generalization were also presented in the reports of E. R. Reiter, K. Ya. Vinnikov and P. Ya. Groysman, G. V. Gruza and E. Ya. Ran'kova, R. D. Madden, O. A. Drozdov, J. M. Wallace and D. S. Gutsler, Ye. M. Dobryshman, M. I. Fortus and Ya. M. Kheyfets, N. V. Kobysheva and L. P. Naumova, L. S. Petrov, et al., V. N. Adamenko, Yu. L. Rauner.

The climate modeling problem was discussed in more than ten reports. Evaluations of the influence of an increase in the content of CO_2 in the atmosphere on the climatic regime, obtained using the Oregon University model, were presented in a report by W. L. Gates. Although the model includes a realistic description of the topography of the earth's surface and the seasonal variation of solar radiation, these evaluations cannot be used for predicting climatic changes, since in this investigation the temperature of the ocean surface is considered stipulated and does not change with an effect on the climatic system.

The necessity for allowance for the influence of thermal inertia of the ocean on the change in air temperature accompanying an anthropogenic increase in the atmospheric content of CO_2 was demonstrated in a report by R. D. Sess. In another report by this author it was stated that the process of global warming can be accelerated as a result of the increasing anthropogenic discharge of the compounds CO, NO_x, CH_4, forming from fuel combustion.

In a report read by V. P. Dymnikov, Academician G. I. Marchuk and his colleagues gave detailed information concerning the status of studies on construction of models in the theory of climate at the Computation Center Siberian Department USSR Academy of Sciences. I. V. Trosnikov told about a model of general circulation of the atmosphere developed at the USSR Hydrometeorological Center.

It was demonstrated in a report by V. P. Meleshko and R. T. Vezerold that allowance for the real geographical distribution of cloud cover exerts a substantial influence on the local characteristics of the climatic and circulatory regime of the atmosphere.

Important problems in study of the laws of behavior and sensitivity of a global climatic system by means of models were also examined in reports by Corresponding Member USSR Academy of Sciences G. S. Golitsyn, G. North, M. Suarez, I. L. Karol' and I. M. Held.

The reports of V. A. Aleksandrov and V. Ya. Sergin, R. M. Chervin and M. Halem were devoted to a study of the statistical characteristics of the meteorological regime, reproducible using models of general circulation

of the atmosphere. The studies of these authors give additional information on how realistic climatic models are and make possible a more correct formulation of numerical experiments for evaluating the sensitivity of climate to external effects.

Without dwelling on the other reports (the materials contained in them have been partially published), we note a paper by I. M. Held, which was discussed from the floor, telling about a new study by Manabe and Wetherhold which gave an evaluation of the influence of doubling and quadrupling of atmospheric CO_2 content on the mean annual climatic regime over the continents and oceans separately. According to these evaluations, the warming of climate can be accompanied by a substantial change of moistening conditions in agriculturally important regions of the continents.

The participants in the symposium expressed the opinion that it is necessary to summarize the results of the series of Soviet-American symposia held during the period 1976-1979 at a conference of Soviet and American experts on the problem of the influence of CO_2 on climate. Upon completion of the symposium this proposal was adopted at a session of the Eighth Working Group of the Soviet-American Commission.

K. Ya. Vinnikov

***

The Tenth Conference of the Danubian Countries on Hydrological Forecasts was held in Vienna during the period 11-14 September 1979. It was attended by delegations from Austria, Bulgaria, Hungary, USSR, West Germany, Czechoslovakia and Yugoslavia, as well as two hydrologists from Switzerland and one each from East Germany and the Netherlands. Three international organizations were represented at the conference: Danubian Commission, World Meteorological Organization and International Institute of Systems Analysis. The total number of participants was 134. The working languages were Russian and German.

In evaluating the organization of the conference work we should note the high level of its preparation and implementation. Before the conference began two volumes of materials were published which contained national reports on the methods used in each country for predicting the water and ice regimes of the Danube (one volume) and the reports presented at the conference (second volume). Also included were author's summaries of reports and detailed programs of the scientific sessions and field trips. Each conferee received these materials. We should also note the exceptionally high quality of simultaneous translation. All this favored the complete success of the conference.

Thirty-four reports were presented and discussed at six scientific sessions. Most of these were devoted to the following problems and aspects of hydrological forecasts for the Danube and its tributaries: short-range

forecasting of levels and discharges, long-range forecasting of levels and discharges, forecasting of ice phenomena, forecasting of channel processes and runoff of sediments, evaluation of the accuracy and economic effectiveness of forecasts.

The greatest number of reports (15) dealt with methods for the short-range forecasting of water discharges and levels in the Danube and its tributaries. The basis for the methods is mathematical models of the channel phase of runoff, differing in complexity, and models known under the name "precipitation-runoff."

Among the first of these models attention was centered on an adaptive linear model of channel runoff whose parameters vary continuously in dependence on the observed error in forecasts on the preceding days. Precomputations of river discharges and levels using an electronic computer on the basis of such a "self-adjusting" forecasting method are probably of considerable practical interest. The model was developed by the Hungarian hydrologist Sh. Ambrush for the reach of the Danube between Dunafoldvar and Baja, but it naturally has quite general significance. In the forecasting methods which were discussed in the reports of Kresser, Gutknecht and Dreher (Austria), Engel and Mendel, Schiller and Tissa (West Germany) and Stefanova (Bulgaria) the emphasis was on computations of the travel-time curve of water on the basis of models of a cascade of linear and nonlinear capacitances. In general, these models are quite well known. Nevertheless, the reports were of considerable interest because they familiarized the conferees with some modifications of these models and procedures for determining their parameters. It is also important that river reaches with a cascade of reservoirs were among the investigated objects.

"Precipitation-runoff" models were discussed in reports by Lutz, Koch and Rosemann (West Germany), Lukachova (Czechoslovakia), Georgevic (Yugoslavia) and Nachtnebel (Austria). In scientific respects the most interesting reports were an investigation of the influence exerted by the intensity of precipitation, runoff losses and some other factors on the form of the unit hydrograph (report by Lutz) and a nonlinear model of the "runoff-precipitation" type (reports by Lukachova and Nachtnebel).

In the reports presented at the preceding conference in Budapest it could be seen that in the "precipitation-runoff" model there is still a part which has not been adequately developed; reference is to computations of runoff losses with time. Unfortunately, this situation still persists, as follows from the conference reports in Vienna. The reason for this is the absence of extensive investigations of the problem of infiltration of rain water, especially investigations on the basis of experimental and representative basins. The use of a mathematical approach alone does not solve this complex problem. Attention was given to this circumstance at the final session of the conference.

The reports on the considered problem also contained important information relating to remote measurements of hydrometeorological elements and the automated collection of the results of these measurements at the

forecast preparation center. Since the maximum possible advance time for predicting rain-induced high waters in many cases is less than 24 and even 12 hours, an acceleration of the collection of initial data for preparation of a forecast is of very great practical importance. A prediction of precipitation, to be sure, makes it possible to increase the advance time for predicting high water. In this connection informational reports on precipitation forecasts were presented at the conference.

It should be noted that in connection with the construction of a large number of reservoirs on the Danube tributaries the problem of their control is becoming increasingly acute. For this reason, and also in relation to the problems involved in monitoring water quality (two reports -- from the USSR and Bulgaria -- were devoted to water quality problems), short-range forecasts are acquiring ever-greater importance. Naturally, the prediction of exceptionally high waters, constituting a danger for the population and enterprises along the shores, also retains its importance in the presence of reservoirs.

At this conference there was not a single report on the problem of long-range forecasting of low levels of the Danube, having great importance for navigation. For that reason particular interest was shown in a report by V. M. Mukhin (USSR Hydrometeorological Center) on a method for predicting the levels of the Danube for 10-20 days in advance. The basis of the method is a mathematical model which takes into account the role of water distribution along the length of the river and the role of the distribution of precipitation over the area of the basin in the formation of water discharges at the lowest-lying station on the river. Such forecasts make it possible to know the depth in the main channel during the movement of a ship in the Danube reach from Bezdan to Tulcea, with an extent of about 1,400 km. The report caused interest as well due to the fact that for solving the problem V. M. Mukhin used a modern approach (component analysis, theory of solution of incorrectly formulated problems).

Four reports were devoted to a superlong-range forecasting of the water volume in the Danube and an analysis of its changes over a period of many years. They did not contain new approaches to solution of the problem of superlong-range forecasting of river runoff. We note that among the hydrologists of the Soviet Union the opinion prevails that there is no firm scientific basis for the superlong-range forecasting at this time and that investigations of this problem have a strictly exploratory nature. The Soviet delegation presented no reports on the superlong-range forecasting of river volume, although at the preceding conference at Budapest we did present reports on this problem.

Six reports were presented on the problem of channel processes and the runoff of sediments. However, only the reports from the Soviet Union were devoted to a quantitative prediction of river channel deformations (B. F. Snishchenko, State Hydrological Institute and V. N. Mikhaylov,

Moscow State University). The reports on sediments, in essence, contained no methods for predicting the solid runoff of the Danube and its tributaries. Nevertheless, they were interesting since they gave the results of investigations which without question will be used in developing methods for predicting the runoff of sediments. For example, in a report presented by Bulgaria there were data characterizing the distribution of the granularity of bottom deposits in a reach of the Danube with an extent of about 2,000 kilometers and casting light on the evolution of the composition of deposits along the length of this river. The acoustic method for measuring bottom sediments is quite novel; it was described in a report by Schlagge (West Germany).

It is well known that the problems involved in predicting the ice regime of rivers in the Danube basin are being studied primarily in the Soviet Union. It is therefore not surprising that only our reports were presented at the conference: one about the hydrological conditions of winter navigation and another about the method for long-range forecasting of the duration of ice phenomena and the times for clearing of the Danube from ice.

There were only two special reports on the problem of evaluating the economic effectiveness of forecasts. The matter of economic effectiveness was touched upon in a number of other reports in which data were cited quantitatively characterizing the advantage gained from different specific forecasts of the water volumes in the Danube and its tributaries.

Upon completion of the scientific program of the conference an excursion was organized for its participants to the Danube Melk and Ibbs-Persenboyg Hydroelectric Power Stations, the first of which is under construction, whereas the second has been in operation since 1958. An exhibition of hydrometeorological instruments was held during the conference.

N. F. Dement'yev and V. D. Komarov

NEWS FROM ABROAD

Moscow METEOROLOGIYA I GIDROLOGIYA in Russian No 3, Mar 80 p 128

[Article by B. I. Silkin]

[Text] As reported in NATURE, Vol 278 and SCIENCE NEWS, Vol 115, No 17, 1979, several years ago the American space probe "Mariner-9" registered evidence of the existence of baroclinic waves in the Martian atmosphere (pressure systems which on earth are usually associated with cyclones). At that time their presence was established at the end of winter in the planet's northern hemisphere. In general, it was found, the north polar region is one of the most meteorologically active.

Now meteorological observations on Mars have been made with a considerably greater accuracy using equipment carried aboard the orbital compartment of the interplanetary station "Viking-1." It was possible to photograph summer cloud structures similar to the classical structures associated with cyclones on the earth. In actuality the orbital compartments of the "Viking" are not meteorological satellites, but the duration of their existence made it possible to accumulate observational data of meteorological value. The directors of the team processing these space photographs, Harry E. Hunt (University College, London, England) and Philip B. Jones (Missouri State University, United States) note that for the first time evidence was obtained that under summer conditions it is possible to observe the baroclinic waves usually predominating in other seasons.

The most interesting atmospheric formation was discovered near 81°N, 160°E on Mars, almost at the very edge of the planet's polar cap. Observations in the IR part of the spectrum indicated the existence here of a steep temperature gradient at the surface; immediately to the south of the postulated cyclone a temperature of 237 K was registered, directly beneath it -- about 230 K, and to the north of it -- approximately 215 K. Under conditions of cyclonic systems it is natural to expect precisely such a gradient. This is because the atmospheric waves causing such disturbances usually are formed within polar fronts separating cold masses of arctic air from the warmer middle-latitude atmosphere.

Still another rotational structure was discovered closer to the equator at about 66°N and 227°E. Evidently it also contained water ice. The elevation of this formation, determined from shadows on the planetary surface, was from 6 to 7 km. The wind speed was about 23.1 m/sec in the clouds and about 9.2 m/sec in the surface layer.

In addition, evidences of the existence of baroclinic systems were detected by the two landing modules of the "Viking" when these systems passed over them. The meteorological instrumentation of these landing modules operated continuously for more than 688 days, that is, more than one Martian year. However, the cameras on the modules were oriented in such a way that they could not record the true configurations of the cyclonic formations. However, the very fact of their existence on Mars is considered completely demonstrated on the basis of the data obtained from the orbital modules.

*****

As reported in NATURE, Vol 280, 1979, and NEW SCIENTIST, Vol 83, No 1163, carbon dioxide, entering into the atmosphere in ever-greater quantities as a result of man's transportation and industrial activity, is creating a so-called greenhouse effect which is an obstacle to heat transfer from the earth's surface. In addition to its warming, it naturally will lead to a cooling of the higher layers of the atmosphere deprived of this heat source.

It was recently established that an insignificant decrease of stratospheric temperature impairs the photochemical balance in such a way that it favors the retention of ozone. The easily vulnerable layer of the ozonosphere in the atmosphere, which is threatened by the increasing discharge of fluorocarbons into air space, thus is acquiring a definite possibility of preservation and renewal.

Scientific specialists of the British Meteorological Service K. Groves and A. Tuck have improved the mathematical model of the atmosphere, including in it data on the influence of carbon dioxide and the temperature effects related to it on the course of 35 different photochemical reactions maintaining the ozone balance in the troposphere.

They ascertained that even if the entry of fluorocarbons into the atmosphere persists at the 1975 level, by the year 2020 the quantity of ozone will only be reduced by 8.6%. Until now, without taking the influence of carbon dioxide into account, it was assumed that this reduction could attain 15-20%.

On the other hand, even such an insignificant reduction in the total concentration of ozone can be accompanied by a substantial displacement of the altitude of the main layer of ozone concentration in air space and also a change in its entire vertical temperature structure. For the time being it is unclear to specialists as to what climatic changes can result from this.

5303 -END-
CSO: 1864